Volume 119, September 2017

ISSN 0927-796X

ELSEVIER

MATERIALS SCIENCE & ENGINEERING

R

Reports: A Review Journal

Spatially and temporally controlled hydrogels for tissue engineering

Jeroen Leijten, Jungmok Seo, Kan Yue, Grissel Trujillo-de Santiago, Ali Tamayol, Guillermo U. Ruiz-Esparza, Su Ryon Shin, Roholah Sharifi, Iman Noshadi, Mario Moisés Álvarez, Yu Shrike Zhang, Ali Khademhosseini

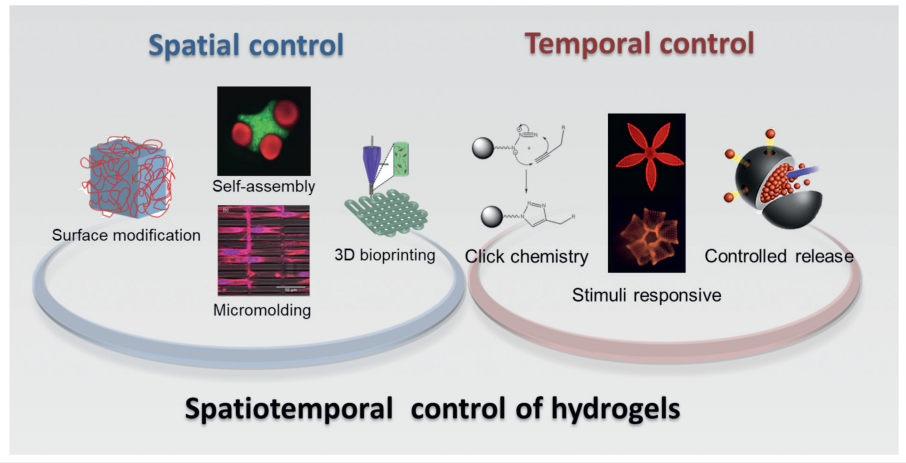

Available online at www.sciencedirect.com

ScienceDirect

Materials Science and Engineering R 119 (2017) 1–35

Contents lists available at ScienceDirect

Materials Science and Engineering R

journal homepage: www.elsevier.com/locate/mser

Spatially and temporally controlled hydrogels for tissue engineering

Jeroen Leijten[a,b,c,1], Jungmok Seo[a,b,d,1], Kan Yue[a,b,1], Grissel Trujillo-de Santiago[a,b,e,f], Ali Tamayol[a,b], Guillermo U. Ruiz-Esparza[a,b], Su Ryon Shin[a,b], Roholah Sharifi[a,b], Iman Noshadi[a,b,i], Mario Moisés Álvarez[a,b,e,f], Yu Shrike Zhang[a,b], Ali Khademhosseini[a,b,g,h,*]

[a] Biomaterials Innovation Research Center, Division of Engineering in Medicine, Department of Medicine, Brigham and Women's Hospital, Harvard Medical School, Cambridge, MA 02139, USA
[b] Harvard-MIT Division of Health Sciences and Technology, Massachusetts Institute of Technology, 77 Massachusetts Avenue, Cambridge, MA 02139, USA
[c] Department of Developmental BioEngineering, MIRA Institute for Biomedical Technology and Technical Medicine, University of Twente, Enschede, The Netherlands
[d] Center for Biomaterials, Biomedical Research Institute, Korea Institute of Science and Technology, Seoul 02792, Republic of Korea
[e] Microsystems Technologies Laboratories, MIT, Cambridge, 02139, MA, USA
[f] Centro de Biotecnología-FEMSA, Tecnologico de Monterrey , CP 64849, Monterrey, Nuevo León, Mexico
[g] Department of Bioindustrial Technologies, College of Animal Bioscience and Technology, Konkuk University, Hwayang-dong, Gwangjin-gu, Seoul 143-701, Republic of Korea
[h] Department of Physics, King Abdulaziz University, Jeddah 21569, Saudi Arabia
[i] Department of Chemical Engineering, Henry M. Rowan School of Engineering, Rowan University, Glassboro, NJ 08028, USA

ARTICLE INFO

Article history:
Received 17 March 2017
Received in revised form 5 July 2017
Accepted 6 July 2017
Available online 25 July 2017

Keywords:
Hydrogel
Tissue engineering
Microfabrication
Bioprinting
Cell-biomaterial interaction
Biomaterials
Cellular microenvironments

ABSTRACT

Recent years have seen tremendous advances in the field of hydrogel-based biomaterials. One of the most prominent revolutions in this field has been the integration of elements or techniques that enable spatial and temporal control over hydrogels' properties and functions. Here, we critically review the emerging progress of spatiotemporal control over biomaterial properties towards the development of functional engineered tissue constructs. Specifically, we will highlight the main advances in the spatial control of biomaterials, such as surface modification, microfabrication, photo-patterning, and bioprinting, as well as advances in the temporal control of biomaterials, such as controlled release of molecules, photocleaving of proteins, and controlled hydrogel degradation. We believe that the development and integration of these techniques will drive the evolution of next-generation engineered tissues.

Abbreviations: 2D, two dimensional; 2PP, two-photon hydrogel polymerization; 3D, three-dimensional; AFM, atomic force microscopy; AgNP, silver nanoparticles; AuNP, gold nanoparticle; α-SMA, alpha-smooth muscle actin; RGD, Arg-Gly-Asp; BMP, bone morphogenetic protein; CNTF, ciliary neurotrophic factor; DMD, digital micromirror device; ECM, extracellular matrix; ESC, embryonic stem cell; FBR, foreign body reaction; FGF1, fibroblast growth factor 1; GelMA, gelatin methacryloyl; HUVEC, human umbilical vein endothelial cell; HA, hyaluronic acid; hESC, human embryonic stem cell; hiPSC, human induced pluripotent stem cell; hMSC, human mesenchymal stem cell; HSC, hepatic stellate cells; IL, interleukin; IPN, interpenetrating polymer network; MSC, mesenchymal stem cell; MMP, matrix metalloprotease; NF-κB, kappa-light-chain-enhancer of activated B cells; NIL, nanoimprint lithography; NIR, near infrared; NorHA, norbornene-functionalized hyaluronic acid; PHEMA, poly(2-hydroxyethyl methacrylate); PA, polyacrylamide; PAA, poly(acrylic acid); PBT, poly(butylene terephthalate); PCL, polycaprolactone; PDMS, polydimethylsiloxane; PDPA, poly(2-(diisopropylamino)ethyl methacrylate); PEG, poly(ethylene glycol); PEGDA, poly(ethylene glycol) diacrylate; PEI, polyethyleneimine; PLGA, poly(lactic-co-glycolic acid); PNIPAAm, poly(*N*-isopropylacrylamide); PMMA, poly(methylmethacrylate); PMPC, poly(2-(methacryloyloxy)-ethyl phosphorylcholine); PVA, poly(vinyl alcohol); PTFE, poly (tetrafluorethylene); RGD, Arg-Gly-Asp; ROMP, ring-opening metathesis polymerization; SHH, sonic hedgehog; SWGA, surface-wettability-guided assembly; SPAAC, strain-promoted alkyne-azide cycloaddition; UV, ultraviolet; VEGF, vascular endothelial growth factor.

* Corresponding author at: Biomaterials Innovation Research Center, Department of Medicine, Brigham and Women's Hospital, Harvard Medical School, Cambridge, MA 02139, USA.
E-mail address: alik@bwh.harvard.edu (A. Khademhosseini).
[1] These authors contributed equally to this work.

http://dx.doi.org/10.1016/j.mser.2017.07.001
0927-796X/

Contents

1. Introduction

Recent advances in biomaterials have allowed for deeper understanding of fundamentals of cell biology and fueled further development of novel pharmacological *ex vivo* models by recapitulating native physiological processes [1]. Moreover, biomaterials play a fundamental role in tissue engineering, which is aiming to fabricate living replacements to restore the functions of affected tissues and organs. The last decades have underlined the essential role of biomaterial design and engineering to improve the function of engineered tissue constructs [2]. Here, we critically review the emerging progresses of spatiotemporal control over biomaterial properties towards advanced biomaterials that facilitate the development of functional tissue-engineered constructs.

Traditionally, research directions on biomaterials have centered on the development of biomaterials with novel compositions and properties [3]. In parallel, an intense effort has been made towards the chemical modification of known biomaterials to endow them with improved performance or specific new functions. Moreover, conventional research has focused on the static behavior of biomaterials, while recent findings suggest that spatial and temporal control of biomaterials provides unique opportunities to recapitulate the dynamic nature of the microenvironments in native tissues, which play a key role in controlling cell behaviors and functions.

In addition to advances in biomaterial chemistry, numerous engineering techniques have also been developed to fabricate biomaterial constructs with unique spatial modifications and complex architectures [4]. We review the recent developments in biofabrication techniques including, but are not limited to, micromolding, photolithography, and spinning techniques for the fabrication of spatially defined biomaterials. The use of constructs fabricated with these technologies has revealed how the geometrical and topological factors of scaffolds can influence the proliferation, migration, and differentiation of cells in contact with engineered scaffolds. Also, we introduce the recent rapid developments in three-dimensional (3D) bioprinting techniques, which have provided practical methods for fabricating biomaterials into relevant sizes, shapes, and compositions for regenerative medicine [5].

We also review the recent achievements in temporal control over biomaterials. While conventional approaches have focused on controlled release of growth factors and drugs, recent studies have been dedicated to transforming passive and static scaffolds into responsive and dynamic matrices [6]. For example, cell-adhesive peptides can be presented in synthetic matrices upon on-demand photo-activation with precise spatial control, while biophysical characteristics such as matrix elasticity or stiffness can also be dynamically changed. Such new approaches are expected to play a major role in recapitulating the unique dynamic features of native extracellular matrix (ECM) to direct multistep biological processes,

such as stem cell differentiation and functional tissue regeneration.

We conclude by providing a perspective on the future challenges and opportunities in the development of biomaterials for tissue engineering applications. Specifically, we discuss the possibilities to generate multiscale materials by combining several recently developed technologies, which can provide instructive cues to cells on multiple length scales and provide unrivaled biomimetic microenvironments. Moreover, since this research direction necessitates the screening of large numbers of variables, the development and integration of high-throughput platforms into the field of biomaterial science is highlighted.

2. Spatial control of hydrogels

Conventional hydrogels can be employed for fabrication of scaffolds, which provide biomimetic chemical and physical microenvironments for the embedded cells to regulate their behaviors. However, these biomaterials lack the heterogeneity and dynamic changes observed in native tissues. Biomimicking the temporal and spatial characteristics of the native tissues and organs requires the development of advanced hydrogels. In this chapter, we will review the recent approaches towards spatial control of hydrogels for tissue engineering to enhance cellular functionality and therapeutic efficacy of implants.

2.1. Surface modification

Adherent mammalian cells need a solid substrate for anchorage to sustain their viability and function. Proteins sequestered in the ECM, components of the cytoskeleton, and trans-membrane receptors can all mediate the anchoring mechanisms between cells and the ECM [7–9]. For biomedical applications, the surface of hydrogels needs to mimic the chemical and physical properties of native ECMs and provide the components required for cell attachment. Incorporating bioactive motifs, such as the Arg-Gly-Asp (RGD) peptide sequences in polymeric hydrogels, is a practical approach to enhance cell attachment and proliferation [7,10]. In addition to cell anchoring motifs, surface characteristics such as stiffness, elasticity, topography, and thickness have been proven to affect the functions of cells and tissue regeneration. Thus, the cellular responses to the physical and chemical properties of hydrogel surfaces are intimately related to functionalities that are important in the context of tissue engineering, such as implant integration, prevention of inflammation, induction of cell differentiation, and antimicrobial activity. In this section, we describe the effects of hydrogel surface properties on cell behaviors to elucidate how additional physical cues can be added to hydrogel matrices to achieve specific functionalities, as well as the practical uses of hydrogels as surface modifiers.

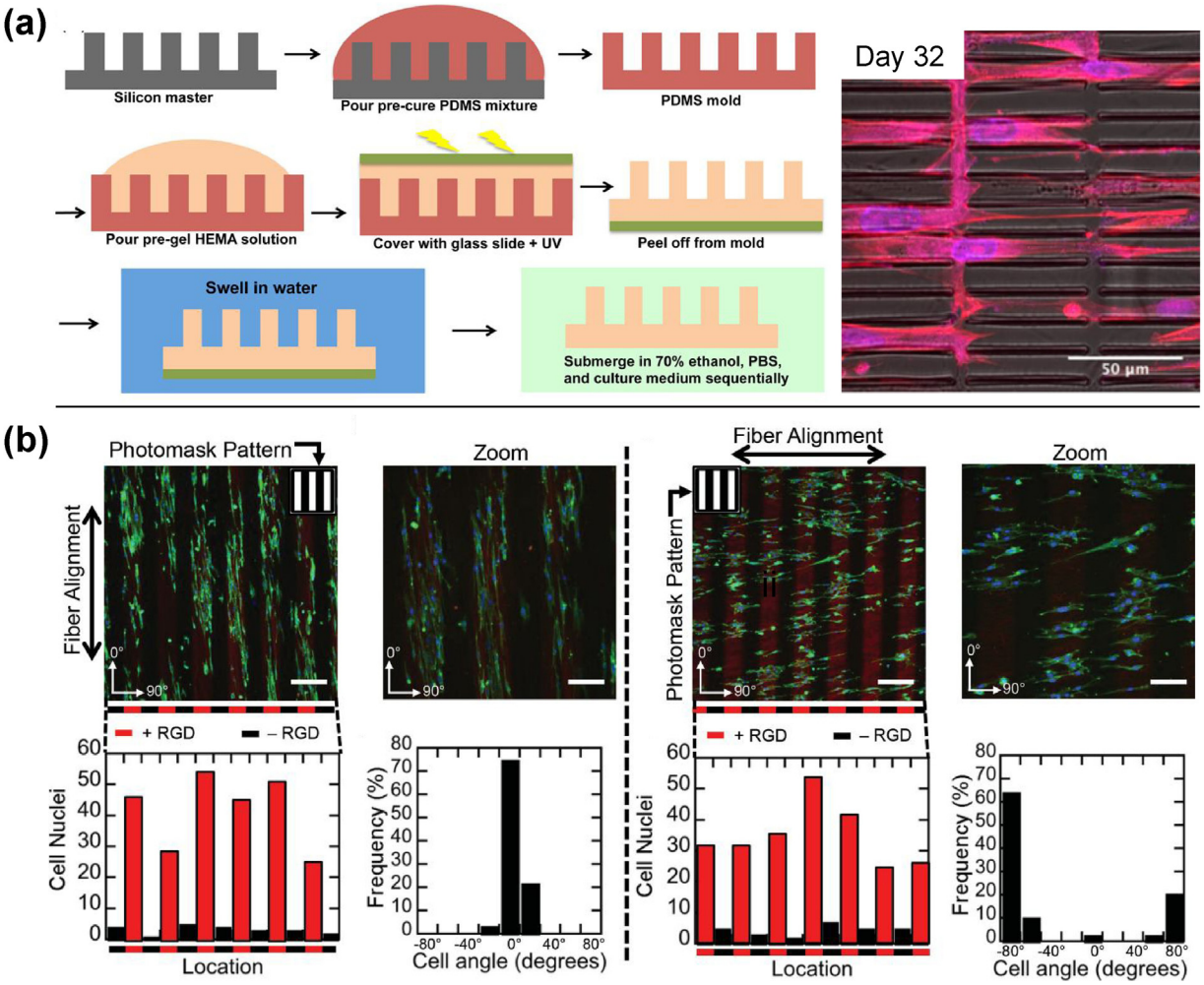

Fig. 1. Patterning hydrogel surfaces to spatially functionalize hydrogels. (a) Schematic representation of a method to transfer patterns to pHEMA hydrogels from a silicon master and the effect of the patterns on the morphology of cells cultured on them. (b) Physical and molecular patterns (RGD) of fibrous HA-based hydrogel functionalized with norbornene and their effect on cell alignment.
Reproduced with permission from: (a) Ref. [16], (b) Ref. [17].

2.1.1. Spatial control of hydrogel surfaces

Not only material properties but also spatial patterns on hydrogels can regulate cell behaviors on the surface. Surface patterning of hydrogels is an effective strategy for aligning cells and manipulating cell functions on the surface. Cell alignment is involved in many important natural processes, such as the formation of functional vascular, muscular, and neural tissues [11]. Cell shape manipulation also can affect the stem cell fate decision process [12,13]. In addition, the surface patterning of hydrogels can be used to steer the immune response by *e.g.* polarizing macrophages towards a non-inflammatory phenotype, which has been used as a strategy to enhance biocompatibility on implantable metal and polymeric surfaces [14].

Segura et al. reported oriented growth of NIH/3T3 fibroblasts on patterned hyaluronic acid (HA)-collagen hydrogels [15]. The patterns were transferred *via* a poly(tetrafluorethylene) (PTFE) mold, on which the hydrogel was cast. After casting, the hydrogel solution was dehydrated, stored, and eventually re-hydrated for cell culture experiments. Although the hydration step limited the pattern resolution, the patterning was sufficiently effective to guide the cell alignment. A more recent study by Hu et al. reported a method that enabled high-resolution micropatterns (5–15 μm spacing) using a poly(2-hydroxyethyl methacrylate) (PHEMA) hydrogel [16]. Fig. 1a shows a schematic depiction of the fabrication method towards micropatterned hydrogels. Human mesenchymal stem cells (hMSCs) were cultured on top of the patterned hydrogels and confocal microscopy results showed that the cells were aligned with the patterned surface. The hMSCs proliferated and formed interconnections along the surface of the micropatterned hydrogel over 32 days of culture (Fig. 1a).

Wade et al. introduced a hydrogel system that incorporated distinct spatial patterns with different chemical properties, thereby providing different sets of topographical and biochemical cues to cells [17]. The topographical cues were provided by utilizing aligned electrospun norbornene-HA hydrogel fibers, whereas the patterned biochemical cues (RGD patterns) were provided by the polymer chemistry design coupled with photo-patterning. The scaffolds were prepared with either parallel or perpendicular biochemical and topological patterns. Interestingly, in both cases, the cells responded more strongly to the topographical cues than to the biochemical patterns. RGD patterns alone proved insufficient to orient cells when they were perpendicular to the fiber direction, but they enhanced cell density along the patterns when both patterns were parallel to each other (Fig. 1b).

Hodde et al. reported another approach to provide topographical cues to hydrogel systems [18]. Individual frames with aligned polycaprolactone (PCL) electrospun nanofibers were prepared, which were then stacked together (with parallel fiber orientation). A fibrin hydrogel was cast around the PCL frames to create a 3D hydrogel system with embedded 2D topographical cues. Schwann cells grown in this system were effectively oriented when they were in contact with the 2D topographical cues provided by the nanofibers, but the cells failed to orient when they were "suspended" in the hydrogel without the presence of the nanofibers. The incorporation of spatial patterns on hydrogel surfaces therefore allows the manipulation of cellular behaviors in diverse ways, and this could have important ramifications for the therapeutic efficacy of hydrogel-based regenerative medicine. Novel approaches also aim to include temporal control over spatial patterns. for example Liu et al. reported on a method for reversible expression of topographical cues by exploiting the thermal responsiveness of poly *N*-isopropylacrylamide (PNIPAAm) [19].

2.1.2. Hydrogels as surface modifiers

Due to the high resemblance of hydrogels to natural ECM and their amenability of customization by incorporating spatial characteristics, hydrogels have been widely used as surface modifiers for various implantable devices [20,21], such as orthopedic implants [22], load-bearing scaffolds [23,24], and biosensors [25]. Antimicrobial activity is desirable for all implantable devices as it reduces the risk of implant-associated infections. However, the specific required properties of hydrogels for each device type are different. For instance, orthopedic implants or load-bearing scaffolds may require a hydrogel coating that modulates the immunological response by diminishing the inflammation and thereby increasing the chance of integration within the body [26]. In the case of implantable sensors, the aim of using hydrogel coatings is to avoid the formation of a fibrous tissue capsule due to the foreign body reaction (FBR), which would act as a barrier between the sensor and the biological environment [25].

Fig. 2 summarizes some representative examples of the use of hydrogel coatings for different implantable devices. Fig. 2a shows two samples of polypropylene surgical meshes for hernia repair, with and without a coating of pig skin-derived ECM hydrogels. Histological results showed a reduced number of foreign body giant cells in the coated samples compared to the control by day 35 [27]. Faulk et al. [23] and Wolf et al. [26] further explored and characterized the same system in terms of macrophage polarization and chronic inflammation, revealing promising results for hydrogel coatings as (artificial) ECM materials for implantable surgical meshes for hernia repair. Fig. 2b illustrates an example of hydrogel coating for implantable sensors [28]. Brain silicon microelectrodes were coated with alginate hydrogels with two different thicknesses and were implanted into rat brains. The microelectrodes with a 400-μm-thick hydrogel coating layer significantly lowered the FBR as compared to the thin-coated and uncoated sensors after 4 months of implantation, because the thick hydrogel layer temporarily could deactivate pro-inflammatory cues within the hydrogel matrix, thus resulting in delayed FBR process. Immunoreactivity was assessed by immunostaining the samples with markers specific for microglial macrophages (CD68 and IBA-1) (Fig. 2b).

Besides the confirmed effectiveness of anti-fouling hydrogels to mitigate the FBRs [29], these hydrogels have also been suggested to confer antimicrobial properties of rubber surfaces for catheters. Fig. 2c shows a rubber piece coated with a poly(ethylene glycol)-based hydrogel chemically engineered with polycarbonate that contain quaternary ammonium groups for antimicrobial and antifouling properties. These hydrogels demonstrated a broad antimicrobial spectrum and highly efficient anti-fouling activity, which resulted in no retaining bacteria on the coated rubber surface [20].

Hydrogels appear to be one of the most widely used biomaterials to improve the surface functionality and favor the biointegration of implants. However, engineering of surface coatings is still an evolving area, and some important challenges remained to be addressed. Coatings need to be customized, depending on the intended application. In surgical implants, coatings can be an important resource to lower inflammatory responses, enhance or accelerate integration, or decrease the risk of infections. These applications will need new material design and fine tune of hydrogel properties, which will demand the incorporation of additional chemical and physical cues. They should be stable with the physiological environments for sufficient time to accomplish their intended purpose, but not overly long to avoid fibrous capsule formation. All of these requirements impose stringent demands of new and smart materials, suitable for conventional microfabrication platforms.

2.2. Microfabrication of hydrogels

Many microfabrication techniques are ideally suited to confer an architecture or functionality to hydrogels. Here, we introduce

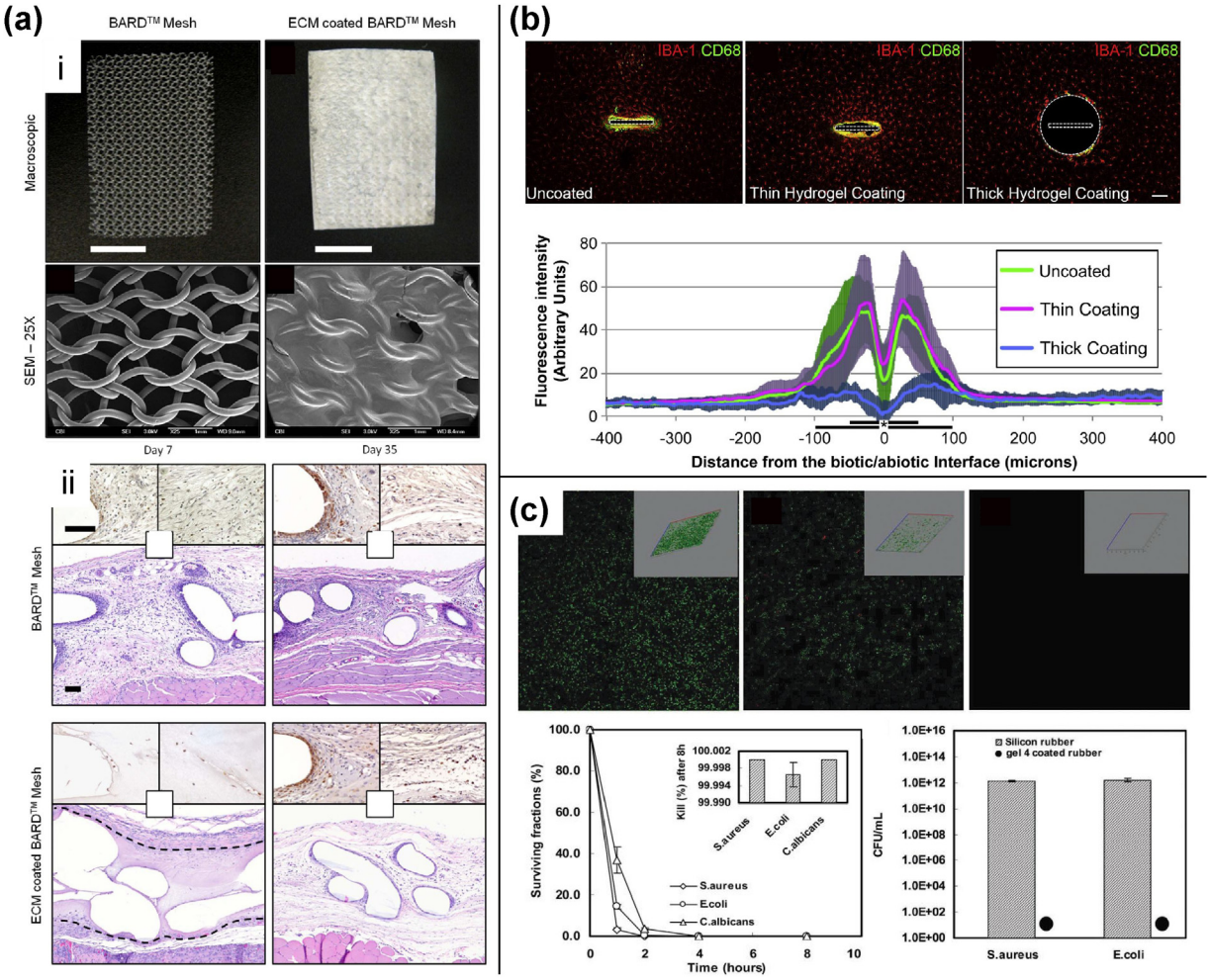

Fig. 2. Hydrogels as surface modifiers. (a) (i) Commercial meshes for hernia repair coated with and without hydrogel layer and (ii) histology images of meshes implanted in rat abdominal regions after 7 and 35 days. (b) Microelectrodes (uncoated or coated with different thickness of alginate hydrogel) implanted into rat brains. Immunostained samples (for CD68 and IBA-1 macrophages) reveal the effect of the hydrogel coating on the immunoreactivity. (c) Antimicrobial and antifouling activity of silicon rubber coated with polycarbonate/PEF hydrogel.
Reproduced with permission from: (a) Ref. [27], (b) Ref. [28], (c) Ref. [20].

examples of the hydrogel microfabrication techniques that are commonly used in the context of tissue engineering applications.

2.2.1. Replica micromolding

Replica micromolding is a facile, reproducible, cost-effective, and intuitive microfabrication technique. It is based on the use of a mold, into which a prepolymer solution is dispensed and later solidified to adopt the shape of the mold. Pioneering work on the replica micromolding technique by different groups have confirmed the versatility of micromolding for casting different hydrogel geometries [30–34].

Polydimethylsiloxane (PDMS) is a commonly used material for the fabrication of micromolds for several reasons including ease of use, tunable mechanical strength and elasticity, transparency, biocompatibility, and high fidelity of copied micro- and nanostructural features [35]. As the PDMS surface is naturally hydrophobic, it facilitates the easy unmolding/detachment of the cast hydrogels. Other materials, such as poly(methylmethacrylate) (PMMA), silicon, PTFE, glass, and metals are also frequently used to produce micromolds, although this often requires a surface functionalization process [36,37]. Recently, the use of 3D printing has significantly expanded the capabilities and flexibility of fabricating complex master molds [38,39]. To crosslink the hydrogels in micromolds, different techniques have been demonstrated including the use of light (most commonly UV light), heat, and chemicals [31,34,40].

Replica micromolding is arguably the simplest microfabrication technique for hydrogels, and yet remarkably flexible and powerful. For example, the use of multiple positive and negative replica molds expands the possibilities of the technique and allows the replication of the superficial features and volumetric shapes of practically any object. Gelatin has been widely used as a sacrificial molding material [41,42]. After crosslinking of the prepolymer solution, the gelatin molding can be sacrificed by heating the mold to above 37 °C. For example, Zhao et al. used gelatin as the sacrificial material to cast channels within microfluidic devices made from silk fibroin-based hydrogels [42]. Other sacrificial materials including sugars and proteins have been demonstrated [38]. Hosseini et al. generated grooved patterns in gelatin methacryloyl (GelMA) hydrogels using nylon fibers as the sacrificial template [43]. Nylon or metal fibers were arranged into planar arrays or wrapped onto cylindrical or planar surfaces, and then submerged into a PDMS prepolymer to make a mold. After curing, the fiber patterns were transferred to poly(ethylene glycol) diacrylate (PEGDA) or GelMA hydrogel to form the grooved patterns. The patterned hydrogels led to the improved alignment of C2C12 myoblasts as compared to conventional channel-ridge patterns. Similarly, hydrogels micromolded with channel-ridge

patterns were used for *in vitro* culture of cardiomyocytes, which can promote cell attachment and proliferation, as well as enhance cell alignment within the channels of the hydrogels compared to non-patterned hydrogel substrates [44].

At present, replica micromolding and other micromolding techniques continue to find relevant therapeutic applications. Rios et al. successfully used a simple micromolding technique to fabricate hydrogel devices that encapsulated islets for the restoration of normal glycemic levels in diabetic mice [45]. A GelMA hydrogel construct fabricated by casting in a PTFE mold was recently used for controlled release applications using an *in vivo* mouse model [37]. In addition, replica micromolding has become a standard technique to create low-attachment microwell arrays to generate cellular spheroids and micro-organoids, which can be used to drive bottom-up tissue engineering, to control stem cell behavior, and to improve drug screening [46–50].

2.2.2. Photo-patterning

Photo-patterning has rapidly evolved into a very powerful and flexible tool with many reported variations. Photo-patterning refers to the use of lights to form patterns using photocrosslinkable hydrogels. In its simplest version, the surface of the material is covered with a photomask containing a predesigned pattern, which locally shields the material from light exposure and subsequent chemical modification of a photosensitive material. The work by Bryant et al. represents an example of photo-micropatterning of crosslinkable hydrogels [51]. The authors used a photomask with microscale circular opaque islands to pattern circular pores onto the surface of photocrosslinkable PHEMA hydrogels (Fig. 3a). In addition to this, the photo-patterning of chemical signals has represented an important step forward to selectively endow (or activate) chemical cues in specific regions of a hydrogel construct with precise spatial control. Gramlich et al. used a norbornene-functionalized HA (NorHA) and the click photoreaction with dithiols to photo-pattern hydrogels (Fig. 3b) [52]. The use of masks with specific patterns enabled the functionalization of specific regions of the hydrogels by exposure to light. The control of the spatial distribution of the dithiol groups allowed the selective induction of secondary reactions.

New laser illumination techniques developed in the last decade have provided new and more precise ways to fabricate 3D microstructures within hydrogels. One of these systems, based on the phenomenon of two-photon absorption, has enabled direct "writing" of micropatterns with nanoscale precision [53]. Two-photon hydrogel polymerization (2PP) platforms use a femtosecond laser source. The intensity of the laser beam is highly regulated and therefore allows for printing within cell-laden hydrogel matrices through the precisely localized excitation of photoinitiator molecules. This polymerization technique enables a uniquely high resolution of 3D patterning (Fig. 3c) [54]. In addition, obtaining complex architectures including perfusable microvessel structures is feasible once proper computer-aided design files are produced [55–57]. However, the potential to produce complex micropatterns at remarkable resolutions comes at the price of low fabrication speed. When fabricating larger constructs, a single structure could take hours to days to complete, thus limiting the practical applications of 2PP for large-scale endeavors towards cell-laden constructs.

A further aspiration in the field is to employ photo-patterning for spatial and temporal applications. Many biomedical applications would benefit from temporal matrix remodeling or temporally controlled release. Such strategies would allow the temporal evolution of cell microenvironments within hydrogels, opening up avenues for the temporal manipulation of cellular processes, which will be described in Section 3.

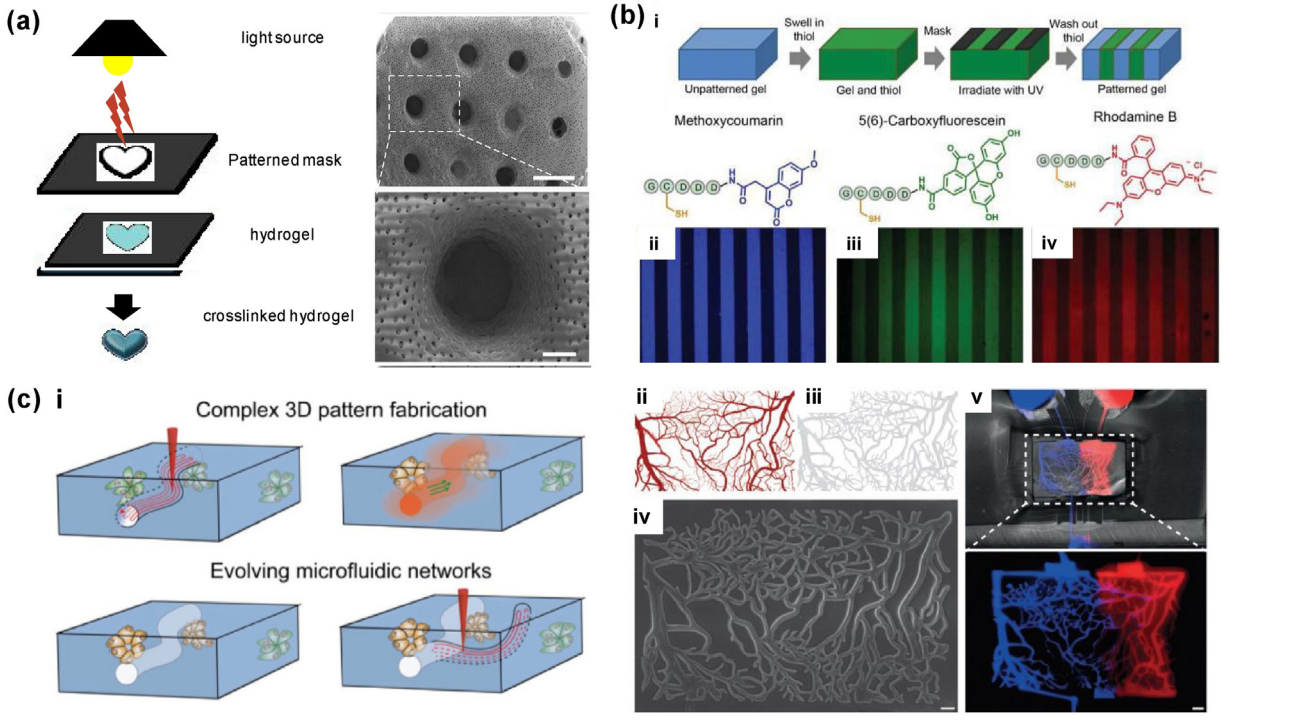

Fig. 3. Photo-pattering of hydrogels. (a) Schematic representation of a simple photo-pattering process using a photo-mask and photo-patterned pores (62 μm) in porous pHEMA hydrogels. (b) Chemical pattering of hydrogels. (i) Schematic of process to photo-patterned NorHA gels with thiol-containing molecules. (ii–iv) Chemical structures of fluorescent-dye-terminated peptides with confocal images of photo-patterned NorHA gels with different dyes. (c) (i) Schematic of a fully controlled mask-less laser system that enabled the microfabrication of convoluted microfluidic channels within hydrogels. (ii, iii) Photograph of a capillary-bed photograph and mask showing the complexity of the fabricated networks. (iv) Resulting microfluidic capillary network. (v) Connected and perfused network using two different fluorescent molecules (Scale bars, 100 μm). Reproduced with permission from: (a) Ref. [51], (b) Ref. [52], (c) Ref. [54].

2.2.3. Microfluidics-assisted fabrication

The term microfluidics refers to a set of scientific/technological disciplines and resources that enable the manipulation of small volumes of fluid (or small flow rates) through narrow channels or small spaces [58]. Microfabrication is one of the many relevant applications of microfluidics; indeed, microfluidics-assisted fabrication has been previously reviewed [59].

Microfluidics has expanded our toolset for engineering the geometry, composition, and functionality of hydrogel constructs. Microfluidic systems are particularly pertinent for engineering hydrogels for a number of reasons including their intrinsic capacity to produce flow alignment. Hydrogels are typically prepared from viscous liquids that can be dispensed, dosed, or extruded through microfluidic systems. The laminar flow that prevails in microfluidic systems is a powerful tool for microfabrication. In addition, the small size of microfluidic systems enables a tight control of relevant fabrication conditions, such as heat transfer rates, mass transfer rates, surface tension, and chemical microenvironments.

The use of microfluidic systems has been widely exploited for the microfabrication of hydrogel structures. Microfluidic platforms have been used to microfabricate hydrogel spheres with well-defined diameters, architectures, and chemical compositions [60–64], as well as fibers of a particular architecture including hollow fibers and gradients within hydrogels [65]. Numerous studies have demonstrated the generation of cell-laden hydrogel microparticles using microfluidic devices [64]. Recent innovations even allowed for microfluidic encapsulation of individual cells in microgels that are only marginally larger than the cell they contain [66]. Spatial placement of the cell in these microgels is of high importance to prevent cell egression; it has been reported that delayed on-chip gelation places cells in the microgel's center, which enables long-term culture [67]. Frequently, hydrophilic hydrogel precursor solutions are co-flown with a hydrophobic liquid, such as oils in a microfluidic channel to generate microdroplets of liquid hydrogel precursor. These microdroplets are subsequently crosslinked within the microfluidic channels or at the outlet by exposure to a crosslinking agent, such as light, heat, chemical reagent, or enzyme that is added downstream. These microfluidic channel systems provide a level of process control that is far superior to those achievable in traditional synthesis methods. Almost perfectly spherical hydrogel microparticles of a precise diameter, and with a very narrow particle size distribution, can be generated in a facile manner using microfluidic methods. Manipulation of operative parameters, such as the nature of the hydrophobic phase, hydrogel precursor solution, hydrophobic/hydrophilic ratio, flow rate, chemical environment within the channel, and the diameter of the microfluidic channel, allow tight control of shape, diameter, and functionality of the generated microparticles [68].

Microfluidic systems allow for the straightforward tailoring of well-defined physical and chemical microenvironments for cell proliferation, function, or differentiation. Each hydrogel particle can be viewed as an individual tissue micro-niche, *i.e.*, a well-defined cell microenvironment, where the chemical and physical properties can be controlled by dosing chemical and physical cues in the precursor solution. As an example, the fabrication of PEGDA/heparin hydrogel microspheres for the high-throughput encapsulation of mouse embryonic stem cell (ESCs) has been explored, which demonstrated the rapid formation of embryonic spheroids with enhanced differentiation [61]. Specifically, a simple microfluidic device was used to co-inject the PEGDA precursors, methacrylated heparin and 8-arm PEG-thiol to produce cell-laden spheroids containing appropriate chemical microenvironments for the proliferation of ESCs and to guide their endodermic differentiation.

Fibers are ubiquitous in natural tissues. Neurons, muscle fibers, and tendons are only some of the many examples of fibrous tissue units in the human body. The fabrication of hydrogel fibers with predefined architectures is therefore of great interest to tissue engineers. Microfluidic platforms have found an important niche in this field, as microfluidic systems behave like microfiber extruders. The fiber-shaped hydrogels could be utilized as woven tissue textiles, which will be covered in Section 2.2.5.

2.2.4. Self-assembly

Microfabrication techniques based on micromolding, photopatterning, and microfluidics enable the construction of the micro-building blocks of tissue constructs, such as cell-laden hydrogel particles, fibers, or mini-constructs of any shape [69]. To engineer micro-tissues, the next level of fabrication is needed, which is capable of organizing the micro-building blocks coherently and rationally into a tissue-like assembly. Here, we will highlight the bio-inspired self-assembly-based strategy for fabricating micro-tissue constructs that can augment the field of tissue engineering.

Self-assembly is a widely studied natural phenomenon. Nature has evolved to use self-assembly to produce complex structures from simple building blocks in an efficient manner. The very basic concepts of self-assembly from nature have been imported to organize microgels and engineer macroscopic hydrogel structures including shape complementarity, chemical affinity, and physical attraction (or repulsion) [70]. In these cases, a driving force is needed to bring equivalent units into proximity and overcome the entropy loss (negative ΔS) of self-assembly. In the context of hydrogels, self-assembly has been induced using magnetic, acoustic, mechanical, capillary forces, surface tension, or polarity (the hydrophobic interactions) [71–73]. Chemical affinity and chemical reactions have also been used in self-assembly [74–77]. Zamanian et al. utilized surface tension and polarity to self-assemble cell-laden microgels [71]. Cell-laden microgels (*i.e.*, cubes of $\approx$1000 μm^3) were placed randomly on top of the surface of a high-density hydrophobic liquid (*i.e.* carbon tetrachloride or perfluorodecalin) and self-assembled to form aggregates of microgels. In this case, surface tension was the driving force for the self-assembly. The system could find a state with reduced free energy. The microgel aggregates could be consolidated *via* a secondary, light-triggered crosslinking step. Similarly, floating microgels with complementary shapes (*e.g.* lock-and-key structures) can promote self-assembly [73], which can be accelerated by mechanical means (*i.e.* simple agitation or vibration induced by acoustic waves). Recently, Chen et al. used standing waves at a liquid surface as a template to self-assemble different materials including cell-laden spheroidal hydrogels. The authors confirmed that numerical finite simulations on the drift of energy field could closely predict the self-assembled structures that were experimentally created [78]. The structures can be dynamically rearranged, in timeframes of seconds, by simply changing the operating parameters of the wave generator (*i.e.* frequency and amplitude). In addition, this strategy is scalable; structures of 100 mm^2 to 10,000 mm^2 could be consolidated using a secondary crosslinking step.

The complementarity between DNA chains is a powerful way to induce self-assembly between microgels [75,77,79,80] and even between cells [81]. Qi et al. demonstrated the self-assembly of cell-laden hydrogel blocks by functionalizing their surface with long single-strand DNA strains [79]. Cubes functionalized with complementary DNA strains were shown to preferentially bind to each other. If each hydrogel block contained different cell types, the aggregations with predesigned patterns could be used to direct 3D cell distribution, which enabled the organized building of complex multi-cellular micro-tissues with micro-resolution. Recently, Todhunter et al. published a detailed report on the use of DNA self-assembly to organize a complex micro-tissue. This technique allowed a high degree of precision, given the built-in specificity of

DNA complementary binding [77]. The self-assembly methods could potentially provide a facile way to re-organize microgels with different cell types, allowing engineered micro-tissue constructs *via* the bottom-up mechanism.

2.2.5. Textile processes for forming complex tissues

Despite the groundbreaking progress of the aforementioned techniques for spatial control of hydrogel shape, it has remained a true challenge to create large constructs with in-depth complexity at the microscale. Textile-like processing of hydrogel fibers has emerged as a powerful tool for fabrication of large 2D and pseudo-3D constructs with tunable mechanical properties, architectures, and patterns. These properties are well aligned with the expectations of ideal scaffolds for tissue engineering applications [82–85]. In addition, the similarity between textile-based fabrics and some tissues, such as muscle, tendon, and ligament, has fueled the interest for their use in tissue engineering [86]. Thus, textile technology based on weaving, braiding, and knitting has been used for the engineering of various tissue constructs [87]. Woven hydrogel fabrics can provide anisotropic mechanical properties usually with a higher mechanical strength in the planar directions. In addition, their mechanical strengths in the through-plane direction can be enhanced by interlocking multiple layers of 2D hydrogel fabrics [88,89].

Interlocking fibers into ordered arrangement of connected loops can generate knitted constructs, which have higher through-plane strength and flexibility. Such constructs have been explored for the engineering of tendon and ligaments tissue constructs [88]. Knitted scaffolds coated with hydroxyapatite have been utilized for engineering bone tissue and have shown excellent osteoconductivity [90]. Braided scaffolds formed from intertwined fibers offer the highest construct density and axial mechanical strength in comparison to those fabricated using other textile techniques. Thus, braided hydrogel constructs can be excellent candidates for engineering tissues with high axial strengths, such as tendons and ligaments [90].

The majority of the textile-based scaffolds have been generated from acellular polymeric fibers as the fabrication process exerts significant mechanical stress, which cannot be tolerated by hydrogels that are commonly used for cell encapsulation [87,91]. In addition, harsh solvent exposure of fibers during the fabrication process is another technological barrier for cell-encapsulated

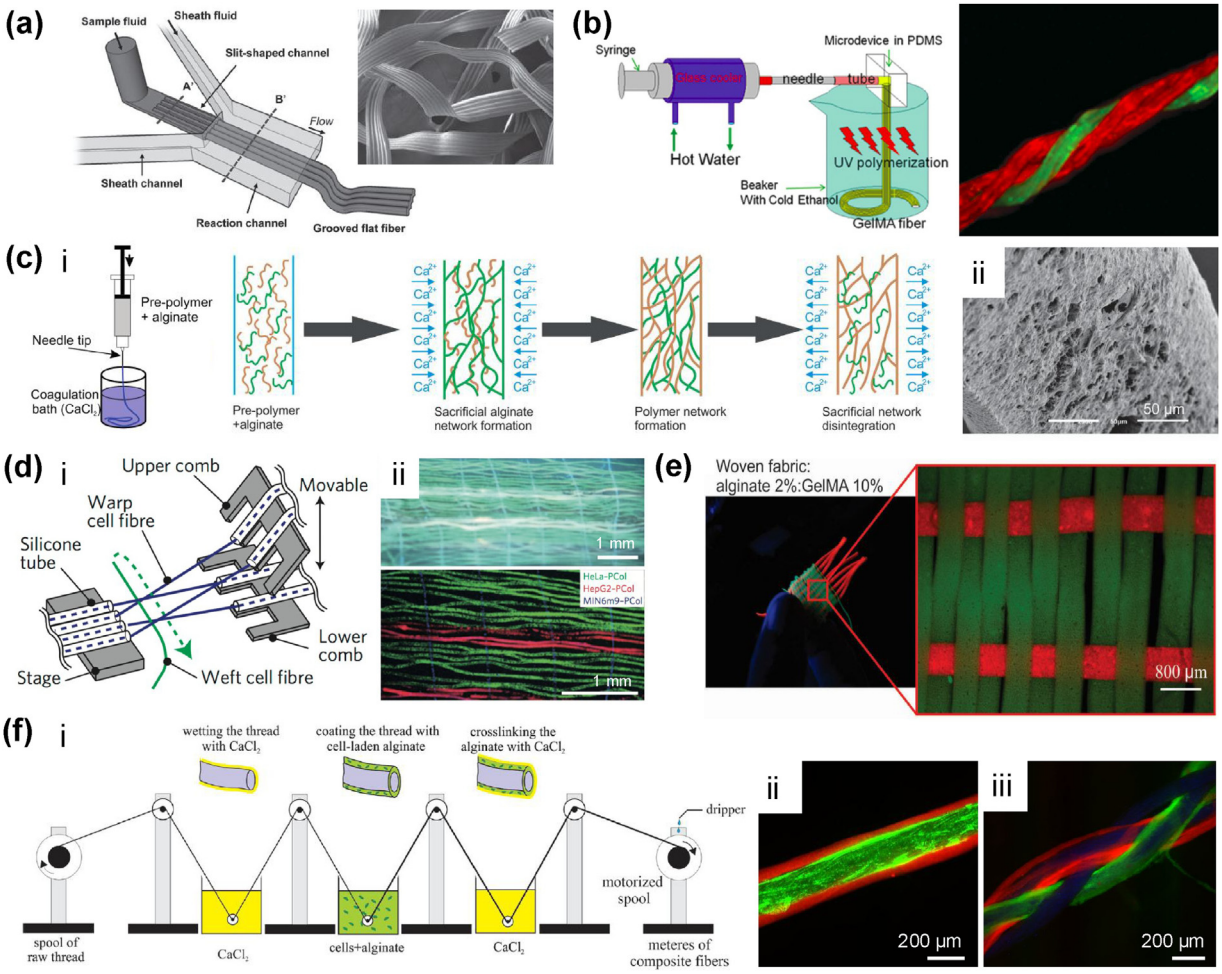

Fig. 4. Various platforms for the engineering of cell-laden fibers and constructs. (a) Fabrication of flat alginate fibers using microfluidic systems. (b) Fabrication of GelMA fibers by injecting GelMA precursor into cold bath of ethanol followed by UV irradiation. The fibers were mechanically stable and multiple fibers could be twisted together. (c) The use of sacrificial templates for engineering hydrogels fibers from different polymers. (i) Schematic of fiber fabrication platform and the fiber formation process. (ii) Typical fabricated GelMA hydrogel fiber after alginate dissociation confirming the stability of the fibers. (d) (i) A microweaving loom for fabrication of hydrogel constructs and (ii) a fabricated construct. (e) Centimeter scale hydrogel fabric engineered from hybrid alginate:GelMA hydrogels. (f) (i) Fabrication of composite fibers by coating polymeric fibers with a layer of cell-laden hydrogel. (ii) A typical composite fiber generated by coating of two distinct layers of microbead-laden hydrogel. (iii) Micrograph showing a typical braided construct from composite fibers.
Reproduced with permission from: (a) Ref. [99], (b) Ref. [103], (c) Ref. [104], (d–e) Ref. [107], (f) Ref. [109].

fibers. Therefore, significant efforts have been dedicated to the fabrication of fibers that can serve as modules for creating cell-incorporated biotextiles.

In the past decade, fibers have been fabricated from a variety of natural polymer-based hydrogels that could carry cells [92–96]. The main methods used for fabrication of cell-laden fibers include wet-spinning, microfluidic spinning, and interfacial complexation [86]. In the case of wet-spinning, the prepolymer is injected into a reservoir containing compounds and the formation of stable fibers requires a rapid crosslinking rate of the prepolymers to limit the undesired diffusion into the surrounding solution. To this end, alginate has been frequently used for the fabrication of cell-laden fibers through wet-spinning, as alginate can be rapidly crosslinked by divalent ions, such as Ca^{2+} to form biocompatible physical hydrogels [89].

Microfluidic-based wet-spinning has a similar crosslinking process with a major difference as the precursor and crosslinker are flown co-axially through a microchannel [97–99]. Both methods have been widely used for the fabrication of cellular and acellular fibers. The use of sophisticated microfluidic systems has enabled the formation of fibers with multiple compartments and materials [99–101]. In addition, the surface topography of the fibers and their shape can be tuned through the use of non-circular nozzles (Fig. 4a) [102]. Although the majority of the cell-laden fibers fabricated using this technique have been limited to alginate-based materials, recent methods have been proposed for fabrication of fibers from other hydrogels with a slower crosslinking rate. In one example, GelMA hydrogel prepolymer solution was injected into a low-temperature solution to induce rapid thermally induced gelation, after which the solidified fibers were photocrosslinked to form stable constructs (Fig. 4b) [99,103]. However, this method suffered from significant dispersion of the hydrogel stream into the cold aqueous solution, resulting in poor controllability of the composition of the final fibers. To challenge this, sacrificial polymeric templates were introduced to assist in generating fibers (Fig. 4c) [103]. In this method, the target polymer was mixed with alginate and then injected into a $CaCl_2$ crosslinking solution. The alginate component was crosslinked to physically entrap the polymer chains. A secondary crosslinking process was carried out to form an interpenetrating polymer network (IPN) hydrogel. Alginate was then dissolved by a calcium-chelating agent to leave behind a stable fiber composed of the targeting polymer. Interfacial complexation is another fabrication method that has been widely used to produce cell-laden fibers [104]. In this method, two solutions with strong interaction (mostly electrostatic) will be interfaced and crosslinked. The interface layer is pulled using a needle to form stable fibers. However, controlling the fiber dimension and morphology using interfacial complexation needs to be improved.

Cell-laden hydrogel fibers are typically fragile and their assembly using textile processes is not trivial. However, a few reports have managed to fabricate cell-laden hydrogel fibers and assemble them using textile processes [105,106]. A microweaving loom was designed to reduce the exerted mechanical forces during the weaving process (Fig. 4d) [104,107]. However, the density of the generated fabric and the resolution of woven patterns were limited. As an another approach, IPN hydrogel fibers were generated with higher mechanical strength and were assembled using manual miniaturized weaving looms and also were braided into centimeter-scale fabrics (Fig. 4e) [107]. The resolution of the generated constructs was comparable to commercial conventional textile platforms for fabrics. Although the engineered hydrogel fabrics did offer anisotropic mechanical properties, their strength was still significantly lower than those observed in native tissues.

Since the successful implantation, integration, and function of engineered constructs rely on mimicking the tissue-level mechanical properties, tremendous effort has been dedicated to the fabrication of composite constructs. Many researchers have used textiles as reinforcing mats to strengthen cell-laden hydrogels [104]. Specifically, the hydrogel provides a nurturing environment for cellular growth, while the fabric provides the mechanical support and ensures the physical stability of the construct. However, controlling both the mechanical properties and the cellular distribution at the same time had remained elusive. A potential solution was coating mechanically strong core fibers with a layer of cell-laden hydrogels [88,108]. It was shown that the mechanical properties of braided constructs could be tuned by three orders of magnitude while the cellular pattern could be preserved in the 3D environment (Fig. 4f) [109]. As such, this technology is uniquely suited to simultaneously control the spatial mechanical properties and the cellular distribution of engineered tissue constructs. Composite fibers have been assembled using manual weaving looms and have been knitted similar to regular threads. However, there were still key challenges associated with these composite fibers including the detachment of the hydrogel layer from the core fiber.

Overall, biotextiles have emerged as a powerful tool for the engineering spatially organized tissue constructs with clinically relevant dimensions. Hydrogel fibers have been widely used as acellular scaffolds and through the recent advancements in the fabrication of cell-laden fibers as miniaturized textile platforms to engineer tissue constructs. A key advantage of the textile processes is their ability in mimicking the tissue-level and cell-level properties independently. This unique feature distinguishes the textile-based technology from all other microfabrication technologies. However, there are several challenges to be resolved to enable their practical translation. The resolution of the textile processes has remained poor and requires improvement. Moreover, the current potential applications of this technology have been limited to the engineering of fibrous tissues.

2.3. Patterning biomaterials using 3D bioprinting

Although conventional biofabrication strategies as discussed in previous sections have enabled convenient patterning and spatial control of biomaterials, they generally suffer from a limited versatility and at times an inability to produce 3D sophisticated structures of macroscale shapes. Recently, 3D bioprinting technologies have provided effective alternatives to pattern biomaterials with high complexity in a volumetric space with high precision, by combining material dispensing or crosslinking with motorized operations. In this section, we will illustrate the recent advances in 3D bioprinting and discuss its applications in shaping biomaterials at the macroscale.

2.3.1. Common bioprinting modalities

Stereolithography is one of the first 3D printing modalities and was initially proposed by Hull in 1986 [110]. In this strategy, a reservoir is filled with the precursor solution of a UV-curable material, which is then crosslinked in a layer-by-layer approach. After the printing of each individual layer, the printed structure is moved away from the light source in the z-direction by a motorized stage to create space for the next print layer (Fig. 5a) [111,112]. While stereolithography was conventionally used for printing resins, it has been adopted in the fabrication of biomaterials, such as hydrogels made from PEGDA and GelMA prepolymers [113–116]. More recently, the pattern projection method has also seen a major improvement by switching the traditional reflection of digital masks with a planar digital micromirror device (DMD). The DMD, unlike a single piece of mirror, is composed of a mechanically adjustable array of thousands to millions of mirrors. By digitally adjusting each mirror, a desired pattern can be created in an

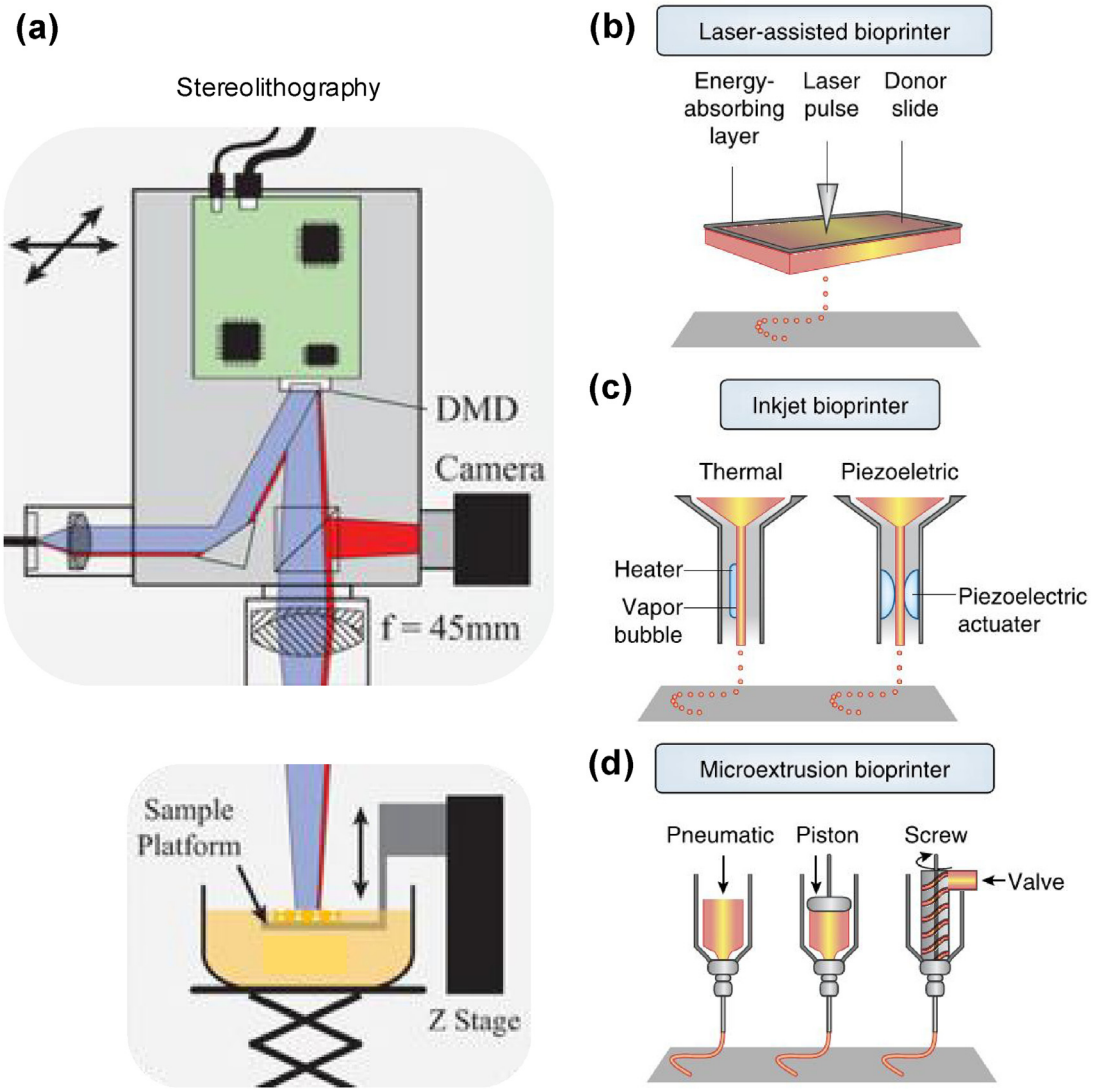

Fig. 5. Common bioprinting modalities. Schematics showing (a) stereolithography/DMD bioprinting, (b) laser-assisted bioprinting, (c) inkjet bioprinting, and (d) microextrusion bioprinting.
Reproduced with permission from: (a) Ref. [111] and (b–d) Ref. [112].

ultrafast manner, thus allowing for dynamic projection of patterns with a higher speed and versatility [113,115,117].

The Laser-assisted forward transfer is another modality featuring high-speed bioprinting [118–120]. In this setup, an energy-absorbing substrate carrying a thin layer of bioink at the bottom side is irradiated by a laser source in a defined pattern. Upon absorbing the laser power, the localized heating of the substrate generates air bubbles that induce the forward transfer of the bioink in droplets to the collecting plate to form the pattern (Fig. 5b). However, the choice over bioinks suitable for bioprinting has remained limited due to their specific requirements *e.g.* proper viscosity and crosslinking mechanisms [121–125].

Among the different bioprinting methods, nozzle-based bioprinting techniques have attracted increasing attention due to their relatively low cost, convenient setup, and their compatibility with a wide range of bioinks [121–126]. Nozzle-based bioprinting modalities can be generally divided into two categories, inkjet bioprinting, and microextrusion bioprinting. Inkjet bioprinting utilizes nozzles actuated by either heating or piezoelectricity to break the bioink stream into discrete droplets, and a stage motorized with programmed movement to allow for controlled deposition of the bioink in 3D (Fig. 5c). In comparison, microextrusion bioprinters rely on pneumatic pressure or mechanical compression to drive extrusion of bioinks to realize continuous deposition of microfibers and generate 3D shapes, in conjunction with the movements of a motorized stage (Fig. 5d). While extrusion bioprinting features easy operation and high bioink compatibility, cells might experience significantly higher shear stress in the extrusion printing process than that encountered in the previously mentioned bioprinting modalities [127,128].

2.3.2. Stereolithography and DMD bioprinting

As mentioned in previous sections, stereolithography bioprinting fabricates 3D shapes in a layer-by-layer manner, and each layer is crosslinked with a projected pattern of choice. As the optically projected digital masks can achieve ultrahigh resolution, the resulting patterns of biomaterials can also inherit the high spatial precision, which is not easily attainable using other bioprinting modalities. Similar high-resolution of bioprinting could also be achieved with mask-free DMD printing coupled with a high-density array of mirrors, which possesses better flexibility in the dynamic patterning of the bioinks than the conventional mask-based methods.

To date, a variety of bioinks have proved their merits in stereolithography/DMD bioprinting including PEGDA, GelMA, poly (acrylic acid) (PAA), collagen, HA, and their blends [113–115,117,129–131]. For example, Zhang et al. directly patterned 3D microscale objects made of PEGDA into a variety of shapes, such as stepwise, spiral, embryo-like, and flower-like microstructures (Fig. 6a) [132]. Of note, these microarchitectures featured resolutions in the range of a few tens of micrometers, which reflected the uniqueness of stereolithography/DMD bioprinting. Another widely used photocrosslinkable biomaterial, GelMA, has also been fabricated using DMD bioprinting into 3D hexagonal structures (Fig. 6b) [114]. The bioprinted GelMA scaffolds showed high cytocompatibility with human umbilical vein endothelial cells (HUVEC) and were able to support the proliferation of cells across the entire volume of the scaffolds (Fig. 6c).

Hybrid biomaterials have also been used to endow bioprinted constructs with enhanced properties that are not achievable by individual components. For example, Suri and Schmidt patterned an IPN hybrid hydrogel by combining HA, a high-molecular weight glycosaminoglycan ubiquitously found in many cartilaginous tissues, and collagen, a major macromolecular component in the ECM, for use as scaffolds in engineering functional tissues [130]. Similarly, Madaghiele et al. used a mixture of PEGDA and acrylic acid for the stereolithographic fabrication of 3D hydrogel scaffolds in the presence of collagen [129]. The grafting of collagen macromolecules through the carbodiimide chemistry to the PEGDA/PAA network further increased both the bioactivity and the mechanical properties of the resulting hydrogel constructs. Despite these unique advantages of high-resolution bioprinting at fast rates, its utility is hampered by the need for large volumes of bioink in the reservoir and the limited selection over biomaterials, which requires both mechanical robustness and photocrosslinkability [122–125].

2.3.3. Shear-thinning extrusion bioprinting

Extrusion-based bioprinting has allowed for convenient deposition of bioinks. Comparing to stereolithography/DMD bioprinting, extrusion bioprinting provides a higher versatility in compatible biomaterials at the expense of reduced spatial resolution (typically in the range of a few hundred micrometers) [123–125]. Extrusion bioprinting typically requires the bioink to be self-supportive to maintain the architectural integrity of the construct upon extrusion. To this end, shear-thinning bioinks are often adopted as they exhibit a fluid-like mobility during the

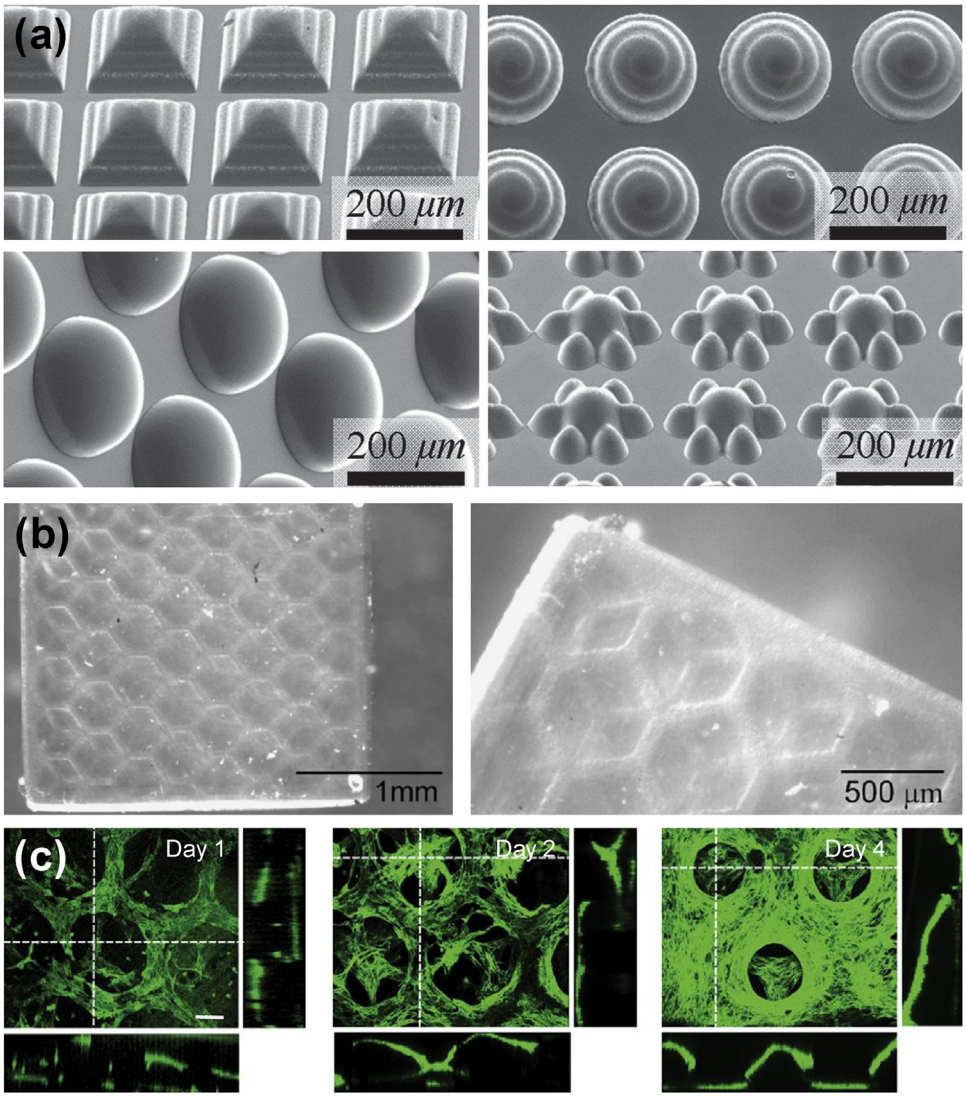

Fig. 6. Stereolithography and DMD 3D bioprinting. (a) Scanning electron microscope images showing DMD-bioprinted PEGDA microstructures. (b) Optical micrographs showing a bioprinted hexagonal GelMA scaffold. (c) Confocal micrographs showing the proliferation of HUVECs seeded in the bioprinted GelMA scaffold. Reproduced with permission from: (a) Ref. [132], (b–c) Ref. [114].

extrusion process due to external shear stress, but revert back to their gel state upon removal of the mechanical force. Poly(ethylene oxide)-poly(propylene oxide) (also known as Pluronic) aqueous solution is a typical example, which demonstrates shear-thinning characteristics at a certain concentration range. Not surprisingly, Pluronic has often been used to bioprint a variety of sacrificial constructs that can be selectively removed by dissolution, as will be further discussed in Section 2.3.4 [133–135].

Bioinks that enable proper cellular activities have also been developed for extrusion-based bioprinting. By rapidly cooling down GelMA solutions to below their gelation points in the printing nozzle, Lee et al. engineered a GelMA-based shear-thinning bioink that enabled direct extrusion. The resulting self-standing structures could then be permanently solidified *via* UV-initiated crosslinking (Fig. 7a) [136,137]. Multi-layered microfibrous structures of GelMA hydrogels could be fabricated using this bioprinting system (Fig. 7b and c). The bioprinted GelMA constructs could support the viability of embedded HepG2 hepatocellular carcinoma cells in a crosslinking density-dependent manner; higher UV exposure dose increased the crosslink density and thus resulted in reduced cell viability (Fig. 7d) [137]. In addition, under proper conditions, the encapsulated cells, such as HepG2 cells and mesenchymal stem cells (MSCs), maintained high viability within the GelMA microfibers for a culture period of over 14 days (Fig. 7e) [137]. Nevertheless, one limitation of this method was the inability to bioprint GelMA bioinks of <7% (w/v) due to the relative slow gelation kinetics of GelMA solutions of low concentrations.

Recently, a different strategy to generate shear-thinning bioinks has been proposed by Ouyang et al. (Fig. 7f) [138]. In this study, a pair of molecules with strong guest-host inteactions, namely, adamantane (Ad) and β-cyclodextrin, were separately immobilized on HA to create two hydrogel precursors. Upon mixing, these two hydrogel precursors immediately formed a supramolecular hydrogel that possessed a unique shear-thinning behavior, which allowed for direct extrusion of the hydrogel bioink into self-standing microfibrous structures. Similar with GelMA, methacrylate groups could be further engrafted to the HA precursors, which enabled a secondary UV-crosslinking step to permanently stabilize the bioprinted structures [139]. By fine-tuning the bioprinting parameters, such as the bioink concentration, extrusion rate, and nozzle moving speed, structures with reproducible fidelity could be obtained (Fig. 7g and h). Moreover, embedded fibroblasts could achieve high viability and pronounced spreading in the HA constructs functionalized with RGD peptide motifs (Fig. 7i).

The major drawback of conventional extrusion-based bioprinting lies in its inability to produce freeform objects due to the gravitational force that would deform the mechanically weak hydrogel structures. Three individual groups recently pioneered an embedded extrusion bioprinting method, which utilizes a supporting hydrogel reservoir to stabilize the extruded bioink, allowing for fabrication of self-sustained shapes with relatively complex architecture.

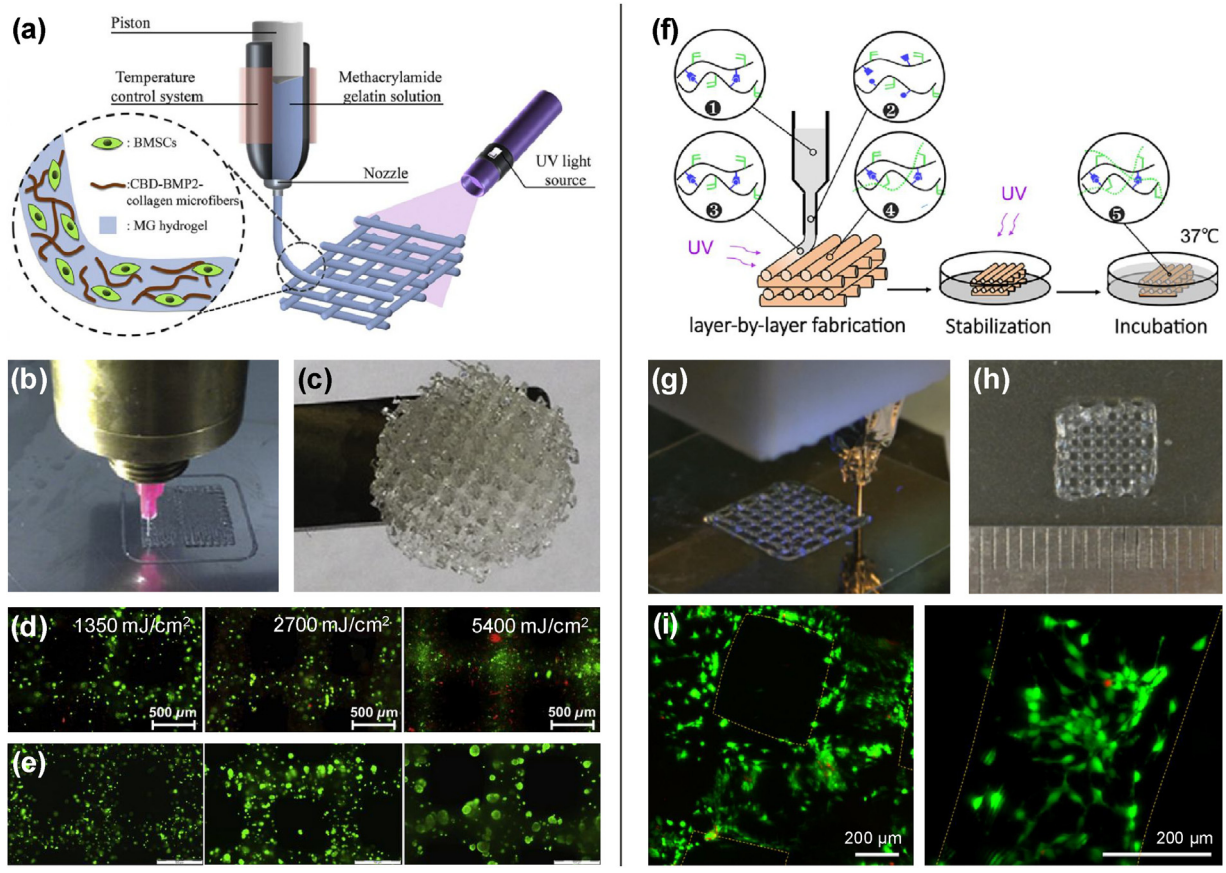

Fig. 7. Nozzle-based 3D bioprinting. (a) Schematic showing the bioprinting process of locally cooled GelMA bioink and the subsequent secondary photocrosslinking. (b, c) Photographs showing the bioprinting process and a bioprinted GelMA scaffold, respectively. (d) Cell viability analysis at different UV crosslinking density; green: live, red: dead. (e) Viability of encapsulated HepG2 cells at Days 1, 7, and 14 post bioprinting. (f) Schematic showing the bioprinting process of the shear-thinning HA-based bioink and the subsequent secondary photocrosslinking. (g, h) Photographs showing the bioprinting process and a bioprinted HA-based scaffold, respectively. (i) Viability and spreading of fibroblasts encapsulated in the bioprinted construct at Day 5.
Reproduced with permission from: (a–e) Ref. [136,137] (f–i) Ref. [138].

During the embedded bioprinting procedure, the extruded bioink forms microfibrous structures that are suspended within the hydrogel matrix. As the nozzle moves through the supporting bath, the supporting hydrogel reservoir automatically heals and interlocks with the macromolecules in the bioink to stabilize the printed shape (Fig. 8a). The unique gravity counteracting the properties provided by embedded bioprinting allow for the first time the direct fabrication of 3D freeform shapes without any structural collapse (Fig. 8b). A secondary photocrosslinking capability might also be incorporated into either the bioink or the supporting matrix, leading to permanently stabilized freeform structures or freeform microchannel structures, respectively [140].

In addition to supramolecular hydrogels, granular gels could also be adopted for use as the supporting matrix due to their shear-thinning and self-healing properties [141,142]. For example, Bhattacharjee et al. used aqueous Carbopol ETD 2020 or oil-based Dow Corning 9041 silicone elastomer blend granular gels as the supporting matrix, where a variety of bioinks including polystyrene microsphere suspension, polyvinyl alcohol, and PDMS were used to print freeform structures of different types (Fig. 8c) [141]. Complex macroscale shapes, such as continuous hollow knots (Fig. 8d) that were unattainable from conventional extrusion bioprinting techniques could be readily achieved. In a parallel work, Hinton et al. utilized gelatin slurry as the support bath to build 3D freeform objects with extrusion bioprinting from an alginate bioink, where a variety of different freeform architectures from simple spirals (Fig. 8e) to dual-layered blood vessels and organ-mimicking volumetric patterns were successfully obtained (Fig. 8f) [142].

2.3.4. Sacrificial bioprinting

Direct bioprinting of sacrificial bioinks provides a unique way to fabricate spatially complex structures that can be subsequently transformed into hollow channels on temporal demand. Particularly, this might be useful for the fabrication of a vascular networks within an engineered tissue construct. In this strategy, a fugitive bioink is first deposited in a desired pattern followed by casting of a hydrogel matrix that surrounds the template structures. Afterward, the bioink is selectively removed to leave a hydrogel block with interconnected microchannels. Compared to the conventional vascularization strategy, sacrificial bioprinting allows for unprecedented flexibility over the size, shape, and pattern of the generated vasculature, which can be conveniently tuned to match the needs of the target tissues.

In an early report, Bertassoni et al. explored agarose solutions as a sacrificial bioink, which formed a robust hydrogel at room

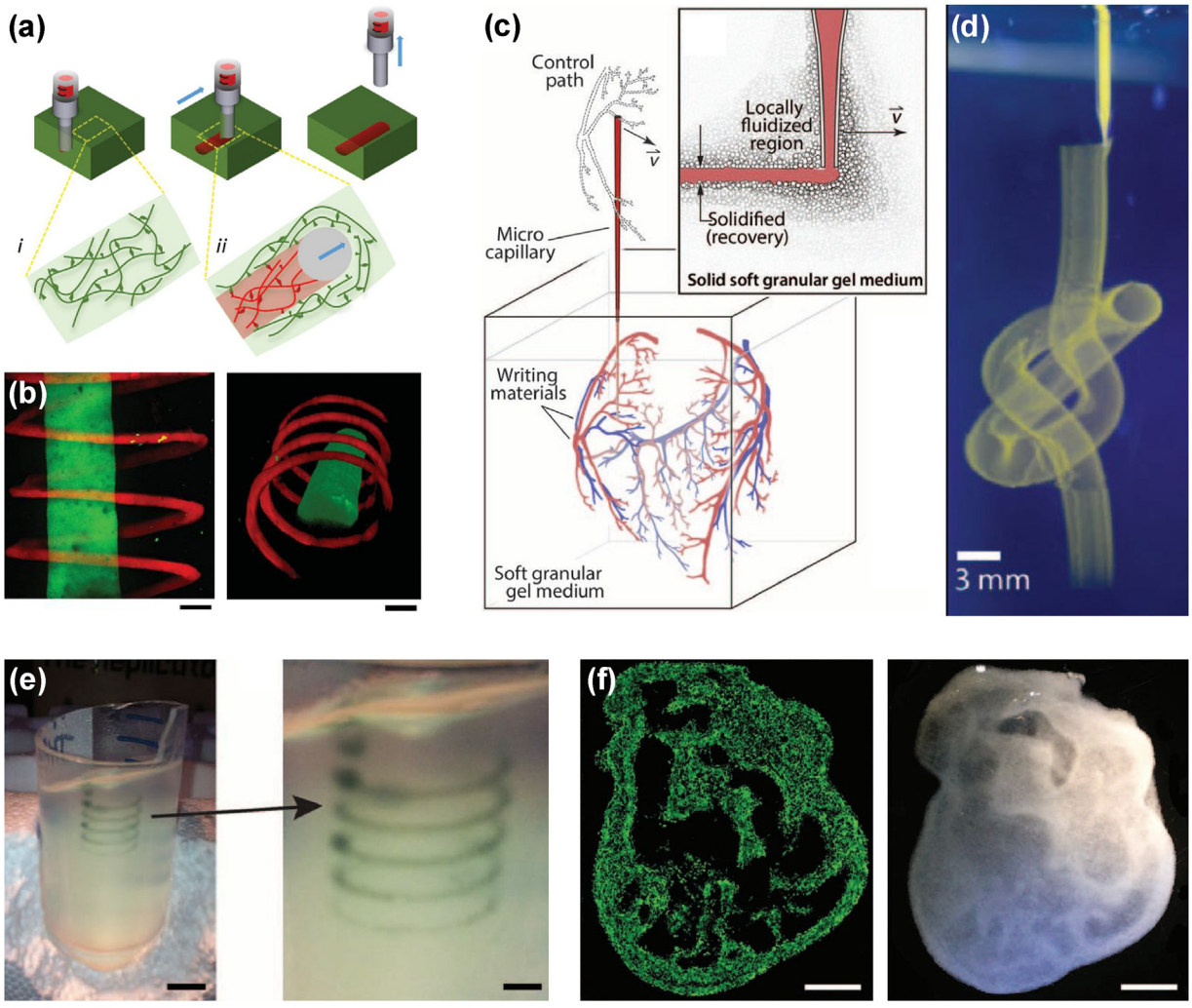

Fig. 8. Embedded extrusion bioprinting (a) Schematic showing the process of directly bioprinting a shear-thinning bioink into a self-healing hydrogel matrix. (b) Confocal reconstruction images showing the bioprinted freeform patterns. (c) Schematic showing the bioprinting of the bioink into a soft granular shear-thinning gel medium. (d) Photograph showing a bioprinted knitted hollow knob. (e, f) Photographs showing bioprinted spiral and heart-like structures.
Reproduced with permission from: (a–b) Ref. [140], (c–d) Ref. [141], (e–f) Ref. [142].

temperature or lower [143]. The deposited agarose microfibers could be efficiently extracted manually, affording interconnected hollow channels inside the surrounding hydrogel constructs (Fig. 9a). In this way, GelMA constructs containing various branching structures can be created (Fig. 9b). Importantly, cells encapsulated within these prevascularized constructs showed higher viability than those in bulk GelMA constructs of similar dimensions without any microchannels. The difference in cell survival rates was attributed to the enhanced oxygen and nutrient diffusion as provided by the internal hollow network. While agarose microfibers can be physically extracted, the ability to fabricate complex hollow structures using this strategy still poses a challenge. To this end, fugitive bioinks featuring convenient removal have been developed by different research groups. For example, Lewis and co-workers reported a Pluronic bioink, which could form a shear-thinning hydrogel at room temperature but

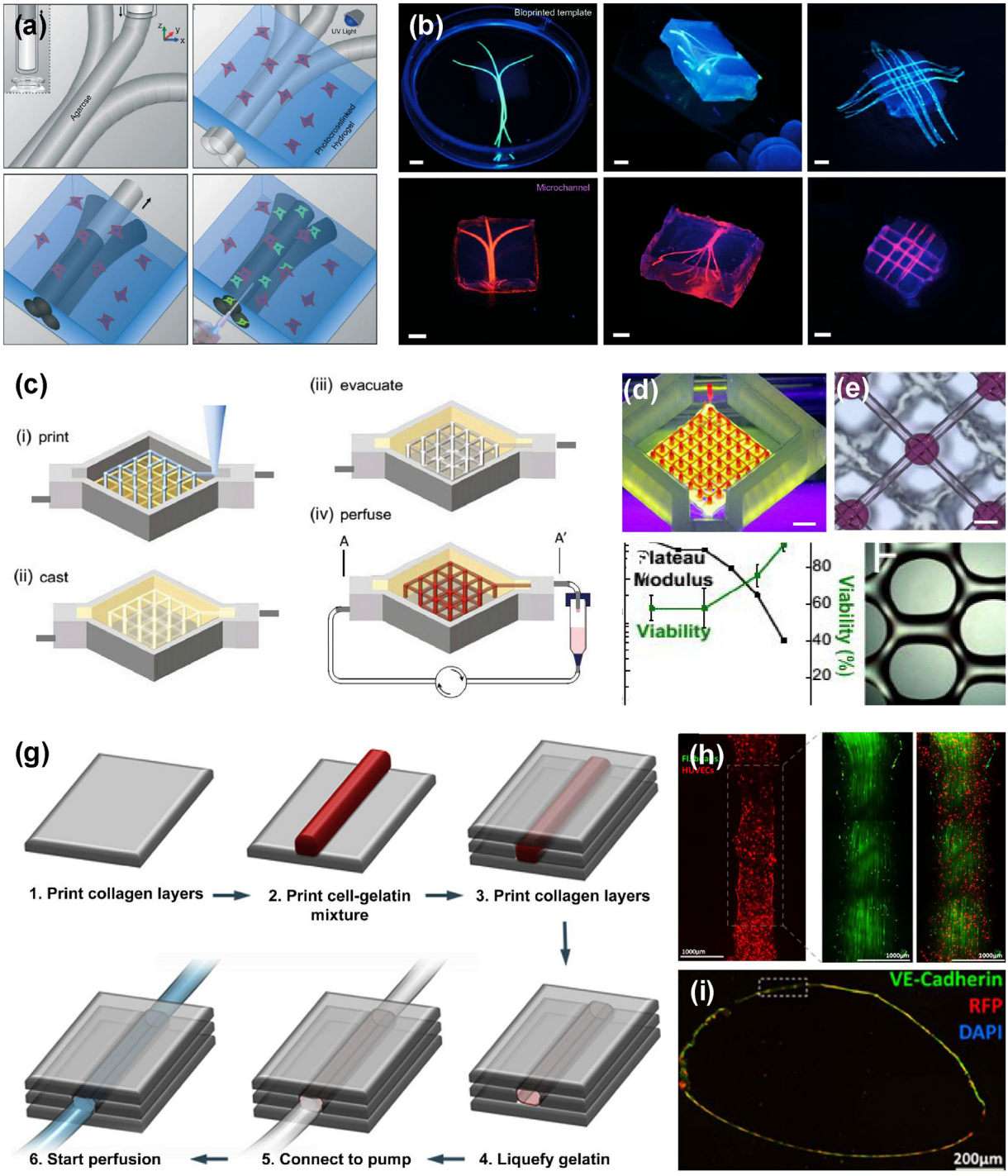

Fig. 9. Sacrificial bioprinting. (a) Schematic showing the sacrificial bioprinting process *via* extraction of bioprinted hydrogel agarose microfibers. (b) Photographs showing the structures before (upper row) and after (lower row) agarose removal. (c) Schematic showing the sacrificial bioprinting process *via* dissolution of bioprinted pluronic microfibers. (d–f) Images showing a thick construct with interconnected microchannels post pluronic removal. (g) Schematic showing the sacrificial bioprinting process *via* dissolution of bioprinted gelatin microfibers. (h, i) Fluorescence micrographs showing the lumen-like structure that are formed by HUVECs along the wall of the hollow microchannel post gelatin removal.
Reproduced with permission from: (a–b) Ref. [143], (c–f) Ref. [135], (g–i) Ref. [144].

liquefied at 4 °C or lower [133,134]. Taking advantage of this property, a framework of the Pluronic bioink could be generated, cased with a hydrogel matrix, and removed to generate thick vascularized tissue constructs (Fig. 9c–f). The use of dried Pluronic bioink simultaneously serving as the scaffolds and the sacrificial template was further developed [135].

Lee et al. utilized gelatin solutions as the fugitive bioink, which gelled at lower temperatures but liquefied when the temperature reached approximately >30 °C (Fig. 9g) [144]. Importantly, rather than seeding endothelial cells after the hollow microchannels were created [133–135,143], in this approach the cells could be directly embedded in the gelatin fugitive bioink during the bioprinting process. As gelatin gradually dissolved over incubation at the culture temperature, the embedded cells would spontaneously attach to the formed microchannel walls (Fig. 9h and i). Sacrificial bioprinting, however, usually relies on the differential properties of the template and the bulk hydrogels, thus limiting the choice of the variety of materials that can be used.

2.3.5. Microfluidic bioprinting

While embedded bioprinting has partially solved the limitations of extrusion bioprinting by providing physical confinement of the extruded bioink using a supporting hydrogel matrix, this process relies on relatively complex multi-step procedures. To this end, Khademhosseini and co-workers have developed a novel microfluidic bioprinting approach [145–147], where essentially any desirable biomaterial (*e.g.* GelMA) can be deposited by combining with alginate, a polysaccharide that features ultrafast physical crosslinking in the presence of divalent ions [148–150]. This was achieved by using a core-sheath microfluidic printhead, where the bioink was delivered through the inner core flow while a $CaCl_2$ solution was carried from the outer sheath flow [145,146]. After the biofabrication step, the biomaterial could be further chemically crosslinked to preserve the permanent shape, while the alginate component, serving as the temporary scaffold, could be selectively removed afterward using a calcium-chelating agent, such as ethylenediaminetetraacetic acid. Of note, the microfluidic printhead could be expanded to more than a single channel. For example, two inlets could be merged into a single outlet sheathed by the $CaCl_2$ crosslinking solution (Fig. 10a), thus enabling alternative or simultaneous bioprinting of two bioinks (Fig. 10b and c) [145]. This microfluidic printhead may have a few additional variations. One prominent example is the use of a tri-layered co-axial device. In this setup, the alginate-containing bioink is extruded from the middle layer while the crosslinking $CaCl_2$ solution is streamed from both interior and exterior, leading to bioprinting of hollow vascular-like structures [147,151–156]. Vascular cells may be encapsulated within the bioink to generate biologically active hollow conduits that mimic blood vessels [147,154].

A similar device without the sheath flow was used by Hardin et al. to extrude two viscoelastic inks [157]. The same group subsequently integrated a rotating impeller into this printhead to achieve active mixing of the two bioinks at prescribed ratios (Fig. 10d and e) [158]. This unique design allowed for complete mixing of the bioinks within the volume of the printhead. By

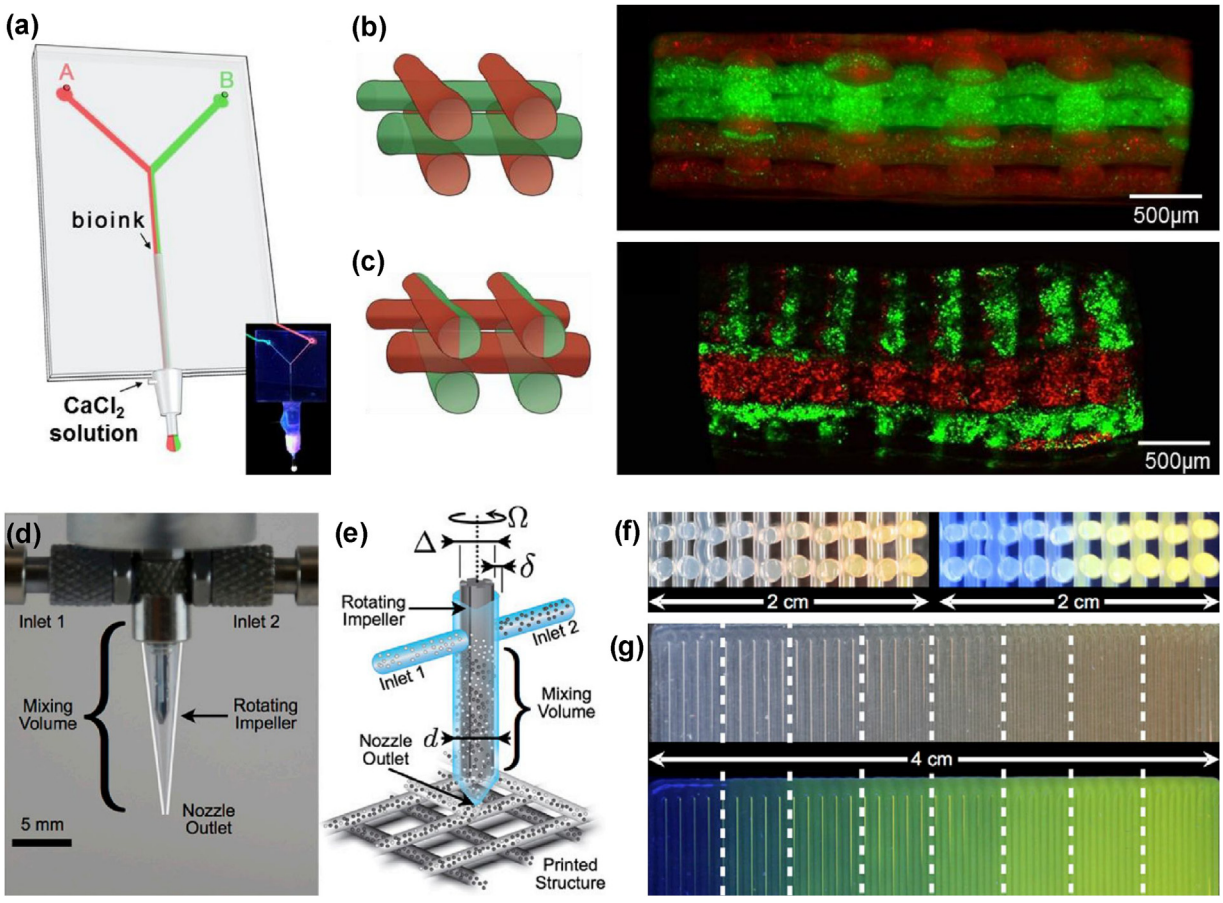

Fig. 10. Microfluidic bioprinting. (a) Schematic showing the design of the bifurcated microfluidic printhead featuring a core-sheath configuration at the tip. (b) Schematic and (c) confocal images showing the sequential and simultaneous bioprinting of two bioinks. (d) Photograph and (e) schematic of a microfluidic printhead with an embedded rotating impeller to achieve active mixing. (f, g) Photographs showing bioprinted gradient structures.
Reproduced with permission from: (a–c) Ref. [145], (d–g) Ref. [158].

meticulously tuning the relative volumes of the two bioinks, gradient structures could be achieved in both vertical (Fig. 10f) and horizontal (Fig. 10g) directions. Such a bioprinting process was unprecedented and enabled direct deposition of heterogeneous and gradient bioinks with relative ease.

2.3.6. Multi-material bioprinting

There is no single natural tissue in our body that is comprised of only single cell types or ECM composition. Thus, to mimic both the structural and the compositional accuracy of the fabricated tissue and organ constructs, it is crucial to achieve simultaneous deposition of bioinks made of different biomaterials. Recent advances have contributed to the development of multi-material bioprinters using stereolithography/DMD and extrusion techniques.

By sequentially changing the input bioinks for the DMD bioprinter along with synchronized patterning with the mirror array, tissue constructs made of multiple materials in a well-organized manner could be obtained [113,159–164]. For example, to mimic the liver microarchitecture, Ma et al. reported the sequential bioprinting of human induced pluripotent stem cell (hiPSC)-derived hepatic cells in a hexagonal lobule structure with supporting cells (non-parenchymal cells from endothelial and mesenchymal originals) filling the lining of the lobules (Fig. 11a) [164]. The bioprinted liver construct demonstrated structural resemblance with its *in vivo* counterparts and exhibited functionality as indicated by long-term cell viability, stable secretion of liver biomarkers, and expression of cytochromes. A similar strategy was also used to fabricate hydrogel micro-robots in the form of micro-fish loaded with iron oxide nanoparticles in its head and platinum nanoparticles in its tail. Platinum nanoparticles decomposed H_2O_2 that was present in water, which generated O_2 and propelled the micro-fish to move forward, in addition to the magnetic control enabled by iron oxide nanoparticles [160].

Multi-material extrusion bioprinters have been significantly improved since the inception of the concept. Since the initial demonstration of the multi-nozzle system that was capable of fabricating hydrogel constructs from multiple materials [133,165], bioprinters now can simultaneously or sequentially extrude biomaterials of several categories including the conventional scaffolding polymers (*e.g.* PCL or PLA), hydrogel bioinks to function as a tissue mass, and sacrificial bioinks that serve as the fugitive template to achieve vascularization. A recent demonstration by Kang et al. proved that, by rationally integrating these different aspects into a bioprinting system, functional tissues at relatively large scales with vascularization, such as the mandible bone, calvarial bone, ear cartilage, and skeletal muscle could be obtained (Fig. 11b) [166].

2.3.7. Advanced bioinks for 3D bioprinting

To further expand the capability of current 3D bioprinting technologies, various bioinks with tunable biochemical and biophysical properties are being developed to engineer tissue constructs with improved biomimetic features. The specific requirements of bioink characteristics depend innately on the type of 3D bioprinting technique and target tissue/organ, since different organs, such as heart, bone, skin or lung, have very different ECM compositions and biomechanical properties. Despite the development of various 3D bioprinting techniques, most of the previously developed bioinks focused on the extrusion-based bioprinting technique due to its high popularity, which posts high demands on the rheological properties of bioinks [125,167].

To design and develop advanced bioinks for various 3D bioprinting techniques, several important parameters have to be considered that dictate the interplay between different materials properties. These properties include viscosity for uniform cell encapsulation, shear-thinning behavior to improve printability and avoid the use of highly viscous inks, gelation kinetics for structural

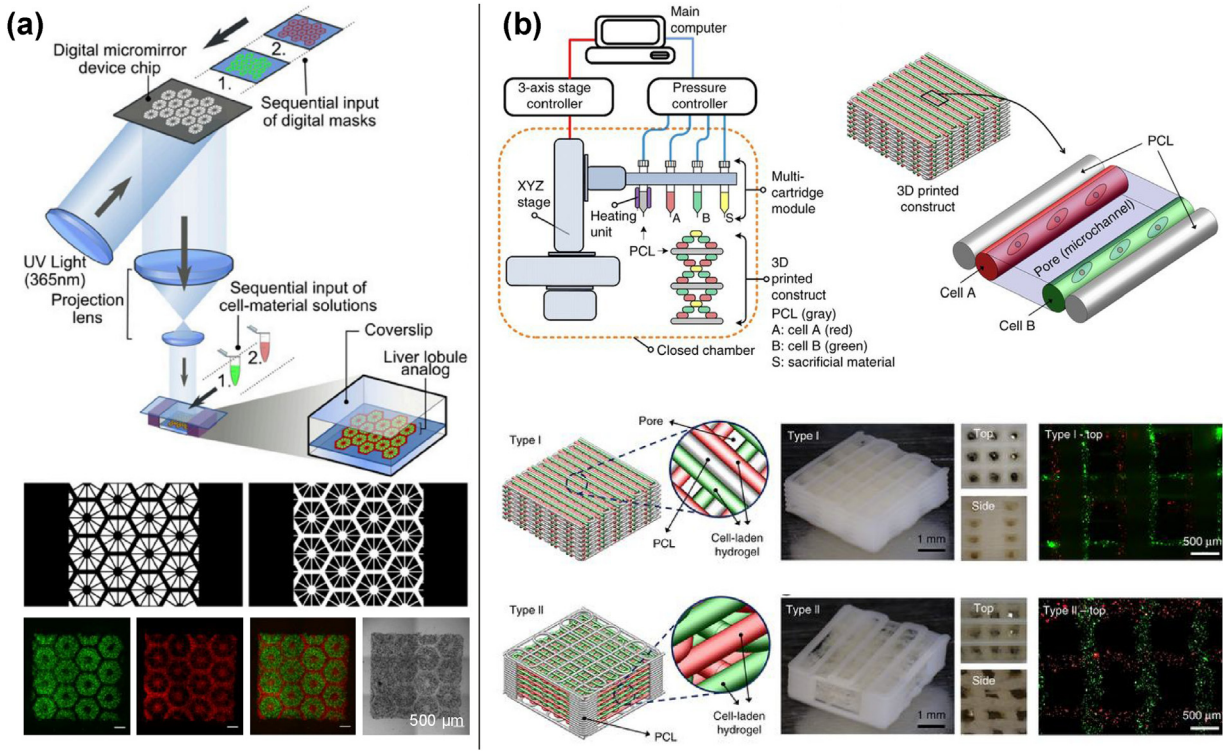

Fig. 11. Multi-material bioprinting. (a) Multi-material DMD bioprinting and fabricated dual-material liver lobule structures. (b) Multi-material extrusion-based bioprinting for simultaneous deposition of scaffolding polymer, tissue bioinks, and sacrificial bioinks for vascularization.
Reproduced with permission from: (a) Ref. [164], (b) Ref. [166].

fidelity, viscoelasticity to protect cells from shear stress, and biocompatibility for supporting cell viability and growth [168]. In particular, to improve structural fidelity, the bioinks can be immediately crosslinked under biocompatible conditions during the printing process. Also, it is important that the bioinks possess biomimetic structural and remodeling aspects of the native ECM to support cellular adhesion, proliferation, and differentiation, which will enhance the function of resulting tissue constructs [169]. In this section, we will roughly divide the various reported bioinks based on the following categories: natural polymers, synthetic polymers, and nanocomposites.

Natural polymers that have been used to design bioinks including alginate, gelatin, collagen, fibrin/fibrinogen, gellan gum, HA, agarose, chitosan, and silk, in general, have promising properties, such as biocompatibility and biodegradability, as compared to synthetic polymers [170]. Alginate is an anionic polysaccharide and has been widely used in bioprinting due to its ultra-fast crosslinking with divalent cations and the sacrificial character, which allows for rapid gelation and feasible on-demand removal [171]. However, as alginate is a biologically inert material, it provides limited support for biological functions, such as cell attachment and growth. This challenge can be resolved by chemically modifying alginate with RGD peptide motifs [172]. Another solution is to physically blend alginate with other bioactive polymers, including fibrin, thrombin, collagen, gelatin, agarose, genetically engineered phages, or nanoparticles. The resulting hybrid alginate-based bioinks can show improved biological functions.

Another widely used natural polymer for bioprinting is gelatin, stemming from its excellent biocompatibility, biodegradability, low antigenicity, inclusion of integrin-binding motifs and matrix metalloproteinase sensitive motifs, good processability, and low cost [173]. In addition, the thermally reversible physical gelation feature of gelatin has been explored to design fugitive bioinks as described above. However, the direct printing of uniform and stacked gelatin fibers was found to be challenging due to the poor mechanical properties and poor stability at body temperature [174]. Blend bioinks based on gelatin have also been demonstrated, such as the cell-laden GelMA/HA bioink to challenge the issue [175].

Collagen is the main structural ECM protein in our body. Several research groups have used collagen bioinks to print cell-laden 3D tissue constructs by using stereolithography, extrusion-based bioprinting, and microfluidic bioprinting systems [176]. In

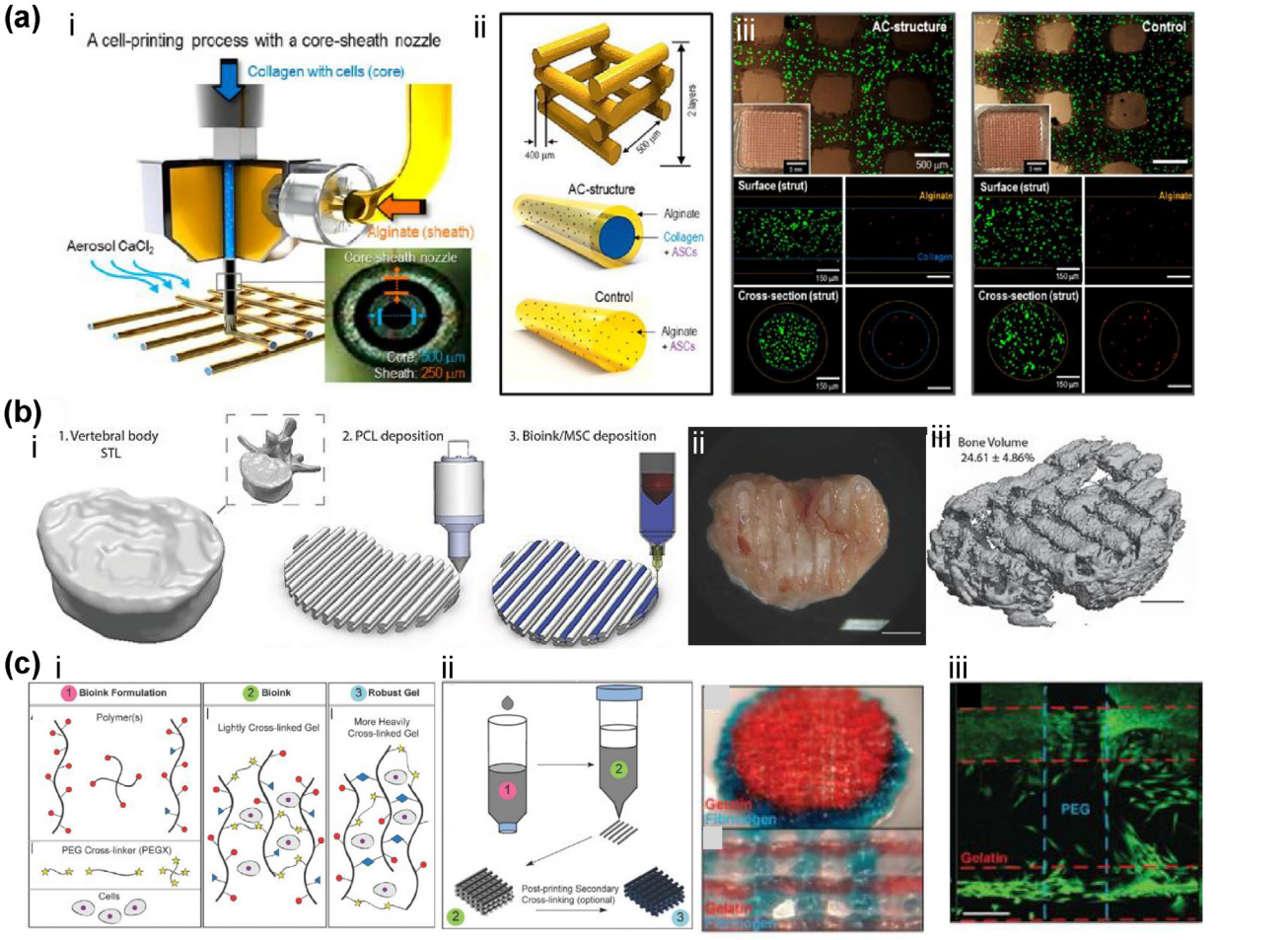

Fig. 12. Advanced natural bioinks for 3D bioprinting and their applications. (a) (i) Cell printing process with a core–sheath nozzle using a collagen-based bioink (core) and pure alginate (sheath). (ii) Designing alginate-collagen core-sheath structure and control. (iii) Live (green)/dead (red) images of human adipose stem cells in alginate-collagen core-sheath structure and a control. (b) (i) 3D bioprinting process: The outer geometry of a human vertebral body was scanned and next layers of PCL filaments were deposited followed by deposition of the MSC laden bioink. (ii) Development of vascularized bone organ *in vivo* following implantation of cartilage rudiment. Macroscopic image of anatomically shaped vertebrae constructs after 12 weeks of implantation (scale bar, 2 mm). (iii) μCT reconstruction and X-ray of whole construct (scale bar, 2 mm). (c) (i) Bioinks consist of natural hydrogels with PEGX crosslinker. The red circles represent amines, blue triangles methacrylate groups, and yellows stars sucinimidyl valerate groups of PEGX. (ii) 3D printing process of PEGX bioink method and corresponding multilayer structures. (iii) Cell viability of 3D bioprinted structures. (For interpretation of the references to colour in this figure legend, the reader is referred to the web version of this article.)
Reproduced with permission from: (a) Ref. [178] (b) Ref. [181] (c) Ref. [182].

addition, collagen was also used in forms of mixture with agarose or alginate to improve the printability and structural integrity [177]. Recently, Yeo et al. fabricated multi-layered cell-laden lattices using a core-sheath nozzle and an aerosol crosslinking method. A cell-laden collagen-based bioink was delivered in the core region, while an alginate bioink was delivered in the sheath region, which created a mechanically robust and biologically functional structure (Fig. 12a) [178]. Fibrinogen is converted into insoluble fibrin catalyzed by thrombin in presence of Ca^{2+} during the blood clot formation process. Both fibrinogen and fibrin are highly biocompatible, biodegradable, and non-immunogenic. In addition, its fibrous network can induce cell attachment and proliferation [179]. However, due to its weak and fragile nature of fibrin, to create robust and stable bioprinted 3D constructs from fibrin bioinks alone is challenging. Nevertheless, this challenge can be resolved by blending fibrin with other polymers, such as alginate, HA, collagen, PCL, or PEG, among others. For example, Gruene et al. utilized a cell-laden blend bioink composed of fibrinogen-HA to create a vascular-like network using stereolithography bioprinting for 3D assembly of multi-cellular arrays [180].

Other natural polymers are used in combination with the above-mentioned polymers to generate bioinks with desirable rheological properties with improved shape fidelity of the bioprinted constructs. However, variations in viscosity tend to dramatically affect the printing resolution. Therefore, the development of modified natural polymers could potentially tackle these limitations as it can improve structural fidelity, tune physicochemical properties, and enhance tissue-remodeling functions of the bioinks, which is a crucial step towards successful bioprinting of engineered tissue constructs that truly mimic native tissues or organs.

Synthetic polymers have attractive properties, such as highly controllable mechanical strength and stability, as well as facile fabrication processes. Among various cytocompatible synthetic polymers, PEG is widely used to prepare bioinks. These materials can be easily tailored in various molecular parameters. However, it is often difficult for cells to grow into and remodel their synthetic polymer matrices. The introduction of enzymatically cleavable moieties can alleviate this challenge. Synthetic polymers have also been functionalized with RGD peptide motifs or growth factors to improve their bioactivity. Another approach to integrate bioactive characteristics is the incorporation of natural biopolymers, such as HA, collagen, gelatin, and fibrinogen with synthetic polymers. Daly et al. deposited PCL and hMSC-laden RGD-modified alginate hydrogel in a layer-by-layer manner to engineer an anatomically accurate cartilage template, which over time evolved to a proper bone organ *in vivo* (Fig. 12b). In this study, printed PCL filaments were used as the framework to create areas for the deposition of cell-encapsulated alginate hydrogels [181].

Mechanical properties of PEG hydrogels can be easily tuned by changing molecular weights or molecular architectures, such as linear or multi-armed, without inducing toxicity or immunogenicity. To date, PEG is probably the most popular synthetic biomaterial due to its water solubility, bioinert nature, ease of chemical modification. Rutz et al. utilized PEG derivatives to develop tunable bioink formulations that provided a wide range of mechanical and rheological properties (Fig. 12c) [182]. They produced PEGs with reactive groups (PEGX), which effectively acted as a crosslinker for various natural materials by reacting with amine groups. This approach was used for the printing of PEGX-PEG, PEGX/gelatin, PEGX-gelatin-fibrinogen, and PEGX-gelatin-atelocollagen bioinks containing several types of cells. These results suggested that chemically modified PEG derivatives are a valuable candidate to tune bioink properties, enhance bioink choices, and control cell responses.

Nanomaterials can be incorporated into polymer-based bioinks to provide valuable characteristics including shear-thinning behavior, unique bioactivity, electrical conductivity, and magnetic property. As such, nanocomposite bioinks represent a highly versatile platform for endowing bioinks with specific functions. As an example, Skardal et al. incorporated gold nanoparticles (AuNPs) into a thiolated HA hydrogel as a bioink to print vascular structures using an extrusion-based bioprinter [183]. The AuNPs showed an affinity to sulfur containing polymers, making them multivalent crosslinkers for thiolated molecules that enabled enhanced control over the bioprinting process. In another studies, electrically conductive silver (AgNPs) or gold (AuNPs) nanoparticles were introduced into an alginate or GelMA bioink to print 3D tissues including cardiac tissue and ears using extrusion-based bioprinting [184,185]. Interestingly, the bioprinted ears were able to receive electromagnetic signals without interfering with the metabolic activity of the encapsulated cells. Furthermore, magnetic iron oxide nanoparticles were used as an additive in alginate bioinks, which allowed an additional level of magnetic control over the bioink during printing *via* an external magnetic field [186]. Nanocomposite bioinks are also highly suitable to steer stem cell differentiation. For instance, nanosilicates mixed with GelMA have been successfully explored as a bioink for bone tissue engineering (Fig. 13a) [187,188]. Moreover, the nanosilicate/GelMA bioinks showed shear-thinning behavior, which was also utilized for the printing of complex-shaped micro-constructs.

Recently, decellularized-ECM based bioinks were developed by Pati et al. to better mimic the natural environments of encapsulated cells [189]. They successfully obtained high cell survival rate, type-specific gene expression, and specific ECM formation in bioprinted structures made of decellularized adipose, heart, and cartilage tissues. DNA hybridization is another novel way to make supramolecular bioinks for 3D bioprinting [190]. Li et al. developed a rapid *in situ* 3D bioprinting method using a supramolecular polypeptide/DNA hybrid hydrogel. They utilized two precursors: one containing a polypeptide–DNA conjugate and another containing the complementary DNA sequences as the linker (Fig. 13b) [191]. DNA hybridization between the complementary DNA sequences enabled fast gelation (within a few seconds). These scaffolds possessed high biocompatibility and selective degradability using either proteases or nucleases. Another recent trend is the use of cell pellets and microaggregates to prepare bioinks in order to achieve scaffold-free tissue growth. Spherical aggregates of Chinese hamster ovary cells were prepared and packaged into micropipettes [192].

Until now, various synthetic and natural biomaterials, nanomaterials, cells, and their combinations have been used as bioinks to print complex and functional tissue constructs *in vitro*. Despite the significant advances, the development of novel bioinks that can temporally change their shapes and compositions to biomimic microenvironments of native tissue is challenging. The combination of advanced multidisciplinary technologies, such as click chemistry and stimuli-responsive biomaterials with advanced 3D bioprinting technologies may provide a new way to create functional complex tissues and organs.

3. Temporal control of hydrogel

In the past few decades, hydrogels have been developed to mimic the native ECMs and are commonly utilized as cell culture substrates, partly due to their high-water content, tunable material properties, and biocompatibility. As chemically or physically crosslinked network structures, hydrogels not only provide the mechanical support for cell attachment and survival, but can also present biophysical and biochemical cues to direct cell function. However, the native ECM of living cells is highly dynamic in nature

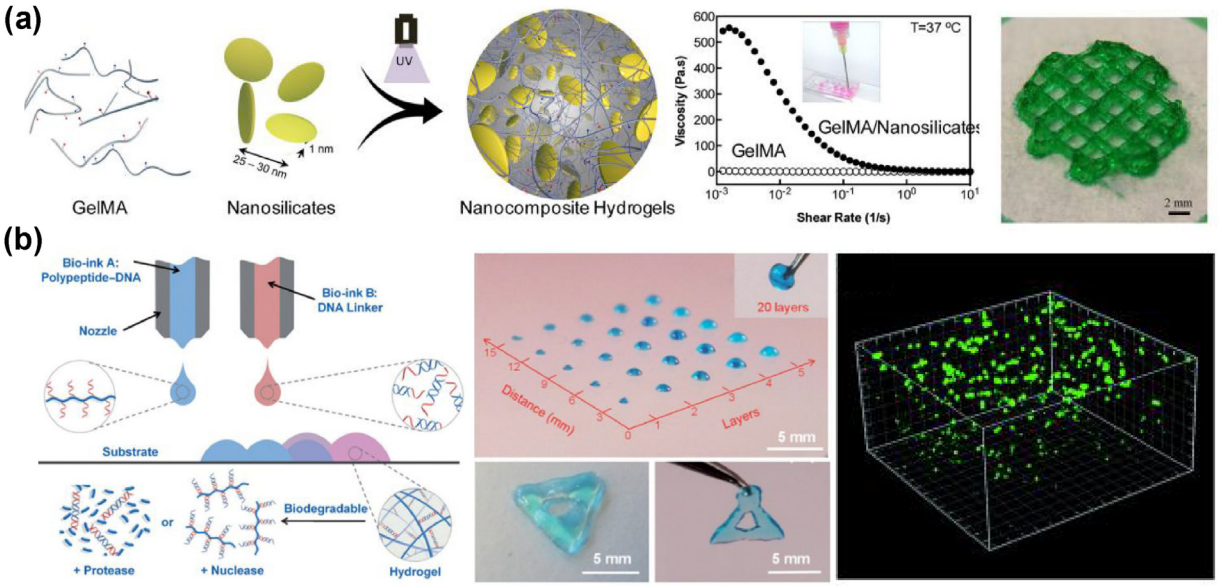

Fig. 13. Advanced bioink-nanomaterial composites for 3D bioprinting. (a) Shear-thinning nanocomposite bioink using nanosilicates incorporated GelMA and their printed construct. (b) Supramolecular bioinks using two bioinks as Bioink A (blue): polypeptide–DNA, and Bioink B (red): DNA linker. Hybridization of these two bioinks results in crosslinking and hydrogel formation. Hydrogels with different sizes and complex structures can be obtained. Encapsulated cells showed high viability in printed construct. (For interpretation of the references to colour in this figure legend, the reader is referred to the web version of this article.)
Reproduced with permission from: (a) Ref. [187], (b) Ref. [191].

and adapts its properties and structures through various biological processes to guide the response of the encapsulated cells to the changing microenvironmental conditions. This temporal control of the chemical and physical microenvironment of cells plays a vital role in tissue development, homeostasis, and pathology. To recapitulate this important dynamic feature, it would be ideal to develop strategies to temporally control the physical and biochemical properties of hydrogels, *e.g.*, in terms of mechanical stiffness, degradation, as well as the presence of drugs and bioactive moieties. In this section, the conventional strategies and recent progress in advanced designs towards temporally controlled dynamic microenvironments of hydrogels is reviewed.

3.1. Delivery of drugs and growth factors

In addition to spatial modulations, temporal control (*e.g.* release of molecules) can be used to manipulate the behavior of engineered tissue constructs. During the last decades, hydrogels have evolved from robust cell-laden structural matrices for tissue engineering applications, to hybrid advanced delivery systems for controlled release of molecules, which can modulate cell microenvironment and develop therapeutic strategies. In this section, the implications of the burst release phenomena in hydrogels, as well as several controlled release modalities, such as on-demand, simultaneous, sequential and spatiotemporal molecular delivery will be discussed.

3.1.1. Burst release and controlled release systems

Much research has been dedicated to prevent the burst release of effector molecules from hydrogels to enable controlled release kinetics. However, it is noteworthy that for some scenarios an initial burst release may be acceptable or even desired. Burst release can be programmed to rapidly and locally deliver bioactive agents in a potentially favorable manner, as long as it is completely predictable to manage the risks related to any side effects or toxicity. It has been demonstrated that many therapeutics might benefit from burst release. For example, in the case of delivering antibiotics, an initial burst release can provide immediate relief, followed by a sustained release for prolonged anti-microbial activity [193]. Regardless, in many other cases, burst release is often considered problematic. As a large fraction of the hydrogel payload is rapidly released and metabolized, issues associated with toxicity or signal saturation might arise.

A principal cause of burst release in hydrogels is the incomplete or non-restrictive encapsulation of therapeutic agents. The use of low molecular weight drugs as payloads might lead to accentuated concentration gradients within the hydrogel system due to their small molecular size and osmotic pressure [194]. Depending on the compositions and properties of hydrogels, burst release can be present in different manners, as the release in drug delivery systems can be classified as chemically controlled, diffusion controlled, magnetically controlled, and swelling controlled [195]. In general, the release profiles of molecules encapsulated in the core region of the hydrogel matrix tend to be affected by the diffusion and permeation kinetics through the network. At the same time, chemical and biological compounds loaded *via* physical entrapment might in turn trigger expansion of the network structure and modification of the release kinetics of the system [196].

Considering that a variety of parameters can govern the burst release process, it is important to study and explore predictive models in order to understand and prevent the release kinetics of several hydrogel formulations for its successful translation to clinical applications. Regardless, several strategies have been developed to modulate the burst release, such as those based on bio-nanocomposite surface extraction, double-walled microspheres, surface modifications, and different coating types [197–199].

In order to modulate the burst release, Park et al. developed polyethyleneimine (PEI)-coated poly(L-lactic acid)/Pluronic blend matrices for controlled protein release [197]. They investigated the burst release of the matrices before and after an aqueous coating using an adsorptive water-soluble polymer, PEI. After the coating, the protein release kinetics were investigated and a remarkable decrease in the burst release accompanied by a significant extension in the release period was observed.

Hezabeh et al. showed in their work that burst release is highly dependent on the degree of crosslinking and the mesh space available for drug diffusion [198]. In their work, the researchers formulated kappa-carrageenan/poly(vinyl alcohol) (PVA) crosslinked hydrogels using genipin as a crosslinker in order to control the release kinetics of β-carotene. Results showed that genipin can modulate and decrease hydrogel burst release as a result of the crosslinking and structural modification of the system. This phenomenon was dependent on genipin concentration changes during the formulation of the system, affecting the strength of the gel network and diffusion coefficient of the molecules.

Another strategy to prevent burst release was reported by Vasudev et al. by applying a chitosan/polyethylene vinyl acetate co-matrix embedded with aspirin and heparin for long sustained release [199]. In order to prolong the release profile and reduce the burst release, the researchers modified the matrices with hydrophobic moieties for effectively controlling burst release.

3.1.2. On-demand targeted delivery by triggered release systems

On-demand drug delivery has been a desired approach for several decades, as most therapeutic interventions could benefit from the controlled delivery of drugs. For patients, pharmaceutical compounds have specific clinical regimens, where on-demand technologies could enable drug dosage at any desired time and thus represent a better method to control therapeutic efficacy and patient care.

Bio-responsive hydrogels have been developed to meet this medical need and generate on-demand drug delivery systems. Several approaches that rely on stimulus, such as light [200–202], ultrasound [203–205], temperature [206–208], or electricity [209–211], have been developed to enable physicochemical responses in synthetic hydrogel materials for on-demand controlled molecular release, and some examples are discussed in the following paragraphs.

Hardy et al. described the development of stimuli-responsive needles based on hydrogels, which could control the release of ibuprofen *via* external light application [212]. The hydrogel needles were fabricated using a micromolding technique using HEMA and ethylene glycol dimethacrylate monomers along with ibuprofen and a light-responsive 3,5-dimethoxybenzoin conjugate to trigger drug release. The system was able to deliver three doses of ibuprofen over an extended period of time upon programmed light exposure. Ultrasound-triggered delivery systems have been developed using alginate hydrogels that displayed self-healing abilities after ultrasound pulses, which allowed on-demand delivery of mitoxantrone to breast cancer xenografts in mice to suppress tumor growth and reduce tumor size [212]. Thermo-responsive hydrogels using *N*-isopropylacrylamide and 1-vinyl-2-pyrrolidinone monomers have been synthesized for on-demand delivery of diclofenac sodium and procaine hydrochloride [206]. This hydrogel system responded on the thermally reversible gelation of the copolymer to tune the dissolution rate as a means to control the release of the drugs. An interesting electroresponsive on-demand technology was developed by Kulkarni et al., who demonstrated the use of poly(acrylamide-grafted-xanthan gum)-based hydrogels for transdermal delivery of ketoprofen [209]. When the hydrogel was positioned on the abdominal skin of a rat, external electrical stimulation could be used to achieve pulsated release and drug permeation through the skin by switching the electrical signals “on” and “off”.

The development of on-demand delivery technologies represents a great opportunity to enable clinicians and patients a better control of drug dosage during different local pathological processes. In the near future, the advent of new smart materials could potentially boost the design of novel responsive hydrogel platforms that can be integrated with electronic devices towards more efficient administration of therapeutic molecules to the diseased sites. Moreover, although these systems are initially developed for the controlled release of drugs, they hold great value in tissue engineering applications for providing timely dosages of bioactive molecules.

3.1.3. Sequential and simultaneous multi-drug delivery

The field of tissue engineering and drug delivery has evolved from using simple hydrogel systems capable of releasing single molecules to designing advanced systems capable of releasing multiple molecules in a simultaneous or sequential manner [213–217]. The advancement in hydrogel fabrication techniques has extended our capacities to investigate biochemical signaling at the nanoscale level by the development of micro- and nanoscale delivery systems. The microgels can act as molecular reservoirs to sense the microenvironment and can be triggered by cellular behavior to release molecules in a controlled fashion [217].

Notably, the spatiotemporal and sequential release of bioactive molecules has been useful in tissue engineering applications, since the natural tissue formation process relies on a well-controlled cascade of sequential exposure to different growth factors. As an example, Greenwood-Goodwin et al. developed a system capable of encapsulating two distinct growth factors and delivering them with different release profiles in order to sequentially promote adipogenesis and adipocyte maturation [218]. In this approach, a pro-adipogenic soluble factor fibroblast growth factor 1 (FGF1), and bone morphogenic protein (BMP)-4 were released from an arginine-based hydrogel system. Researchers showed that the dual release of these two growth factors within a 3D hydrogel system in a staged manner resulted in higher lipid accumulation compared to simultaneous delivery in 2D culture systems, and an upregulation of key genetic adipogenic markers, which were indicative of development and maturation of brown-like adipocytes that were prevenient from white fat tissues (Fig. 14a).

Kempen et al. have also demonstrated that releasing distinct growth factors that regulate either angiogenesis or osteogenesis in a spatiotemporal and sequential manner could significantly enhance ectopic bone formation [219]. In their study, poly (lactic-co-glycolic acid) (PLGA) microspheres containing BMPs were embedded within a poly(propylene) scaffold, which was surrounded by a gelatin hydrogel matrix containing vascular endothelial growth factor (VEGF). After ectopic and orthotropic implantation in rats, the system exhibited an initial burst release of VEGF within the first 3 days and a sequential sustained release of BMP, resulting in ectopic bone formation and regeneration (Fig. 14b). The spatiotemporal and sequential release of these factors enabled a proper signaling dynamics at the required time to guide cellular response, which showed enhanced tissue formation capacity of the hydrogel system.

The main challenge for simultaneous drug delivery is conferring drug synergy. While synergistic effects have been highly sought in conventional pharmacological approaches, they are rarely realized given the disparate pharmacokinetic profiles of drugs, different routes of administration, and their non-specific distribution in healthy tissues and organs. The development of hydrogel systems that are capable to locally deliver several drugs simultaneously has opened the possibility to remedy this clinical challenge and thus possesses great potentials to increase therapeutic efficacies of current treatment modalities. For example, Seo et al. demonstrated an enhanced therapeutic efficacy in the treatment of tumors using a chitosan-based hydrogel that could co-encapsulate and simultaneously release granulocyte-macrophage colony-stimulating factor with several anticancer drugs (doxorubicin, cisplatin, and cyclophosphamide) [220]. After implantation in a murine model of cervical carcinoma, tumor growth was significantly reduced in mice treated with hydrogels co-encapsulated with both

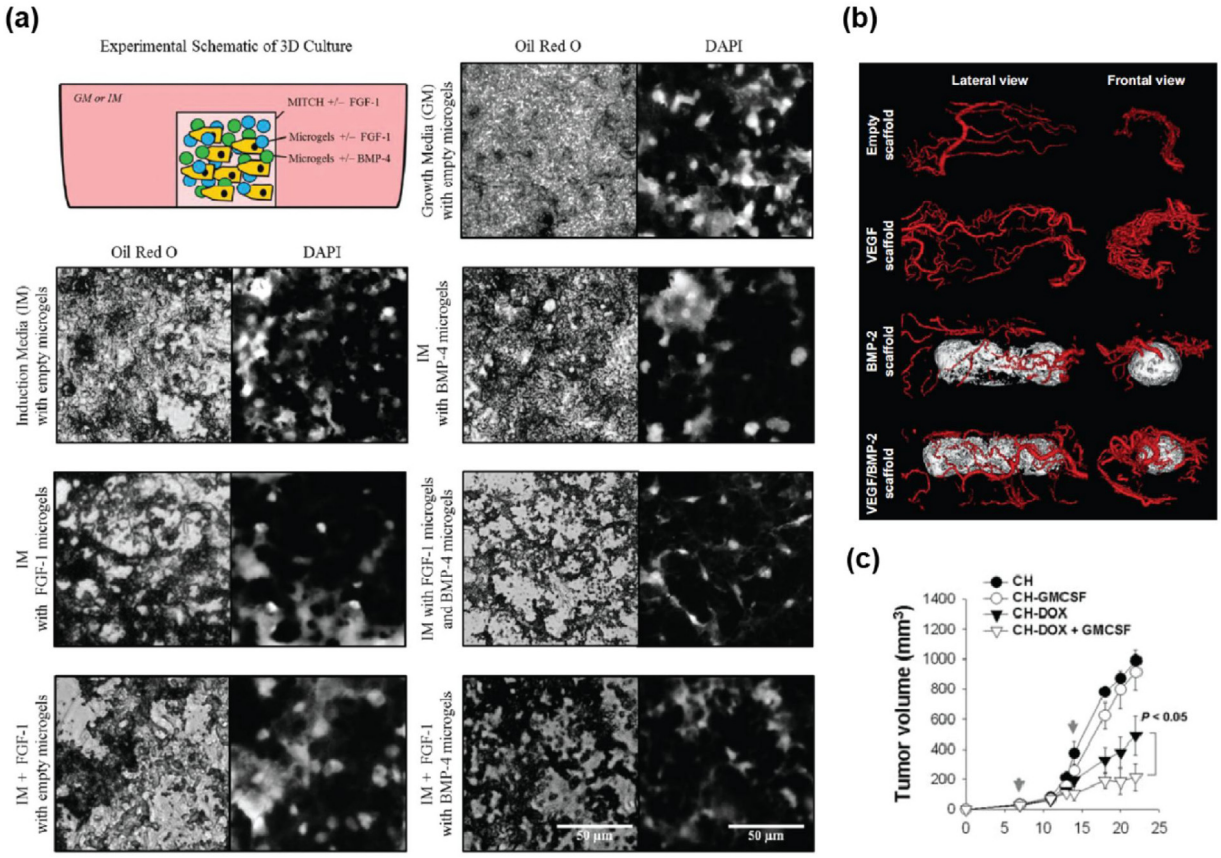

Fig. 14. Sequential and simultaneous chemical delivery. (a) Increased lipid accumulation as a correlation of adipogenesis after FCG-1 and BMP-4 sequential delivery, compared to other combination groups, lipid accumulation is shown by Oil Red O staining (left panels) and cell nuclei shown by DAPI staining (right panels). (b) 3D volume rendering of enhanced formation of the vascular network and bone using VEGF/BMP-2 compared to other groups after 8 weeks of implantation in a rat subcutaneous model. (c) Synergistic anti-cancer therapeutic effects in tumor growth after intratumoral injection of a hydrogel containing a doxorubicin and granulocyte-macrophage colony-stimulating factor, compared to other treatment combination groups. (For interpretation of the references to colour in this figure legend, the reader is referred to the web version of this article.)
Reproduced with permission from: (a) Ref. [218], (b) Ref. [219], (c) Ref. [220].

doxorubicin and granulocyte-macrophage colony-stimulating factor, compared to other groups using hydrogels that had a single therapeutic agent (Fig. 14c). Together, these examples have demonstrated the immense clinical potential of temporally controlled delivery kinetics in controlling tissue fate by delivering molecules in specific, user-defined, and timed fashion, which enables cellular modulation with great precision and at a molecular level.

3.2. Temporal biochemical modification of hydrogels

In native ECMs, growth factors and cytokines are ubiquitously dispersed throughout the network with unique and dynamic distributions, which are essential to direct cell function and fate. Therefore, hydrogel matrices for cell-based applications should also present biochemical and biophysical stimuli in a temporal manner to mimic this *in vivo* microenvironment.

To induce *in vivo*-like cell function in hydrogels, early efforts have been devoted to load bioactive species, such as proteins and growth factors homogenously within the network by directly loading them into the hydrogels. However, this simple strategy only worked well for molecules with sufficiently high molecular weights, which diffused slowly through the hydrogel meshes. Thus, immobilization onto the network backbone was required for small signaling molecules, such as small growth factors, cytokines, or peptides, to improve the functions of delivered molecules. In this section, we will introduce recent progress of biochemical modifications of the hydrogel to control temporal biochemical microenvironments.

3.2.1. Photoinitiated addition reactions

There are numerous studies to use photoinitiated reactions to control spatiotemporal characteristics. Hahn et al. reported some of the first examples to biochemically pattern hydrogels after gelation. In their study, the central idea was to take advantage of the residue photo-reactive groups after the photocrosslinking of PEGDA hydrogels. Peptide sequences holding an acrylate functional group was allowed to diffuse into the preformed PEGDA hydrogel, and further tethered to the network *via* new kinetic chain formation during the second irradiation [221,222]. When combined with the two-photon laser scanning photolithography, this method was used to form biochemically functionalized channels within hydrogel matrices to direct cell migration [223]. Ligation of multiple bioactive molecules to the same hydrogel network combined with spatial control was also demonstrated by a multi-step patterning process to diffuse individual ligands into the hydrogel in a stepwise manner [224].

The Anseth's group introduced sequential click reactions to temporal control of chemical microenvironment [225,226]. They used strain-promoted alkyne–azide cycloaddition (SPAAC) reaction, where the introduction of a difluorinated cyclooctyne moiety instead of the normal alkyne prevented the use of copper salt as the catalyst. As a result, the crosslinking reaction could take place at physiological conditions to result in an "ideal" step-growth

network structure. *In situ* cell encapsulation was also demonstrated with high viability. After the formation of the click hydrogel, the pendant alkene groups on the matrix metalloprotease (MMP)-cleavable peptide crosslinker could be patterned using photolithography techniques and thiol-bearing molecules. Importantly, by using PEG prepolymers with different molecular weights, mechanical properties of the patterned network could also be tuned independently, thus providing a user-defined system to study spatiotemporal cell-material interactions [226,227].

The idea to use click reactions in preparing the hydrogels provides more well-defined spatiotemporally controllable chemical network structures. For example, Fairbanks et al. first reported the use of the photoinitiated thiol-norbornene click reaction to fabricate PEG hydrogels. Different from the chain polymerization of PEGDA or other multi-armed PEG acrylates, this click reaction resulted in step-growth crosslinked networks with much less defects and structural heterogeneity [228]. Moreover, temporal control of chemical hydrogel chemical microenvironments could be realized by adding a slight extra amount of the norbornene groups during the photocrosslinking. Afterwards, the remaining norbornene groups can be modified in a second step to biochemically pattern the hydrogel in 3D. The thiol-bornornene chemistry was also applied to fabricate 3D patterned HA-based click hydrogels [52]. By combining click chemistry with electrospinning, the authors were able to investigate the competing and/or synergetic effects of fibrous orientation and temporal biochemical modification on cell spreading [17]. The concept of click hydrogel systems was expanded to the tetrazine-norbornene [229] and the furyl-maleimide Diels-Alder reactions [230], which could proceed at physiological conditions to result in well-defined hydrogel networks with 3D patterning capability.

From the chain-growth polymerization of methacrylated polymers to the well-designed click hydrogels, recent progress in click chemistry offers unprecedented opportunities towards the fabrication of hydrogels with precise chemical structures and spatiotemporally controllable biochemical properties. It is believed that further advances in this direction could lead to better *in vitro* models for mimicking ECM as well as valuable understanding in cell-material interactions.

3.2.2. Photocleavage reactions

Photoinitiated reactions offer unique advantages for spatiotemporal control over hydrogel modification. Photo-reactions applied in dynamic biochemical modifications to hydrogels can be roughly classified into two categories: 1) an addition reaction takes place upon irradiation to conjugate molecules to hydrogels [221], and 2) chemical bonds are broken by photo-induced cleavage to uncover the reactivity or bioactivity of caged moieties preexisting in hydrogels [231,232]. Both approaches have been demonstrated with the capability to achieve dynamic chemical regulation of hydrogel properties in the presence of cells to direct their behaviors.

Luo et al. first reported the use of photoliable hydrogels to achieve spatiotemporal control of biochemical modifications within preformed hydrogel matrices [233]. They used an agarose-based hydrogel functionalized with protected cysteine moieties by 2-nitrobenzyl groups. Upon UV irradiation, the protection groups could be cleaved to release the reactive thiol groups. Bioactive molecules (*e.g.*, RGD sequences) bearing maleimide tags were diffused into the hydrogel and reacted *in situ* with the free thiols for immobilization. Using photolithography techniques, patterned existence of thiol groups within selected volumes of the hydrogels could be readily achieved *via* focused laser, thus enabling the formation of 3D biochemical channels (Fig. 15a i–iii). *In vitro* cell culture experiments demonstrated that controlled presentation of RGD motifs could direct 3D growth of neural cells (Fig. 15a iv–vi). Similar results of 3D channel patterning and directed cellular behaviors were observed in an HA-based hydrogel system [234]. Moreover, this technique was proven to be compatible with protein loading to achieve patterned presence of proteins at selected volumes within the hydrogel matrices [235]. In addition, it was reported that coumarin derivatives could replace the nitrobenzyl group as the photoliable protection for thiol groups, which opens up more possibilities for designing desired functionalities [236]. Later, Aizawa et al. studied the proliferation and immigration of endothelial cells within agarose hydrogels patterned with cell adhesion peptides and VEGF. Tubule-like structures were observed that followed the guidance of a VEGF gradient in the hydrogel, suggesting a practical approach to grow vascular networks *in vitro* [237].

The presence of multiple different biomolecules at different places within the ECM is a crucial aspect of native ECM and is imperative to control cellular behaviors. Interestingly, the caged-thiol based technology has been demonstrated to simultaneously immobilize different full-length proteins at desired places within the hydrogel [238]. In this study, Wylie et al. applied the agarose hydrogels containing coumarin-protected thiol groups. They selected two pairs of recognizing moieties, namely barnase-barstar and streptavidin-biotin, to assist the multi-protein patterning of amino-terminal sonic hedgehog (SHH) and ciliary neurotrophic factor (CNTF) (Fig. 15b). By applying two consecutive 3D photocleavage steps, barnase and streptavidin were tethered to the agarose network as the binding sites for fusion proteins of barstar-SHH and biotin-CNTF, respectively [238]. The ability to achieve simultaneous patterning of multiple proteins provides a step further towards the fabrication of complex synthetic ECM mimetics for various biomedical applications.

Although elegant, the 3D patterning of full-length proteins using the specific interactions between binding pairs introduced additional factors and required engineered proteins to include the recognition sequences. To mimic the generic process of protein loading on ECM, Mosiewicz et al. developed a photo-patterning technique *via* enzyme-catalyzed coupling reactions [239]. They incorporated a designed peptide containing an *o*-benzyl-protected lysine residue into PEG hydrogels, which, upon photo-deprotection, was the substrate of the transglutaminase factor X to couple biomolecule loads *via* the γ-carboxamide group on a glutamine residue (Fig. 15c). This method could ligated a myriad of proteins with the PEG network under mild conditions, which suggested that it could represent a powerful method to fabricate complex hydrogel matrices with spatiotemporal control over protein distribution [239]. A similar approach was reported by Griffin et al. to prepare hydrogels with 3D protein patterns in the presence of cells [240].

In addition, the photoliable groups can also be used to deactivate the functions of bioactive moieties, which could be temporally activated upon removal of the protection groups. Lee et al. reported the light-triggered activation of a cyclic RGD peptide to control cell behavior in both *in vitro* and *in vivo* models (Fig. 15d) [241]. By selectively removing the nitrobenzyl protection group on the aspartic acid residue *via* UV irradiation in a spatiotemporally controlled manner [242], the activated RGP motifs can promote several processes including cell adhesion, inflammation, and vascularization. Importantly, although suffering from attenuation and scattering issues, the UV-triggered control over patterned hydrogel activation could be realized *in vivo* through transdermal UV light exposure, thus suggesting feasibility for translation in biomedical applications [241].

The use of photocleavable groups in the temporal tuning of biochemical properties of ECM-like hydrogels holds great potentials as it simultaneously allows for spatiotemporal control of chemical microenvironments. Potential future directions could be

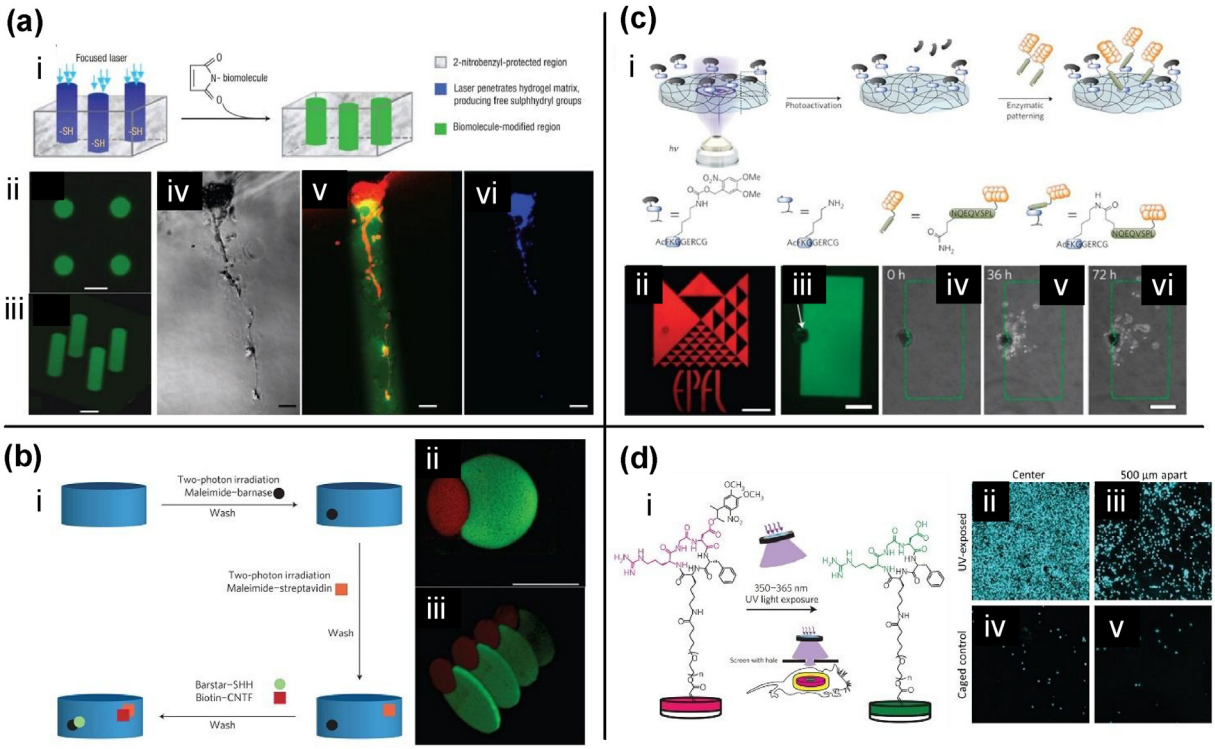

Fig. 15. Dynamic control of hydrogel biochemical properties using photocleavage reactions. (a) (i) Schematic illustration of the biochemically patterned channels with cell-adhesion property in agarose hydrogel matrices using a focused laser. (ii-iii) Representative images of green fluorescently labelled oligopeptide channels (scale bar, 200 μm). (iv-vi) Primary rat dorsal root ganglia cells seeded on agarose gels with patterned channels grew into the channel only at day 3, as revealed by (iv) optical microscopy, (v) confocal fluorescent microscopy with labelled dyes, and (vi) fluorescent microscopy with DAPI-stained nuclei (scale bars, 100 μm). (b) (i) Schematic illustration of the simultaneous immobilization of SHH and CNTF *via* specific interactions between barnase-barstar (the black-green circle pair) and biotin-streptavidin (the orange-red square pair), respectively. (ii-iii) Reconstructed confocal images from different angles showing the simultaneous patterned immobilization of different dye molecules in the hydrogel (scale bar: 100 μm). (c) (i) Schematic illustration of the light-triggered enzymatic patterning of hydrogels. (ii) Light-triggered enzymatic patterning of hydrogels using enzyme-catalyzed coupling reaction and light-exposed regions can generate user-defined precise patterns (scale bar, 200 μm). (iii-vi) Confocal images of a RGD patterned region that covered half of a MSC cluster (scale bar, 100 μm). MSCs quickly grew into the patterned hydrogel regions within 3 days. (d) (i) Schematic illustration of the light-triggered activation of caged RGD peptide on PEGDA hydrogels. Inset: Patterning *in vivo* using transdermal UV light through a mask. (ii-v) Light-triggered activation of caged RGD peptide in PEGDA hydrogels allowed for the examination of cell adhesion on explanted hydrogels from mice that were stained with DAPI to show cell nuclei. (scale bar, 40 μm). (For interpretation of the references to colour in this figure legend, the reader is referred to the web version of this article.)
Reproduced with permission from: (a) Ref. [233], (b) Ref. [238], (c) Ref. [370], (d) Ref. [241].

the development of more photo-sensitive motifs that can respond to light of different wavelengths [243]. Especially, the use of NIR light could benefit the *in vivo* applications due to its excellent penetration through tissues [243].

3.2.3. Reversible tuning of biochemical properties

The complexity of native ECM is further reflected by not only the presence of certain signaling molecules but also the removal of them at proper time points. Therefore, it is of great interest to develop strategies towards reversible tuning of the ligation and release of bioactive moieties, such as the cell-adhesive RGD peptide sequences to control cell spreading and migration, in the hydrogel microenvironment [244].

To achieve this, an elegant combination of photocleavable linkages and the biorthogonal, 3D-patternable click hydrogel systems was reported. A benzyl ether linker was introduced between the thiol groups and the bioactive motifs [245]. 3D patterning of the click hydrogels could be finished with a visible light source [226], while the photocleavage was realized under UV light. Using this design, the authors demonstrated patterned addition and subsequent removal of the bioactive molecules within the hydrogel network [245].

Recently, another study reported fully reversible patterning of full-length proteins in a synthetic click PEG hydrogel system. Here the hydrogel network was formed by the SPAAC reaction, functionalized with benzyl ether-protected alkoxyamine groups [246]. As the first step, selective cleavage of the protection groups permitted protein ligation *via* the oxime bond formation. Moreover, treatment of proteins with a special linker molecule with both *o*-benzyl ether linkage and aldehyde groups enabled both controlled photo-patterning and photocleavage. Dual protein patterning was demonstrated with selective subsequent removal of each individual component. The reversible presence of biochemical cues represented a step forward in our capability to spatiotemporally control hydrogels.

Gandavarapu et al. developed another reversible ligand exchange strategy for dynamic modulation of biochemical motifs [247]. The authors reasoned that allyl sulfide functional groups could be applied to achieve reversible exchange of functional moieties, due to the fast equilibrium switching when the allyl sulfide group was attacked by a thiyl radical [247]. By consecutively adding new thiolated ligands and a photoinitiator, the present motifs could be *in situ* replaced *via* an exchange reaction mechanism. Co-patterning of multiple ligands could be possible by careful kinetic control of the exchange reaction.

These seminal examples illustrated the concepts and potential methods towards fully reversible control of the dynamic presentation of biochemical cues in hydrogels.

3.3. Temporal biomechanical modification of hydrogels

3.3.1. Mechanical stiffness modulation

During the past decade, the effects of mechanical cues in cellular microenvironments to direct cell behaviors have gained increasing attention. Mechanotransduction, which refers to the process to transfer mechanical stimuli to chemical or electrical signals, has been found to play important roles in dictating cell proliferation and differentiation. Engler et al. first identified that the *in vitro* differentiation of MSCs could be tuned by merely changing the mechanical stiffness of the culture substrate [248]. Lineage specification affected by substrate mechanical characteristics was attributed to nonmuscle myosin II, which is an actin-binding protein that controls cell adhesion and migration. Moreover, a recent study revealed that stem cells might potentially possess mechanical memory by sensing and storing the mechanical information from culturing history, which could determine their fate at a later stage [249]. These results highlight the necessity to develop strategies to temporally control the mechanical properties of hydrogel matrices in cell culture studies.

The mechanical strengths of hydrogels rely on its crosslinking density. Therefore, hydrogel stiffness can be increased or decreased with time by increasing or decreasing the number of crosslinking sites. To obtain hydrogels that can stiffen over time, several approaches have been explored. For example, Young et al. reported the use of a kinetically slow crosslinking reaction to achieve hydrogel stiffening within a time scale that is reminiscent of tissue development [250]. In their study, they characterized the crosslinking kinetics of thiolated HA with a PEGDA crosslinker of different molecular weights and found a hydrogel formulation that gradually stiffened from 1 kPa to 8 kPa over a period of two weeks. This kinetic evolution was similar to the tissue elasticity evolution during the development of a chicken heart, which resulted in enhanced cardiac cell marker expression of cells cultured on the dynamic hydrogels. Despite of this elegant design, the reaction kinetics between the thiol and acrylate groups are fixed by the reaction conditions and offer little space for further manipulation.

Sequential multi-step crosslinking mechanisms towards temporal tuning of hydrogel stiffness have also been explored *via* user-trigged methods, which allow for abrupt changes in hydrogel stiffness at precise points post-gelation. Photopolymerization has traditionally been one of the powerful methods to prepare chemically crosslinked hydrogels, which allows convenient spatial and temporal control of the crosslinking reaction. Importantly, the degree of photopolymerization is dependent on the light irradiation dose [251]. As a result, it is possible to take advantage of the dose-dependent crosslinking density, which leaves unreacted functional groups within the hydrogel matrix, which can be subsequently crosslinked in a second step to increase mechanical strengths at a time point of choice [251–257].

Khetan et al. reported a novel sequentially crosslinked hydrogel system towards spatial and temporal control over hydrogel compositions and properties [252]. They synthesized an acrylate-modified HA, which could be crosslinked *via* the addition reaction using peptide crosslinkers with two end-capped thiol groups and a MMP-cleavable sequence. This first crosslinking step generated hydrogels that allowed cell remodeling by breaking the peptide crosslinkers. By tuning the feed ratio of the peptide crosslinker, a portion of the reactive acrylate groups remained unchanged after the first crosslinking reaction, which permitted a second crosslinking by photopolymerization (Fig. 16a). The resulting double-crosslinked hydrogels were mechanically stiffer than their precursor hydrogels, and the enzymatically inactive crosslinking sites blocked the cell spreading *via* matrix remodeling [252]. This study provided the possibility to manipulate cell behaviors through temporal control over matrix properties. Moreover, this system was also compatible with spatial patterning procedures due to the application of the photopolymerization technique. Besides tuning cell spreading, the authors further demonstrated that the spatially patterned hydrogels could lead to entirely different adipogenic/osteogenic fate of encapsulated MSCs through spatiotemporal control of hydrogel crosslinking modes [254].

Stiffening the HA hydrogels *via* a second photocrosslinking mechanism provided a unique and dynamic platform to investigate the effects of abrupt changes in matrix stiffness on cellular behavior and responses, given the fact that matrix stiffening in native ECM might be related to tissue regeneration or disease development. Using this platform, Khetan et al. investigated the cell responses to matrix stiffening in both short-term and long-term time scales in 2D models (Fig. 16b). Their results indicated that MSCs cultured on the stiffened hydrogels could sense stiffness changes quickly and showed increased area and traction within hours of the second crosslinking [254]. On the other hand, when MSCs were cultured in a mixed medium that supported both osteogenic and adipogenic differentiation, the differentiated cell populations demonstrated interesting dependence on the cultured time over hydrogel matrix with different stiffness. MSCs cultured longer on softer matrix tended to differentiate towards adipogenic lineage, while early stiffening of the hydrogels resulted in preferred osteogenic differentiation [254]. These results were consistent with the discovery that stem cells could hold memory of mechanical information [258].

It should be noted that the secondary crosslinking by photopolymerization of acrylate groups not only stiffened the HA-based hydrogels, but also introduced more non-degradable crosslinking sites. This temporal change of degradability along with mechanical characteristics in the HA-based dynamic hydrogel systems was found to influence stem cell differentiation in 3D cell culture [253]. Khetan et al. further revealed that when encapsulated in this HA hydrogels, differentiation of MSCs showed dependence on the generation of cellular traction due to degradation of the matrix, which was found to be independent of hydrogel stiffness and cellular morphology. In particular, even at identical hydrogel elasticity, when embedded in an MMP-degradable HA hydrogels after the first crosslinking, MSCs exhibited high traction and enhanced osteogenesis; on the other hand, the secondary crosslinking resulted in hydrogels with restricted cell-mediated degradation, and preferred adipogenesis of encapsulated MSCs [253]. These findings provide more information to understand cell-biomaterial interactions in 3D dynamic, biomimetic microenvironments.

With this dynamic biomaterials-based *in vitro* cell culture model that recapitulates *in vivo* ECM stiffening, both Burdick and Wells groups investigated how the differentiation of hepatic stellate cells (HSCs) was influenced by matrix stiffness. Differentiation of HSCs into myofibroblasts has been closely related to tissue fibrosis, which might be partially attributed to ECM stiffening during disease development. Their results confirmed that HSCs cultured on stiffer hydrogels (~24 kPa in elasticity) expressed higher levels of alpha-smooth muscle actin (α-SMA) and type I collagen, as compared to HSCs on softer hydrogels (~2 kPa) [255,257]. These results suggest that the dynamic nature of such hydrogels could be leveraged to study biological processes related to ECM stiffening *in vitro*; a feat that is not easily achieved in traditional static hydrogels.

In situ stiffening of hydrogels to tune cellular behavior has also been demonstrated by Marby et al. in a PEG hydrogel system with

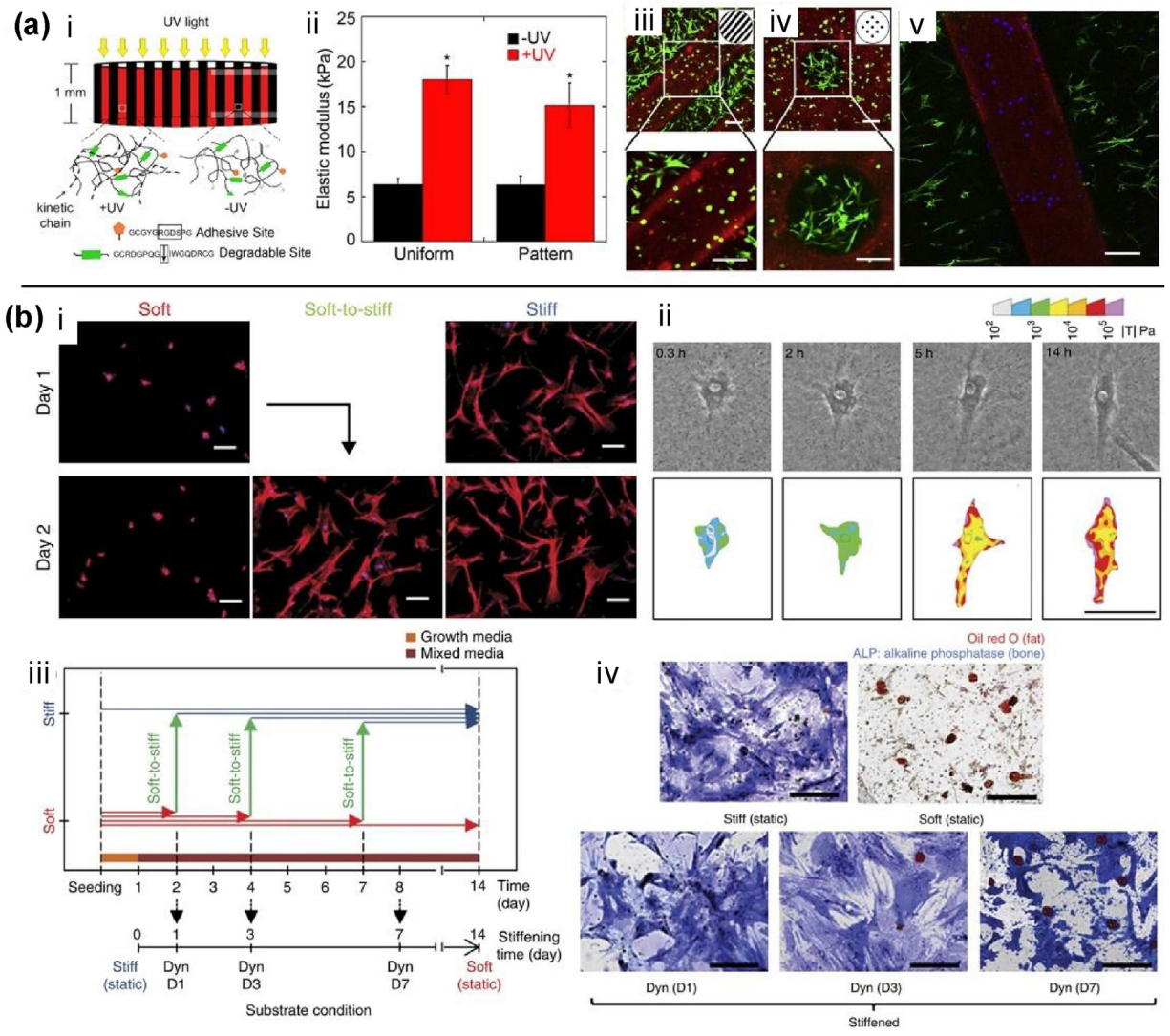

Fig. 16. Representative examples of dynamic stiffening hydrogels. (a) (i) Schematic illustration of a two-step crosslinking strategy to selectively stiffen HA hydrogel zones *via* photopatterning. (ii) Comparison of elastic moduli of uniform HA hydrogels and selectively stiffened HA hydrogel zones measured by atomic force microscopy (AFM) ($p < 0.05$). (iii–iv) Images showing that spreading of encapsulated hMSCs in uniform and photopatterned HA hydrogels only occurred in regions not exposed to UV light (scale bars, 100 μm). (v) Representative immunostaining images showing selective differentiation of hMSCs towards adipogenic and osteogenic lineage in +UV or −UV HA hydrogels, respectively. Fatty acid binding protein was stained as blue while osteocalcin green (scale bar, 100 μm). (b) (i) Spreading of hMSCs cultured on MeHA substrates showed dependence on substrate stiffness (scale bar, 100 μm). (ii) Time-resolved phase-contrast images and traction stress maps of a hMSC showed response of cell traction force to *in situ* substrate stiffening (scale bar, 50 μm). (iii) Schematic illustration of time line for temporal stiffening experiments of hMSCs' osteogenic differentiation. (iv) Representative images of hMSCs stained for ALP (osteogenesis) and lipid droplets with oil red O (adipogenesis) after 14 days of culture (scale bars, 50 μm). (For interpretation of the references to colour in this figure legend, the reader is referred to the web version of this article.)
Reproduced with permission from: (a) Ref. [252], (b) Ref. [254].

MMP-cleavable peptide crosslinkers. Stiffening of cell-laden PEG hydrogels was achieved by diffusing 8-arm PEG derivatives into the base hydrogel to form the second crosslinking network. Responses of valvular interstitial cells encapsulated in 3D hydrogels to the mechanical change were evaluated to reveal different behaviors with those from 2D cell culture models [259]. Recently, dynamic hydrogels capable of *in situ* secondary crosslinking was obtained by using an ABA-triblock copolymer. The A-blocks were modified with coumarin side groups, which could undergo photodimerization upon UV irradiation to introduce additional crosslinking sites. The UV-initiated crosslinking reaction led to varied viscoelastic properties of the hydrogel matrix, which was found to influence the behavior of encapsulated cells [260]. However, as the photodimerization reaction of coumarin moieties is kinetically slow and of relatively low efficiency, potential cell damage associated with long-time exposure to UV light could be a potential concern.

3.3.2. Controlled hydrogel degradation

In contrast to the temporal increment of hydrogels' mechanical properties, strategies to modulate degradation of hydrogels were also developed to weaken hydrogels over time. Early attempts towards controlling the degradation properties of hydrogels focused on the tunability of degradation kinetics through the design of proper hydrolytically or enzymatically degradable crosslinkers. For example, the introduction of short polyester oligomers (such as oligo(lactic acid) or oligo(glycolic acid)) adjacent to crosslinking sites has been demonstrated to tune the hydrolytic degradation rates of hydrogels based on PEG [261–263], PVA [264], or HA [265]. Depending on the lengths of polyester oligomers, crosslinking density, as well as the feed ratio of degradable and non-degradable macromers, degradation profiles of the engineered hydrolytically degradable hydrogels could be tuned from weeks to months. Using these model systems, the

effects of hydrogel degradation profiles on behaviors of encapsulated cells were investigated using different types of cells including chondrocytes [266,267], osteoblasts [268], neural precursor cells [234], and MSCs [265]. However, the major drawback of hydrolytically degradable hydrogels is that the intrinsic degradation properties of the engineered hydrogels are merely dependent on precursor formulations, and do not readily allow for on-demand control of hydrogel properties.

User-defined degradation of hydrogels over time was further explored using hydrogels crosslinked with specific peptide sequences, which were substrates of specific enzymes secreted by encapsulated cells or added exogenously towards controlled cleavage of the crosslinking sites [269–272]. As an example, MMP-cleavable peptide crosslinkers have been used in the temporally tunable HA-based hydrogels as described above [252–257]. Besides MMP-sensitive peptides, peptide sequences that are subject to proteolytic cleavage by other enzymes, such as collagenase [269], plasmin [273], among others, have also been developed. One unique feature of enzymatically degradable hydrogels is the tunability of proteolytic kinetics through screening of a library of peptide sequences, which allows feasible tuning of degradation kinetics for particular requirements [274]. Nevertheless, proteolytic degradation by either cell-secreted or exogenous enzymes still cannot provide spatially precise control over for patterned degradation. Moreover, the use of exogenous proteins might potentially induce adverse effects in cell behavior.

Similar to photoinitiated crosslinking to stiffen hydrogels, photodegradation of hydrogels could also offer advantages like precise spatiotemporal control, compatibility with cell encapsulation, and triggered tuning of hydrogel properties. In particular, the nitrobenzyloxycarbonyl group is among the most commonly used photocleavable motifs, which can degrade into an aldehyde and a carboxylic acid parts upon UV light activation. Johnson et al. investigated the photodegradation of model PEG hydrogels that contained nitrobenzyloxycarbonyl linkages, and confirmed the structures of polymer fragments after photoinduced cleavage of the networks [275,276].

Kloxin et al. first investigated the on-demand modulation of physical and chemical properties of a PEG hydrogel *via* photoinduced degradation, and demonstrated the effects of temporal changes in hydrogel properties on behavior of encapsulated cells (Fig. 17a) [277]. In addition, the incorporation of a photocleavable tether allowed triggered release of certain functional pendant moieties. Coupled with a two-photon laser scanning microscope, 3D patterned features can be readily created within the cell-laden hydrogels by arbitrarily controlling the laser focus to achieve localized degradation [278,279]. As a result, the creation of hollow 3D channels within the hydrogel promoted directed cell immigration along the edge of channels. This unique system provided unprecedented feasibility for *in situ* modulation of hydrogel properties, and precise spatiotemporal patterning of biophysical and biochemical cues in the cell microenvironment. For example, using this hydrogel system, Kloxin et al. observed that the substrate elasticity of the dynamic hydrogels could direct differentiation of valvular interstitial cells through creation of a hydrogel film with a gradient of mechanical stiffness [280].

With modifications to prepolymer structures and crosslinking reactions for primary network formation, this platform could be used towards fabrication of cell culture matrix with gradient degradation, patterned surface erosion, as well as 3D interconnected local erosion, which could serve as excellent *in vitro* models to isolate individual factors to study cell-material interactions and cell behaviors [281–285]. For example, McKinnon et al. reported a photodegradable step-growth PEG hydrogel based on the SPAAC reaction [285]. Temporal control over localized photodegradation of hydrogel was applied to direct the growth direction of encapsulated ESC-derived motor neurons, suggesting that temporal dynamic hydrogels are useful cell culture models for *in vitro* formation of neural networks. In another example, Kloxin et al. revealed that the combination of both photolabile motifs and enzyme-degradable peptide crosslinkers could interestingly offer more dimensions towards spatiotemporal control of cellular microenvironments [286].

Based on the photolabile nitrobenzyloxycarbonyl motifs, DeForest et al. further proposed a chemical strategy to achieve independent spatiotemporal control over both biochemical photoconjugation and biophysical photodegradation in a single hydrogel system crosslinked *via* cytocompatible SPAAC click chemistry (Fig. 17b). A peptide crosslinker bearing both a photocleavable nitrobenzyl ether linkage and a photo-reactive alkene group was synthesized and crosslinked with a four-armed PEG crosslinker with cyclooctyne moieties [287]. After hydrogel formation, biochemical cues can be feasibly introduced *via* the photoinitiated thiol-ene reaction in a spatially controlled manner. The controlled degradation was modulated through photocleavage of the nitrobenzyl ether linkage, similar to the techniques described above. Using this system, it was observed that NIH/3T3 fibroblasts encapsulated in a fibrin clot trapped within this dynamic hydrogels could only outgrow and fill the hollow channels when they were modified with chemical cues (RGD motifs) [287]. This study offered opportunities to create more complex 3D cell culture models to direct cell behavior towards fabrication of tissue constructs.

The nitrobenzyl ether linkage has also been utilized in other platforms to introduce dynamic modulation of network degradation. For example, Truong and Tsang et al. investigated dynamic hydrogels based on gelatin and PEG crosslinkers [288,289]. An organogel system containing the *o*-benzylether motifs based on ring opening metathesis polymerization (ROMP) was demonstrated to degrade into fluorescent polymer fragments upon UV irradiation [290]. Besides the most widely used nitrobenzyl ether linkages, other photoresponsive motifs have also been developed. When combined with other hydrogel systems, diverse dynamic hydrogels have been reported to enrich the toolbox for *in vitro* cell culture models. For example, Azagarsamy et al. developed a novel coumarin methylester-based photocleavable unit that responded to different UV wavelengths than nitrobenzyl ether [244]. The combination of both photolabile units allowed wavelength-controlled orthogonal release of molecular loadings from the hydrogel matrix. A new type of dynamic hydrogel based on this coumarin motif has been investigated to reveal the fundamentals of the degradation kinetics and optimization for property modulation [291]. To overcome the light attenuation problem associated with nitrobenzyl ether and coumarin-based photocleavable moieties, a novel photodegradable and photoadaptable PEG hydrogel has been reported, which relied on the reversible fragmentation and addition of disulfide bonds in the presence of free radicals. Rapid degradation of hydrogel specimens with millimeter thickness was demonstrated, along with the capability of photo-healing due to the disulfide bond rearrangement through photo-activation [292]. The development of novel photocleavable motifs is expected to lead to diverse selections of dynamic hydrogel systems for advanced spatiotemporal control over hydrogel properties and cell-material interactions.

3.3.3. Reversible tuning of hydrogel mechanical properties

Despite of the recent progresses in the development of hydrogels to mimic the dynamic nature of native ECM, the examples of dynamic hydrogels discussed above showed only increasing or decreasing mechanical stiffness over time. Considering that the elasticity of ECM could fluctuate during various biological processes, it is thus of interest to prepare hydrogels that recapitulate the reversible dynamic nature of cell

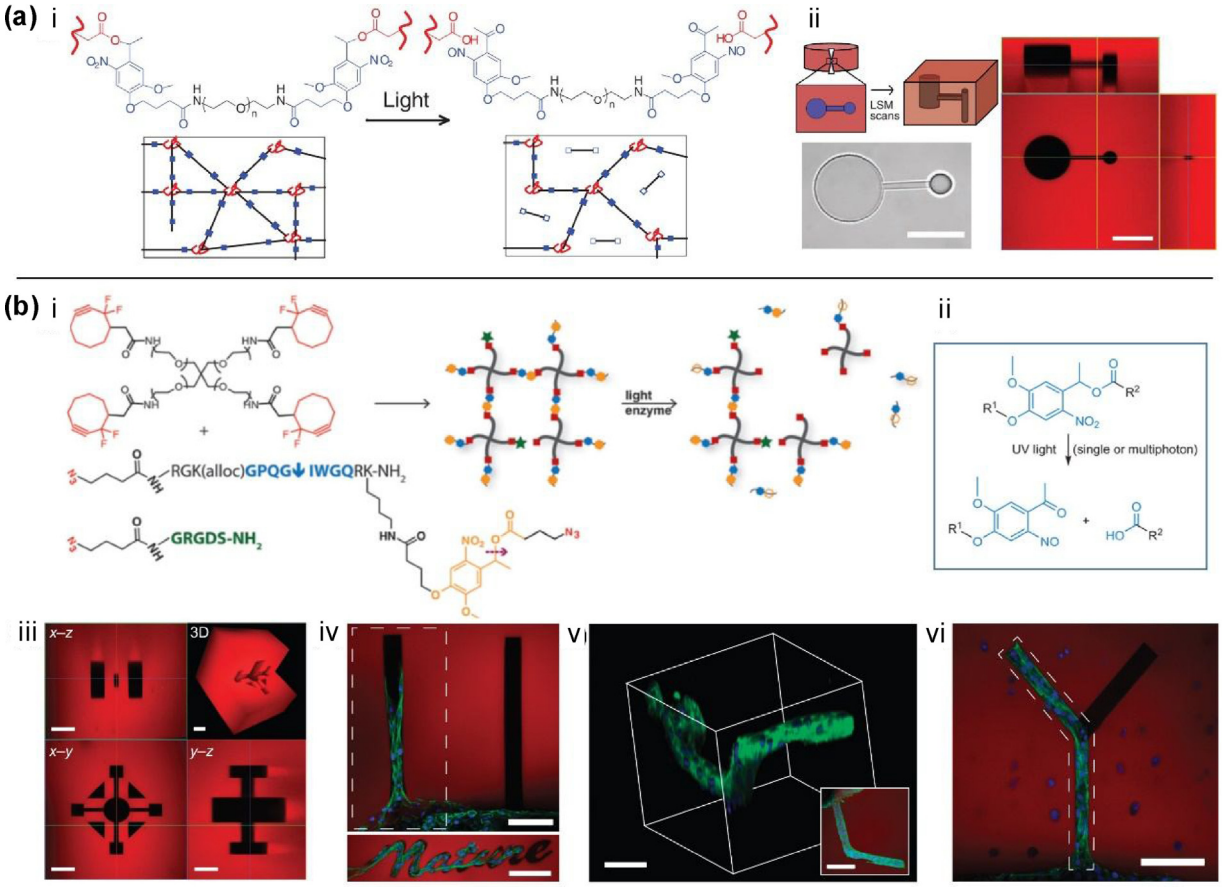

Fig. 17. Representative examples of dynamic degradable hydrogels. (a) (i) Dynamic hydrogels were formed by photopolymerization of a designed PEG diacrylate with a photodegradable photocleavable tether. The photolabile motif cleaved to break the crosslinking and soften the hydrogel. (ii) Schematic and microscopic images showing the fabrication of interconnected 3D channels within the photodegradable hydrogel using a two-photon LSM. The hydrogel was labelled with rhodamine B for easy visualization (scale bar, 100 μm). (b) (i) Design of a photodegradable, enzyme-responsive, click hydrogel for dynamic modulation of biochemical and biophysical properties. (ii) Photo-induced cleavage reaction of the nitrobenzyl ether moiety. (iii) Use of two-photon laser scanning photolithography to create complex 3D patterns in the click hydrogel (scale bar, 100 μm). (iv-vi) Dynamic control of hydrogel properties to directed 3D cell migration within patterned hydrogels. 3T3 cells migrated only within the physically eroded regions modified with RGD peptides, which were denoted by the dashed boxes in (iv) and (vi) (scale bar, 100 μm).
Reproduced with permission from: (a) Ref. [277], (b) Ref. [287].

microenvironments in native tissues. Although hydrogels that reversibly respond to external stimuli has been well explored [293–296], reversibly tunable hydrogels that are prepared and tuned under physiological or cytocompatible conditions are limited.

Yoshikawa et al. reported a pH-responsive hydrogel that showed a reversible change of mechanical stiffness by varying the pH between 7.0 and 8.0. The hydrogel was based on an ABA triblock copolymer, with the A block being the pH-sensitive poly(2-(diisopropylamino)ethyl methacrylate) (PDPA) and the B block being the poly(2-(methacryloyloxy)-ethyl phosphorylcholine) (PMPC) [297]. Interestingly, when the pH was adjusted from 7.0 to 8.0, elasticity of the resulting hydrogel showed a 40-fold increase (from ~1 kPa to 40 kPa), which was found fully reversible with reversible pH changes. Due to the sharp and reversible change under cytocompatible conditions, this system was applied to culture myoblast cells to investigate the effects of substrate elasticity on cellular behavior. Cells exhibited enhanced stress fiber formation and flattening on stiffer hydrogels as compared to softer hydrogels [297]. Importantly, the cell morphology on this hydrogel substrate was also found to be fully reversible along with the change of substrate elasticity, which provided new insights in the mechanobiology of cells.

The Langrana's group reported a series of hydrogels with DNA crosslinking sites enabling a reversible change in mechanical rigidity modulated, which was modulated by the introduction of additional DNA crosslinkers [298–300]. In their design, the initial hydrogel network was crosslinked by DNA recognition, which resulted in extra single-strands within the system. Subsequently, the addition of another single-stranded DNA crosslinker (the fuel strand) with a toehold region could form further crosslinking sites to stiffen the hydrogel. Reversible change of hydrogel properties could be achieved by the addition of a second DNA strand complementary to the fuel strand to generate waste double-strand DNA byproducts and restore the initial state of hydrogels [298]. This DNA-crosslinked hydrogel system was used to investigate effects of substrate stiffness on fibroblasts [299] and neuron cells [300]. However, the presence of exogenous DNA might affect cell signaling and functions.

A composite hydrogel composed of type I collagen and alginate were reported as a dynamic hydrogels with switchable properties [301]. The type I collagen composite provided cell adhesion sites and a moderate degree of crosslinking through fibril formation; the alginate could bind to calcium ions to further crosslink the hydrogel. Interestingly, it is known that calcium ions could be removed by sodium citrate to uncrosslink the alginate, and the reversible process was compatible with cell encapsulation [301]. It was revealed that encapsulated fibroblasts could only spread in pure collagen hydrogels or inside the composite hydrogels with uncrosslinked alginate. Upon crosslinking with calcium ions, the

cells were trapped in the matrix without the capability to spread or immigrate.

Dixon et al. modified the collagen/alginate composite hydrogels to investigate effects of 3D microenvironments on the self-renewal and differentiation of encapsulated hiPSCs [302]. It was found out that the microenvironment with alginate crosslinked by calcium ions could enhance self-renewal of hiPCSs. However, when the alginate was washed away to switch the matrix to a collagen-dominant microenvironment, hiPSCs were found to undergo enhance differentiation towards specific lineages. Interestingly, the switching time of matrix properties was identified to influence the differentiation of encapsulated hiPCSs. This study highlighted the potential applications of dynamic hydrogels for *in vitro* culturing of human stem cells and tissue regeneration [302]. As an elegant design to recapitulate the 3D dynamic cell microenvironments, however, this system lacked precise spatial control over the reversible regulation of mechanical properties.

Stowers et al. successfully engineered a photo-modulation strategy to demonstrate spatiotemporal control of mechanical stiffness of alginate-based hydrogels [303]. Instead of directly adding calcium ions as the crosslinker or chelators agents to crosslink alginate, the authors loaded calcium or chelator molecules along with gold nanorods in separate liposomes, which can be activated *via* irradiation with NIR light to induce elevated temperature for controlled release. The photo-activated release permitted both spatial and temporal control of stiffness changes in the hydrogels, resulting in matrices with patterned or gradient compositions and mechanical characteristics, which could be utilized as *in vitro* models to investigate cellular behaviors. More importantly, the use of NIR light to trigger the mechanical change allowed the transfer of this technology to *in vivo* models, due to the penetrating capability of NIR light.

Dynamic tuning of hydrogel properties based on photo-reversible reactions is an attracting strategy due to the convenient features related to photo-activated reactions. However, early attempts to develop hydrogels with photo-switchable properties relied on the photodimerization and photocleavage of certain motifs [304,305], which required high light intensity and the use of short-wavelength UV light. Therefore, these harsh conditions are not compatible with cell encapsulation. Recently, a hydrogel platform with photo-responsive elastic properties by introducing azobenzene moieties into the crosslinker has been reported [306]. The resulting PEG hydrogels showed reversible stiffening and softening behaviors by multiple light stimuli processes due to the photoisomerization of the azobenzene motifs. The softened hydrogel with *cis*-isomers of azobenzene could be maintained for several hours before thermally converted to the more stable *trans*-isomers. This dynamic hydrogel offered a non-invasive approach to reversibly tune hydrogel rigidity without the necessity to adding reagents to the system.

Besides these examples, many other strategies to fabricate dynamic hydrogels with reversible biophysical features have been reported. For example, genetically engineered protein-based hydrogels showed the potential to transfer the change in protein conformation to differences of the macroscopic properties of hydrogels [307–309]. Very recently, dynamic hydrogels that were responsible for external magnetic field were demonstrated with stiffness change of several orders of magnitude, which could be applied to modulate stem cell behavior including osteogenesis and secretion of proangiogenic molecules [310]. These novel approaches might find important biomedical applications due to the versatility and tunability of these systems.

3.3.4. Hydrogel-based actuators

In addition to the spatial biochemical control, many advances have been made in controlling the biophysical character of biomaterials. In is of note that biophysical control over hydrogels can effectively create actuators. Most commonly this is achieved by controlling the hydromorphic behavior of the hydrogel's polymeric network. Temperature [311], electricity [312], pH [313], magnetism [314], ionic strength [315], and light [316] can be used to contract or expand a hydrogel's polymeric network. Hydrogels can actuate in a homogenous manner to shrink or swell to enable an omnidirectional volume change or in an inhomogenous manner to enable complex hydrogel deformation such as bending, folding, twisting or curling. The controlled deformability allows biomaterials to grip objects [313,317] or move on substrates [311,318–320]. For example, Kim et al. reported that L-shaped hydrogels of PNIPAAm containing cofacially oriented unilamellar electrolyte titanate (IV) nanosheets could be motivated to undergo unidirectional locomotion *via* controlled volumetric alterations by leveraging its anisotropic electrostatic properties [311]. Regardless, many of the current hydrogels can only generate slow deformations or low level of mechanical forces, which limits their direct implementation in various approaches. Several novel hydrogel systems aim to address these limitations. Yuk et al. reported on the fabrication of serially connectable hydraulic actuator units based on polyacrylamide (PA)-alginate hydrogel, of which the design was inspired by the sea animal leptocephali [321]. This approach provided short response times (<1 s) and with high forces (>1 N). Based on their functionality, hydrogel-based actuators are expected to advance the engineering of soft-robots and tissues *e.g.* muscles *via* biologically inspired designs.

4. Future perspectives

4.1. Biomaterials with multiple length scales

Native tissues have precise control over cell behaviors *via* an arsenal of stimuli that spans across multiple length scales. Developing functional multiscale materials that provide predesigned cues to cells at the nano- (atomic and molecular-sized), micro-, and macroscale in a unified architecture is a prerequisite toward truly biomimetic biomaterials (Fig. 18) [322]. As discussed in previous sections, the engineering strategies to gain spatiotemporal control over biomaterials through sophisticated chemistries and fabrication techniques are expected to pave the way for the realization of such biomimetic systems. The concept of bottom-up tissue engineering offers a promising pathway to generate multiscale structures *via* assembling heterogeneous synthons, such as proteins, nucleic acids, cells, nanoparticles, and other bioactive components within the cell-laden hydrogel matrices [66,78,323–325].

The hierarchical arrangement of nanoscale compartments in a microscale unit is crucial to achieve the desired mechanical, physical, and chemical characteristics of the multiscale materials. Such precise hierarchical arranging of, for example, cells inside the tissue eventually outline the cell–cell contacts and paracrine signaling to dictate cellular behavior and subsequently construct function. Such harmonic performance requires contribution by all compartments to the functioning of the construct. The hierarchical organization in spider silk represents an elegant example, as its properties depend on atomic/molecular level (*i.e.*, electron density), nanoscale (*i.e.*, hydrogen bonded β-sheet nanocrystals) and microscale (*i.e.*, hetero-nanocomposite of rigid nanocrystals assembled in core-shell structure) structural features to form silk fibrils, which allow structuring patterns on the macroscale [326]. Creation of sophisticated multiscale units not only necessitates the understanding of interactions ranging from molecular level to macro scale, but also permits reconstruction and reengineering of the complexity that nature has developed over billions of years. As yet, several strategies have been developed to fabricate multiscale

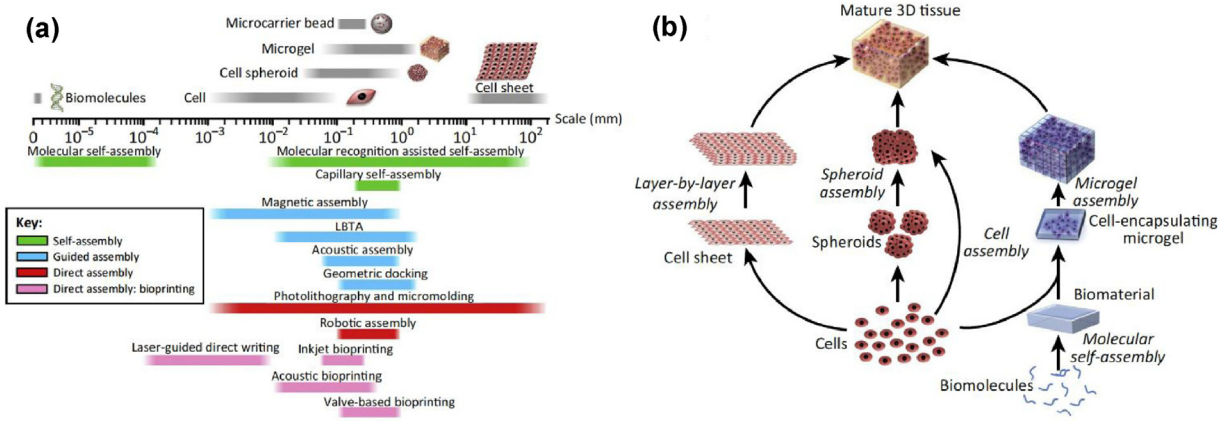

Fig. 18. (a) Existing technologies for assembling building units (shown above the scale) at varying sizes. (b) Schematic of multiscale organization technologies from bottom to top for designing 3D tissue architectures.
Reproduced with permission from: Ref. [322].

architectures, which have provided new opportunities to mimic the organization of native tissues to realize biomimetic engineered tissue constructs.

Supramolecular chemistry based on biomacromolecules in which biological information can be loaded using self-assembling units of DNA or proteins represent a promising method to engineer multiscale structures. It has been shown that the supramolecular structures can be constituted from single-stranded *ss*-DNA and peptides (*e.g.*, RGDs), which offered a facile pathway to investigate the effects of nanotube architecture and peptide bioactivity in cellular function (Fig. 19a) [327]. DNA origami is another promising approach to create nanoarchitectures and decorate specific functionalities at precise and controlled locations, which not only can help to understand the function of individual moieties, but also can controllably emulate cellular microenvironment. It has been shown that the precise positioning of ephrin-A5 in nanofabricated DNA origami scaffolds can regulate the degree of activation in EphA2 receptor in human breast cancer cells and control the invasive characteristics of cancer cells [328]. This opens a unique opportunity to control the nano-organization and macroscale function by spatially positioning ligands for the activation of specific receptors to dictate cellular behavior.

Electrospinning has proven to be a practical method to fabricate nanoscale fibers of wide range of materials in a facile step. However, premade nanofibers might find novel application when merged in bioinks to afford macroscale hydrogel constructs with nanoscale spatial control. It has been shown that solutions of nanofibrillated cellulose had excellent shear thinning characteristics, which can be combined with alginate to yield a unique cell-laden bioink for 3D bioprinting of living tissues [329]. Simultaneous electrospinning of nano and microfiber has led to the formation of multiscale fibrous scaffolds of PCL, which was combined with a chitosan hydrogel for ligament regeneration [330]. This scaffold induced rabbit ligament fibroblast cells to elongate along the aligned PCL fibers, which is required for the native ligament tissue microenvironment (Fig. 19b). Furthermore, electrospinning has been integrated with 3D fiber deposition to create a multiscale scaffold of a PEG/poly(butylene terephthalate) (PBT) block copolymer that possessed a microarchitecture similar to the native tympanic membrane [331]. *In vitro* studies have revealed that hMSCs cultured on these scaffolds remained viable and metabolically active, and arranged along architectural directions of the scaffold. This study paved the way for multiscale, multi-compound, and multi-functional engineered tissues, which could potentially better mimic the complexity of native tissues.

Multiscale hierarchical architectures can also be controllably engineered by combining capillary force lithography and micro wrinkling, as it can mimic the topographical and orientation cues of the ECM. Nanopatterning of materials through UV assisted capillary force lithography technique, and subsequent pressing of

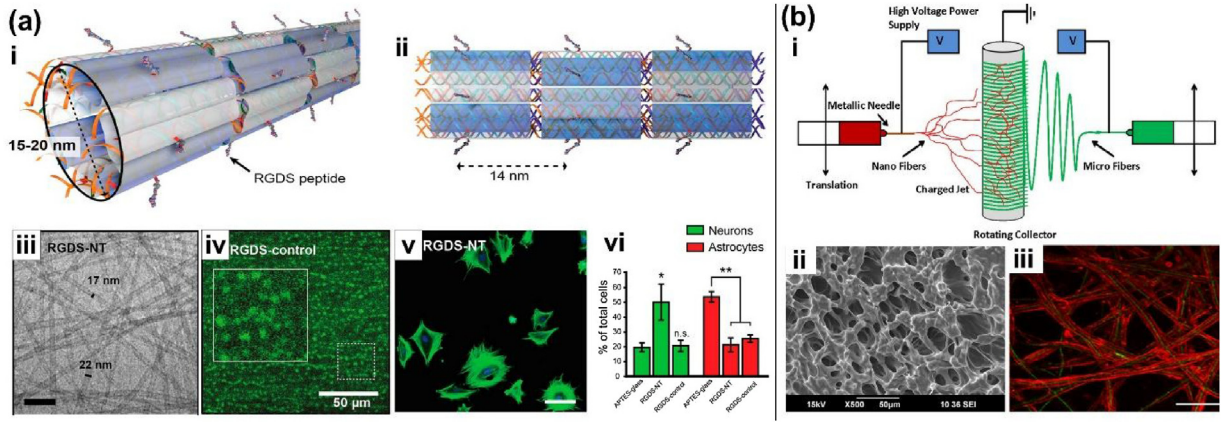

Fig. 19. (a) (i, ii) Schematic illustration of RGD functionalized DNA nanotubes with a comparable organization of the tiles and size of the peptide with respect to the DNA, (iii) its cryo-TEM characterization (iv–v) and cellular behavior. (b) (i) Schematic depicting a dual-electrospinning setup. (ii, iii) Characterization of generated multiscale PCL nano/micro fiber and *in vitro* cellular reaction of PCL random multiscale fibers coated with Ch-HA.
Reproduced with permission from: (a) Ref. [327], (b) Ref. [330].

the materials, affords multiscale topography cues for ECM deposition, which can ultimately regulate cellular morphology and directionality. It has been shown that the structures and directions of fibroblast cells were predominantly influenced by nanotopography, rather than by microtopography [332]. This approach opens a window of opportunity to engineer biomimetic well-defined 3D structures for biomedical applications. Moreover, the capillary force lithography/wrinkling combinatory technique has been used to generate hierarchically micro/nanopatterned transplantable patches composed of PLGA [332]. Besides expressing significant flexibility, such multiscale PLGA patches exhibited augmented tissue adhesion to the underlying native tissue, as opposed to merely nanopatterned counterparts. Integration of such PLGA patches with hMSCs also expressed enhanced bone generation in an *in vitro* model. This combinatory technique contributes to our capability to manipulate the substrate of cell culture to guide cell fate and function.

Multi-component polymers with multiscale pore sizes permit another class of multiscale tissue engineering, which was recently explored for the regeneration of damaged heart muscles [333]. Such multiscale structures were built from a combination of poly (limonene thioether) and poly(glycerol sebacate) porous membrane to function as a vascular–parenchymal interface. Hierarchical structures with micro- and macrosized pores were fabricated by casting the poly(limonene thioether) prepolymer onto PMMA spheres with a $\sim$35 μm diameter inside a precisely patterned mold. The casted prepolymer was later photocrosslinked, detached from mold, and underwent leaching process with acetone to remove the PMMA spheres and afford microsized pores inside of the main scaffold. *In vitro* studies revealed that macrosized channels enabled enhanced perfusion and assisted heart cell to align, while microsized pores improved heart cell retention with reducing polymer content. Moreover, it has been shown that the poly(glycerol sebacate) component functioned as a microporous vascular–parenchymal interface to afford high oxygen permissibility. This approach offers a versatile strategy that can bridge micro- and macroscale structures to mimic native tissue microenvironments. Although extensive research is needed to extend this technology into 3D shaped cell-laden hydrogel, a combination with multimaterial bioprinting approach can be envisioned.

Engineering 3D architectures with designer physical, chemical, and biological properties to accurately control cellular behavior is a key challenge for biomedical engineers. Developing biomaterials that provide cells with synergistic cues at multiple length scales can be expected to extend our capability to control cells in a spatiotemporal manner. Despite advent of novel combinatory techniques, these developments are still in their infancy and require a significant progression to mature in a widely useful platform to provide solutions for biomedical needs.

4.2. High-throughput screening for optimal biomaterial compositions

As described in previous sections, unprecedented hydrogels with different chemical and physical properties have been developed to regulate cellular behaviors by mimicking the microenvironments of native tissues. Although it has been found that the spatial and temporal engineered microenvironmental factors of hydrogels can synergistically affect cellular behaviors in a diverse way, conventional *in vitro* approaches are cumbersome and inefficient to find the optimal compositions from a vast number of hydrogels.

High-throughput screening platforms have been considered as a promising technology to screen the cellular responses to the effects of the vast combinations of factors in hydrogels [334,335]. Diverse high-throughput strategies have been proposed to generate comprehensive libraries of hydrogels' microenvironmental factors to map the cellular responses. Typically, high-throughput screening platforms consist of hydrogel microarrays with different material compositions, which enable the simultaneous analysis of a large number of interactions between cells and hydrogels. To this end, various techniques including contact printing, soft lithography, and wettability patterning have been used to manufacture hydrogel microarrays [336–343].

Contact printing utilizes the capillary force of hollow pin arrays to build high-throughput screening platforms. Briefly, nanoliter volumes of biomaterials could be inserted into the tips of pin arrays *via* the capillary force and transferred *via* contact between the tips and a substrate [344–346]. Combinatorial screenings of 2D and 3D cellular behaviors on biomaterial microarrays have been conducted by utilizing contact printing technique [336,339,344–350]. For instance, Dolatshahi-Pirouz et al. utilized the contact printing method to print 3D cell-laden GelMA hydrogel arrays for the investigation of osteogenic differentiation of hMSCs [339]. It was observed that the osteogenic differentiation of hMSCs was significantly promoted by incorporating bone tissue-related ECM components, such as fibronectin, osteocalcin, and laminin into the hydrogel. Through this approach, an optimal composition of ECM components and growth factors for osteogenic differentiation of hMSCs could be identified.

In addition to contact printing, wettability patterning has also been developed as a facile way to create 3D biomaterial arrays. Wettability patterned surfaces enable the isolation of cell-laden biomaterials onto the hydrophilic region surrounded by hydrophobic borders, resulting in the formation of biomaterial arrays [36,351–356]. Wettability patterning can potentially be used for screening 3D cellular behaviors in spatially engineered hydrogels. Recently, Li et al. developed a simple method to generate spatially engineered 3D cell microenvironments using a surface-wettability-guided assembly (SWGA) method [336]. To make wettability patterns, a thin PDMS layer with microarray patterns was transferred to a clean glass substrate by using soft lithography. The wettability contrast between the hydrophobic PDMS layer and the hydrophilic glass surface allowed for accurate patterning of 3D cell-laden biomaterial arrays. Various shapes of hydrogels that contain different cell types could be readily fabricated using this SWGA method. In addition, heterogeneous biomaterial microarrays could be fabricated by interconnecting two hydrogel arrays printed on separated substrates with different shapes. This method enables the individual and spatial control of 3D cellular microenvironments, which can be used as a powerful tool for the investigation of spatial cell-biomaterial interactions in high-throughput manner.

Most of the conventional high-throughput screening platforms have focused on the investigation of 2D and 3D cellular behaviors in different biomaterial compositions. In addition to the biomaterial compositions, recent findings suggest that the interfacial geometry and temporally applied mechanical/electrical stimuli can synergistically influence cell-biomaterial interactions in a diverse way [357–362]. Thus, screening the synergistical effects of geometric features of biomaterials and external dynamic stimuli on cell behaviors would provide valuable information to design smart biomaterials for therapeutic applications. To investigate the cell-biomaterial interactions under dynamic compressive strains, Moraes et al. developed a high-throughput device that can precisely apply controlled compressive strains to each individual actuating micropillar in a 3D cell-laden hydrogel microarray [363]. A range of 0–26% compressive strains could be dynamically applied to PEG hydrogel, allowing the characterization of deformation of cell nuclei under the compression. Similarly, the capability of applying tensile stress to 3D cell-laden hydrogels is also crucial as various tissues in the body, such as muscles, blood vessels, and heart are under constantly varying tensile strains. To this end,

high-throughput screening platforms that can apply tensile stress to 3D cell-laden hydrogel arrays have been developed [364,365]. The proliferation, spreading, and differentiation of cells were different from those cultured under static conditions, which provided insights in cell behavior upon dynamic biomechanical stimuli in 3D cell culture.

In addition to the dynamic mechanical stimuli, electrical stimulation can also influence cell behaviors and functions, such as proliferation, differentiation, and maturation [366,367]. Particularly, the electrical signaling is regarded as one of the most crucial microenvironmental cues to direct neuronal cell functions. For instance, Jin et al. recently investigated the electrical stimulation effects by a direct reprogramming of fibroblasts to functional neuronal cells [368]. A triboelectrical nanogenerator was implemented as an electrical stimulation source, which generated biphasic electrical current pulse (1 Hz, ~270 nA) from frictional movements. The electrical stimulation combined with nonviral delivery of neuronal linage specific transcription factors showed significantly enhanced cell reprogramming efficiency for both *in vivo* and *in vitro* scenarios.

Despite the significance of electrical stimulation in cellular behavior, high-throughput approaches to find optimized electrical stimuli for enhancing cellular functions remain a largely unexplored area. As a potentially useful platform, Dai et al. developed 3D flexible nanoelectronics to interface a 3D cardiac tissue construct for not only monitoring electrical signals, but also applying electrical stimulation [369]. The nanoelectronics consisted of individually addressable electrical stimulation electrode arrays with sensors to map electrical signals across the 3D cardiac tissue construct. The array configuration enabled spatial manipulation of action potential propagation of a cardiac tissue by applying electrical stimulation (1 V, 1.25 Hz). This miniaturized nanoelectronic platform can potentially be used in various hydrogel-based 3D engineered tissue models including blood brain barriers, blood vessel regeneration, a neuronal network for drug discovery and regenerative medicine.

High-throughput approaches have shown promising results for the investigation of the interactions between cells and their complex chemical and physical microenvironments with minimized use of materials at a significantly enhanced efficiency. Although various high-throughput platforms are developed to screen 2D and 3D cellular behaviors in response to ECM compositions, stiffness, and active mechanical stimulation, to date there is no integrated platform to monitor and analyze the cell behaviors at time scales relevant to tissue development and regeneration. For the true success of high-throughput platforms, there is an urgent need to develop a standardized platform that is compatible with conventional cell cultures and instruments for analyses. As the recent development of biomaterials has been focused on the smart biomaterials that can dynamically change their chemical and physical properties, *in situ* high-throughput analytical platforms that can be integrated with high-throughput screening devices could prove of high value in the high-throughput investigation of dynamic interactions between cells and biomaterials.

5. Conclusions

In summary, the field of hydrogel based biomaterials is rich with strategies for engineering material constructs with innovative functionalities and physicochemical properties. Of particular note are the chemical modifications and technological platforms that have granted spatial and temporal control over various hydrogel systems. Advancing hydrogels from static to dynamic experimenter-controlled systems is expected to expand our capability to guide complex and multi-faceted cellular processes such as stem cell differentiation and tissue regeneration. Recently developed high-throughput platforms are expected to aid in the identification of high performing formulations, which might accelerate the translation of these promising advanced biomaterials.

Acknowledgements

This paper was supported by National Science Foundation (EFRI-1240443), ONR PECASE Award, the Department of Defense Congressionally Directed Medical Research Programs (OR110196) and the National Institutes of Health (AR066193, AR063194, HL092836, DE019024, EB012597, AR057837, DE021468, DE022376, HL099073, EB008392, AR069564, AR007505, HL137193, and EB024403). Dr. Leijten acknowledges financial support from Innovative Research Incentives Scheme Veni #14328 of the Netherlands Organization for Scientific Research (NWO). Dr. Seo was partially supported by Basic Science Research Program through the National Research Foundation of Korea (NRF) funded by the Ministry of Education (2016R1A6A3A03006491). Dr. Zhang acknowledges the National Cancer Institute of the National Institutes of Health Pathway to Independence Award (K99CA201603). This paper has been partially funded by the Tec de Monterrey and MIT Nanotechnology Program.

References

[1] J. Leijten, A. Khademhosseini, Cell Stem Cell 18 (2016) 20–24.
[2] G. Kaushik, J. Leijten, A. Khademhosseini, Stem Cells 35 (2016) 51–60.
[3] M.P. Lutolf, J.A. Hubbell, Nat. Biotechnol. 23 (2005) 47–55.
[4] J. Leijten, J. Rouwkema, Y.S. Zhang, A. Nasajpour, M.R. Dokmeci, A. Khademhosseini, Small 12 (2016) 2130–2145.
[5] C. Mandrycky, Z. Wang, K. Kim, D.H. Kim, Biotechnol. Adv. 34 (2016) 422–434.
[6] C.M. Kirschner, K.S. Anseth, Acta Mater. 61 (2013) 931–944.
[7] R.H. Schmedlen, K.S. Masters, J.L. West, Biomaterials 23 (2002) 4325–4332.
[8] E. Ruoslahti, M.D. Pierschbacher, Science 238 (1987) 491–497.
[9] L. Perlin, S. MacNeil, S. Rimmer, Soft Matter 4 (2008) 2331–2349.
[10] E. Jabbari, J. Leijten, Q.B. Xu, A. Khademhosseini, Mater. Today 19 (2016) 190–196.
[11] Y. Li, G. Huang, X. Zhang, L. Wang, Y. Du, T.J. Lu, F. Xu, Biotechnol. Adv. 32 (2014) 347–365.
[12] R. McBeath, D.M. Pirone, C.M. Nelson, K. Bhadriraju, C.S. Chen, Dev. Cell 6 (2004) 483–495.
[13] C.Y. Tay, M. Pal, H. Yu, W.S. Leong, N.S. Tan, K.W. Ng, S. Venkatraman, F. Boey, D.T. Leong, L.P. Tan, Small 7 (2011) 1416–1421.
[14] M.M. Alvarez, J.C. Liu, G. Trujillo-de Santiago, B.-H. Cha, A. Vishwakarma, A.M. Ghaemmaghami, A. Khademhosseini, J. Controll. Release 240 (2016) 349–363.
[15] T. Segura, B.C. Anderson, P.H. Chung, R.E. Webber, K.R. Shull, L.D. Shea, Biomaterials 26 (2005) 359–371.
[16] Y. Hu, J.-O. You, J. Aizenberg, ACS Appl. Mater. Interfaces 8 (2016) 21939–21945.
[17] R.J. Wade, E.J. Bassin, W.M. Gramlich, J.A. Burdick, Adv. Mater. 27 (2015) 1356–1362.
[18] D. Hodde, J. Gerardo-Nava, V. Wöhlk, S. Weinandy, S. Jockenhövel, A. Kriebel, H. Altinova, H.W. Steinbusch, M. Möller, J. Weis, Eur. J. Neurosci. 43 (2016) 376–387.
[19] D. Liu, C.W. Bastiaansen, J.M. den Toonder, D.J. Broer, Langmuir 29 (2013) 5622–5629.
[20] S.Q. Liu, C. Yang, Y. Huang, X. Ding, Y. Li, W.M. Fan, J.L. Hedrick, Y.Y. Yang, Adv. Mater. 24 (2012) 6484–6489.
[21] J.A. Chikar, J.L. Hendricks, S.M. Richardson-Burns, Y. Raphael, B.E. Pfingst, D.C. Martin, Biomaterials 33 (2012) 1982–1990.
[22] S.B. Goodman, Z. Yao, M. Keeney, F. Yang, Biomaterials 34 (2013) 3174–3183.
[23] D.M. Faulk, R. Londono, M.T. Wolf, C.A. Ranallo, C.A. Carruthers, J.D. Wildemann, C.L. Dearth, S.F. Badylak, Biomaterials 35 (2014) 8585–8595.
[24] N.C. Rivron, E.J. Vrij, J. Rouwkema, S. Le Gac, A. van den Berg, R.K. Truckenmüller, C.A. van Blitterswijk, Proc. Natl. Acad. Sci. 109 (2012) 6886–6891.
[25] J.-W. Jeong, G. Shin, S.I. Park, K.J. Yu, L. Xu, J.A. Rogers, Neuron 86 (2015) 175–186.
[26] M.T. Wolf, C.L. Dearth, C.A. Ranallo, S.T. LoPresti, L.E. Carey, K.A. Daly, B.N. Brown, S.F. Badylak, Biomaterials 35 (2014) 6838–6849.
[27] M.T. Wolf, C.A. Carruthers, C.L. Dearth, P.M. Crapo, A. Huber, O.A. Burnsed, R. Londono, S.A. Johnson, K.A. Daly, E.C. Stahl, J. Biomed. Mater. Res. A 102 (2014) 234–246.
[28] J.L. Skousen, M.J. Bridge, P.A. Tresco, Biomaterials 36 (2015) 33–43.
[29] L. Zhang, Z. Cao, T. Bai, L. Carr, J.-R. Ella-Menye, C. Irvin, B.D. Ratner, S. Jiang, Nat. Biotechnol. 31 (2013) 553–556.

[30] M.D. Tang, A.P. Golden, J. Tien, J. Am. Chem. Soc. 125 (2003) 12988–12989.
[31] W. Bian, B. Liau, N. Badie, N. Bursac, Nat. Protoc. 4 (2009) 1522–1534.
[32] A. Khademhosseini, G. Eng, J. Yeh, J. Fukuda, J. Blumling, R. Langer, J.A. Burdick, J. Biomed. Mater. Res. A 79 (2006) 522–532.
[33] J. Yeh, Y. Ling, J.M. Karp, J. Gantz, A. Chandawarkar, G. Eng, J. Blumling Iii, R. Langer, A. Khademhosseini, Biomaterials 27 (2006) 5391–5398.
[34] J. Fukuda, A. Khademhosseini, Y. Yeo, X. Yang, J. Yeh, G. Eng, J. Blumling, C.-F. Wang, D.S. Kohane, R. Langer, Biomaterials 27 (2006) 5259–5267.
[35] V. Hosseini, S. Ahadian, S. Ostrovidov, G. Camci-Unal, S. Chen, H. Kaji, M. Ramalingam, A. Khademhosseini, Tissue Eng. Part A 18 (2012) 2453–2465.
[36] J. Seo, S.-K. Lee, J. Lee, J.S. Lee, H. Kwon, S.-W. Cho, J.-H. Ahn, T. Lee, Sci. Rep. 5 (2015) 12326.
[37] D. Loessner, C. Meinert, E. Kaemmerer, L.C. Martine, K. Yue, P.A. Levett, T.J. Klein, F.P. Melchels, A. Khademhosseini, D.W. Hutmacher, Nat. Protoc. 11 (2016) 727–746.
[38] V. Rodriguez-Rivera, J.W. Weidner, M.J. Yost, Three-dimensional Biomimetic Technology: Novel Biorubber Creates Defined Micro- and Macro-scale Architectures in Collagen Hydrogels, J. Vis. Exp. 108 (2016), doi:http://dx.doi.org/10.3791/53578 e53578.
[39] J.S. Miller, K.R. Stevens, M.T. Yang, B.M. Baker, D.-H.T. Nguyen, D.M. Cohen, E. Toro, A.A. Chen, P.A. Galie, X. Yu, Nat. Mater. 11 (2012) 768–774.
[40] H. Qi, Y. Du, L. Wang, H. Kaji, H. Bae, A. Khademhosseini, Adv. Mater. 22 (2010) 5276–5281.
[41] A.P. Golden, J. Tien, Lab Chip 7 (2007) 720–725.
[42] S. Zhao, Y. Chen, B.P. Partlow, A.S. Golding, P. Tseng, J. Coburn, M.B. Applegate, J.E. Moreau, F.G. Omenetto, D.L. Kaplan, Biomaterials 93 (2016) 60–70.
[43] V. Hosseini, P. Kollmannsberger, S. Ahadian, S. Ostrovidov, H. Kaji, V. Vogel, A. Khademhosseini, Small 10 (2014) 4851–4857.
[44] N. Annabi, K. Tsang, S.M. Mithieux, M. Nikkhah, A. Ameri, A. Khademhosseini, A.S. Weiss, Adv. Funct. Mater. 23 (2013) 4950–4959.
[45] P.D. Rios, X. Zhang, X. Luo, L.D. Shea, Biotechnol. Bioeng. 113 (2016) 2485–2495.
[46] E. Vrij, J. Rouwkema, V. LaPointe, C. van Blitterswijk, R. Truckenmuller, N. Rivron, Adv. Mater. 28 (2016) 4032–4039.
[47] E.J. Vrij, S. Espinoza, M. Heilig, A. Kolew, M. Schneider, C.A. van Blitterswijk, R. K. Truckenmuller, N.C. Rivron, Lab Chip 16 (2016) 734–742.
[48] J. Leijten, L.S. Teixeira, J. Bolander, W. Ji, B. Vanspauwen, J. Lammertyn, J. Schrooten, F.P. Luyten, Sci. Rep. 6 (2016) 36011.
[49] J. Bolander, W. Ji, J. Leijten, L.M. Teixeira, V. Bloemen, D. Lambrechts, M. Chaklader, F.P. Luyten, Stem Cell Rep. 8 (Mar (3)) (2017) 758–772.
[50] L.S. Moreira Teixeira, J.C. Leijten, J. Sobral, R. Jin, A.A. van Apeldoorn, J. Feijen, C. van Blitterswijk, P.J. Dijkstra, M. Karperien, Eur. Cell Mater. 23 (2012) 387–399.
[51] S.J. Bryant, J.L. Cuy, K.D. Hauch, B.D. Ratner, Biomaterials 28 (2007) 2978–2986.
[52] W.M. Gramlich, I.L. Kim, J.A. Burdick, Biomaterials 34 (2013) 9803–9811.
[53] J. Torgersen, X.H. Qin, Z. Li, A. Ovsianikov, R. Liska, J. Stampfl, Adv. Funct. Mater. 23 (2013) 4542–4554.
[54] N. Brandenberg, M.P. Lutolf, Adv. Mater. 28 (2016) 7450–7456.
[55] A. Ovsianikov, A. Deiwick, S. Van Vlierberghe, P. Dubruel, L. Möller, G. Dräger, B. Chichkov, Biomacromolecules 12 (2011) 851–858.
[56] A. Ovsianikov, A. Deiwick, S. Van Vlierberghe, M. Pflaum, M. Wilhelmi, P. Dubruel, B. Chichkov, Materials 4 (2011) 288–299.
[57] A. Ovsianikov, S. Mühleder, J. Torgersen, Z. Li, X.-H. Qin, S. Van Vlierberghe, P. Dubruel, W. Holnthoner, H. Redl, R. Liska, Langmuir 30 (2013) 3787–3794.
[58] G.M. Whitesides, Nature 442 (2006) 368–373.
[59] B.G. Chung, K.-H. Lee, A. Khademhosseini, S.-H. Lee, Lab Chip 12 (2012) 45–59.
[60] K. Krutkramelis, B. Xia, J. Oakey, Lab Chip 16 (2016) 1457–1465.
[61] C. Siltanen, M. Yaghoobi, A. Haque, J. You, J. Lowen, M. Soleimani, A. Revzin, Acta Biomater. 34 (2016) 125–132.
[62] J.-Y. Leong, W.-H. Lam, K.-W. Ho, W.-P. Voo, M.F.-X. Lee, H.-P. Lim, S.-L. Lim, B.-T. Tey, D. Poncelet, E.-S. Chan, Particuology 24 (2016) 44–60.
[63] B. Yang, Y. Lu, G. Luo, Ind. Eng. Chem. Res. 51 (2012) 9016–9022.
[64] S. Henke, J. Leijten, E. Kemna, M. Neubauer, A. Fery, A. van den Berg, A. van Apeldoorn, M. Karperien, Macromol. Biosci. 16 (2016) 1524–1532.
[65] M.J. Hancock, F. Piraino, G. Camci-Unal, M. Rasponi, A. Khademhosseini, Biomaterials 32 (2011) 6493–6504.
[66] T. Kamperman, S. Henke, A. van den Berg, S.R. Shin, A. Tamayol, A. Khademhosseini, M. Karperien, J. Leijten, Adv. Healthc. Mater. 6 (2017) 1600913.
[67] T. Kamperman, S. Henke, C.W. Visser, M. Karperien, J. Leijten, Small 13 (Jun 22) (2017), doi:http://dx.doi.org/10.1002/smll.201603711 Epub 2017 April 28.
[68] N.G. Min, M. Ku, J. Yang, S.-H. Kim, Chem. Mater. 28 (2016) 1430–1438.
[69] A. Leferink, D. Schipper, E. Arts, E. Vrij, N. Rivron, M. Karperien, K. Mittmann, C. van Blitterswijk, L. Moroni, R. Truckenmüller, Adv. Mater. 26 (2014) 2592–2599.
[70] U.A. Gurkan, S. Tasoglu, D. Kavaz, M.C. Demirel, U. Demirci, Adv. Healthc. Mater. 1 (2012) 149–158.
[71] B. Zamanian, M. Masaeli, J.W. Nichol, M. Khabiry, M.J. Hancock, H. Bae, A. Khademhosseini, Small 6 (2010) 937–944.
[72] F. Xu, C.a.M. Wu, V. Rengarajan, T.D. Finley, H.O. Keles, Y. Sung, B. Li, U.A. Gurkan, U. Demirci, Adv. Mater. 23 (2011) 4254–4260.
[73] F. Xu, T.D. Finley, M. Turkaydin, Y. Sung, U.A. Gurkan, A.S. Yavuz, R.O. Guldiken, U. Demirci, Biomaterials 32 (2011) 7847–7855.
[74] V. Jayawarna, M. Ali, T.A. Jowitt, A.F. Miller, A. Saiani, J.E. Gough, R.V. Ulijn, Adv. Mater. 18 (2006) 611–614.
[75] A. Harada, R. Kobayashi, Y. Takashima, A. Hashidzume, H. Yamaguchi, Nat. Chem. 3 (2011) 34–37.
[76] D. Rogozhnikov, W. Luo, S. Elahipanah, P.J. O'Brien, M.N. Yousaf, Bioconjugate Chem. 27 (2016) 1991–1998.
[77] M.E. Todhunter, N.Y. Jee, A.J. Hughes, M.C. Coyle, A. Cerchiari, J. Farlow, J.C. Garbe, M.A. LaBarge, T.A. Desai, Z.J. Gartner, Nat. Methods 12 (2015) 975–981.
[78] P. Chen, Z. Luo, S. Güven, S. Tasoglu, A.V. Ganesan, A. Weng, U. Demirci, Adv. Mater. 26 (2014) 5936–5941.
[79] H. Qi, M. Ghodousi, Y. Du, C. Grun, H. Bae, P. Yin, A. Khademhosseini, Nat. Commun. 4 (2013) 2275.
[80] Y. Du, E. Lo, S. Ali, A. Khademhosseini, Proc. Natl. Acad. Sci. 105 (2008) 9522–9527.
[81] D. Rogozhnikov, W. Luo, S. Elahipanah, P.J. O'Brien, M.N. Yousaf, Bioconjug Chem. 27 (Sep (9)) (2016) 1991–1998.
[82] J.P. Gong, Y. Katsuyama, T. Kurokawa, Y. Osada, Adv. Mater. 15 (2003) 1155–1158.
[83] M.A. Haque, T. Kurokawa, J.P. Gong, Polymer 53 (2012) 1805–1822.
[84] Z. Li, J. Shen, H. Ma, X. Lu, M. Shi, N. Li, M. Ye, Mater. Sci. Eng.: C 33 (2013) 1951–1957.
[85] Y. Guo, T. Yuan, Z. Xiao, P. Tang, Y. Xiao, Y. Fan, X. Zhang, J. Mater. Sci. 23 (2012) 2267–2279.
[86] A. Fallahi, A. Khademhosseini, A. Tamayol, Trends Biotechnol. 34 (2016) 683–685.
[87] A. Tamayol, M. Akbari, N. Annabi, A. Paul, A. Khademhosseini, D. Juncker, Biotechnol. Adv. 31 (2013) 669–687.
[88] F.T. Moutos, L.E. Freed, F. Guilak, Nat. Mater. 6 (2007) 162–167.
[89] M. Akbari, A. Tamayol, S. Bagherifard, L. Serex, P. Mostafalu, N. Faramarzi, M. H. Mohammadi, A. Khademhosseini, Adv. Healthc. Mater. 5 (2016) 751–766.
[90] P. He, S. Sahoo, K.S. Ng, K. Chen, S.L. Toh, J.C.H. Goh, J. Biomed. Mater. Res. A 101 (2013) 555–566.
[91] K.P. Chellamani, D. Veerasubramanian, R.S.V. Balaji, J. Acad. Ind. Res. 3 (2014) 127.
[92] C.M. Hwang, A. Khademhosseini, Y. Park, K. Sun, S.-H. Lee, Langmuir 24 (2008) 6845–6851.
[93] T. Majima, T. Funakosi, N. Iwasaki, S.-T. Yamane, K. Harada, S. Nonaka, A. Minami, S.-I. Nishimura, J. Orthop. Sci. 10 (2005) 302–307.
[94] M. Horst, S. Madduri, V. Milleret, T. Sulser, R. Gobet, D. Eberli, Biomaterials 34 (2013) 1537–1545.
[95] K.H. Lee, S.J. Shin, Y. Park, S.-H. Lee, Small 5 (2009) 1264–1268.
[96] A. Subramanian, D. Vu, G.F. Larsen, H.-Y. Lin, J. Biomater. Sci. Polym. Ed. 16 (2005) 861–873.
[97] B.R. Lee, K.H. Lee, E. Kang, D.-S. Kim, S.-H. Lee, Biomicrofluidics 5 (2011) 022208.
[98] L. Fan, Y. Du, R. Huang, Q. Wang, X. Wang, L. Zhang, J. Appl. Polym. Sci. 96 (2005) 1625–1629.
[99] E. Kang, Y.Y. Choi, S.-K. Chae, J.-H. Moon, J.-Y. Chang, S.-H. Lee, Adv. Mater. 24 (2012) 4271–4277.
[100] S. Ghorbanian, M.A. Qasaimeh, M. Akbari, A. Tamayol, D. Juncker, Biomed. Microdevices 16 (2014) 387–395.
[101] M.A. Daniele, S.H. North, J. Naciri, P.B. Howell, S.H. Foulger, F.S. Ligler, A.A. Adams, Adv. Funct. Mater. 23 (2013) 698–704.
[102] E. Kang, G.S. Jeong, Y.Y. Choi, K.H. Lee, A. Khademhosseini, S.-H. Lee, Nat. Mater. 10 (2011) 877–883.
[103] X. Shi, S. Ostrovidov, Y. Zhao, X. Liang, M. Kasuya, K. Kurihara, K. Nakajima, H. Bae, H. Wu, A. Khademhosseini, Adv. Funct. Mater. 25 (2015) 2250–2259.
[104] A. Tamayol, A.H. Najafabadi, B. Aliakbarian, E. Arab-Tehrany, M. Akbari, N. Annabi, D. Juncker, A. Khademhosseini, Adv. Healthc. Mater. 4 (2015) 2146–2153.
[105] A.C.A. Wan, I.C. Liao, E.K.F. Yim, K.W. Leong, Macromolecules 37 (2004) 7019–7025.
[106] A.C.A. Wan, M.F. Leong, J.K.C. Toh, Y. Zheng, J.Y. Ying, Adv. Healthc. Mater. 1 (2012) 101–105.
[107] H. Onoe, T. Okitsu, A. Itou, M. Kato-Negishi, R. Gojo, D. Kiriya, K. Sato, S. Miura, S. Iwanaga, K. Kuribayashi-Shigetomi, Y.T. Matsunaga, Y. Shimoyama, S. Takeuchi, Nat. Mater. 12 (2013) 584–590.
[108] M. Kim, B. Hong, J. Lee, S.E. Kim, S.S. Kang, Y.H. Kim, G. Tae, Biomacromolecules 13 (2012) 2287–2298.
[109] M. Akbari, A. Tamayol, V. Laforte, N. Annabi, A.H. Najafabadi, A. Khademhosseini, D. Juncker, Adv. Funct. Mater. 24 (2014) 4060–4067.
[110] C.W. Hull, Apparatus for production of three-dimensional objects by stereolithography, Google Patents, 1986.
[111] M.P. Lee, G.J. Cooper, T. Hinkley, G.M. Gibson, M.J. Padgett, L. Cronin, Sci. Rep. 5 (2015) 9875.
[112] S.V. Murphy, A. Atala, Nat. Biotechnol. 32 (2014) 773–785.
[113] Y. Lu, G. Mapili, G. Suhali, S. Chen, K. Roy, J. Biomed. Mater. Res. A 77 (2006) 396–405.
[114] R. Gauvin, Y.-C. Chen, J.W. Lee, P. Soman, P. Zorlutuna, J.W. Nichol, H. Bae, S. Chen, A. Khademhosseini, Biomaterials 33 (2012) 3824–3834.
[115] P. Soman, P.H. Chung, A.P. Zhang, S. Chen, Biotechnol. Bioeng. 110 (2013) 3038–3047.
[116] T.Q. Huang, X. Qu, J. Liu, S. Chen, Biomed. Microdevices 16 (2014) 127–132.
[117] A. Chiappone, E. Fantino, I. Roppolo, M. Lorusso, D. Manfredi, P. Fino, C.F. Pirri, F. Calignano, ACS Appl. Mater. Interfaces 8 (2016) 5627–5633.
[118] B. Guillotin, A. Souquet, S. Catros, M. Duocastella, B. Pippenger, S. Bellance, R. Bareille, M. Rémy, L. Bordenave, J. Amédée, Biomaterials 31 (2010) 7250–7256.

[119] M. Ali, E. Pages, A. Ducom, A. Fontaine, F. Guillemot, Biofabrication 6 (2014) 045001.
[120] E. Hoch, G.E.M. Tovar, K. Borchers, Eur. J. Cardiothorac. Surg. 46 (2014) 767–778.
[121] Y.-C. Li, Y.S. Zhang, A. Akpek, S.R. Shin, A. Khademhosseini, Biofabrication 9 (2017) 102001.
[122] R. Sheth, E.R. Balesh, Y.S. Zhang, J.A. Hirsch, A. Khademhosseini, R. Oklu, J. Vasc. Interv. Radiol. 27 (2016) 859–865.
[123] Y.S. Zhang, M. Duchamp, R. Oklu, L.W. Ellisen, R. Langer, A. Khademhosseini, ACS Biomater. Sci. Eng. 2 (2016) 1710–1721.
[124] J. Malda, J. Visser, F.P. Melchels, T. Jüngst, W.E. Hennink, W.J. Dhert, J. Groll, D. W. Hutmacher, Adv. Mater. 25 (2013) 5011–5028.
[125] S.V. Murphy, A. Atala, Nat Biotech 32 (2014) 773–785.
[126] Y.S. Zhang, K. Yue, J. Aleman, K. Moghaddam, S.M. Bakht, V. Dell'Erba, P. Assawes, S.R. Shin, M.R. Dokmeci, R. Oklu, A. Khademhosseini, Ann. Biomed. Eng. 45 (2017) 143–163.
[127] A. Blaeser, D.F. Duarte Campos, U. Puster, W. Richtering, M.M. Stevens, H. Fischer, Adv. Healthc. Mater. 5 (2016) 326–333.
[128] R. Chang, J. Nam, W. Sun, Tissue Eng. Part A 14 (2008) 41–48.
[129] M. Madaghiele, F. Marotta, C. Demitri, F. Montagna, A. Maffezzoli, A. Sannino, J. Appl. Biomater. Funct. Mater. 12 (2014) 183–192.
[130] S. Suri, C.E. Schmidt, Acta Biomater. 5 (2009) 2385–2397.
[131] S.A. Zawko, S. Suri, Q. Truong, C.E. Schmidt, Acta Biomater. 5 (2009) 14–22.
[132] A.P. Zhang, X. Qu, P. Soman, K.C. Hribar, J.W. Lee, S. Chen, S. He, Adv. Mater. 24 (2012) 4266–4270.
[133] D.B. Kolesky, R.L. Truby, A.S. Gladman, T.A. Busbee, K.A. Homan, J.A. Lewis, Adv. Mater. 26 (2014) 3124–3130.
[134] D.B. Kolesky, K.A. Homan, M.A. Skylar-Scott, J.A. Lewis, Proc. Natl. Acad. Sci. 113 (2016) 3179–3184.
[135] Y.S. Zhang, F. Davoudi, P. Walch, A. Manbachi, X. Luo, V. Dell'Erba, A.K. Miri, H. Albadawi, A. Arneri, X. Li, X. Wang, M.R. Dokmeci, A. Khademhosseini, R. Oklu, Lab Chip 16 (2016) 4097.
[136] M. Du, B. Chen, Q. Meng, S. Liu, X. Zheng, C. Zhang, H. Wang, H. Li, N. Wang, J. Dai, Biofabrication 7 (2015) 044104.
[137] T. Billiet, E. Gevaert, T. De Schryver, M. Cornelissen, P. Dubruel, Biomaterials 35 (2014) 49–62.
[138] L. Ouyang, C.B. Highley, C.B. Rodell, W. Sun, J.A. Burdick, ACS Biomater. Sci. Eng. 2 (2016) 1743–1751.
[139] W. Schuurman, P.A. Levett, M.W. Pot, P.R. van Weeren, W.J. Dhert, D.W. Hutmacher, F.P. Melchels, T.J. Klein, J. Malda, Macromol. Biosci. 13 (2013) 551–561.
[140] C.B. Highley, C.B. Rodell, J.A. Burdick, Adv. Mater. 27 (2015) 5075–5079.
[141] T. Bhattacharjee, S.M. Zehnder, K.G. Rowe, S. Jain, R.M. Nixon, W.G. Sawyer, T. E. Angelini, Sci. Adv. 1 (2015) e1500655.
[142] T.J. Hinton, Q. Jallerat, R.N. Palchesko, J.H. Park, M.S. Grodzicki, H.-J. Shue, M. H. Ramadan, A.R. Hudson, A.W. Feinberg, Sci. Adv. 1 (2015) e1500758.
[143] L.E. Bertassoni, M. Cecconi, V. Manoharan, M. Nikkhah, J. Hjortnaes, A.L. Cristino, G. Barabaschi, D. Demarchi, M.R. Dokmeci, Y. Yang, Lab Chip 14 (2014) 2202–2211.
[144] V.K. Lee, D.Y. Kim, H. Ngo, Y. Lee, L. Seo, S.-S. Yoo, P.A. Vincent, G. Dai, Biomaterials 35 (2014) 8092–8102.
[145] C. Colosi, S.R. Shin, V. Manoharan, S. Massa, M. Constantini, A. Barbetta, M.R. Dokmeci, M. Dentini, A. Khademhosseini, Adv. Mater. 28 (2015) 677–684.
[146] Y.S. Zhang, A. Arneri, S. Bersini, S.-R. Shin, K. Zhu, Z.G. Malekabadi, J. Aleman, C. Colosi, F. Busignani, V. Dell'Erba, C. Bishop, T. Shupe, D. Demarchi, M. Moretti, M. Rasponi, M.R. Dokmeci, A. Atala, A. Khademhosseini, Biomaterials 110 (2016) 45–49.
[147] W. Jia, P.S. Gungor-Ozkerim, Y.S. Zhang, K. Yue, K. Zhu, W. Liu, Q. Pi, B. Byambaa, M.R. Dokmeci, S.R. Shin, A. Khademhosseini, Biomaterials 106 (2016) 58–68.
[148] O. Smidsrød, G. Skjak-Brk, Trends Biotechnol. 8 (1990) 71–78.
[149] J.A. Rowley, G. Madlambayan, D.J. Mooney, Biomaterials 20 (1999) 45–53.
[150] A.D. Augst, H.J. Kong, D.J. Mooney, Macromol. Biosci. 6 (2006) 623–633.
[151] Y. Yu, Y. Zhang, J.A. Martin, I.T. Ozbolat, J. Biomech. Eng. 135 (Sept (9)) (2013) 091011.
[152] Y. Zhang, Y. Yu, H. Chen, I.T. Ozbolat, Biofabrication 5 (2013) 025004.
[153] Y. Zhang, Y. Yu, I.T. Ozbolat, J. Nanotechnol. Eng. Med. 4 (2013) 020902.
[154] Y. Zhang, Y. Yu, A. Akkouch, A. Dababneh, F. Dolati, I.T. Ozbolat, Biomater. Sci. 3 (2015) 134–143.
[155] F. Dolati, Y. Yu, Y. Zhang, A.M. De Jesus, E.A. Sander, I.T. Ozbolat, Nanotechnology 25 (2014) 145101.
[156] Y. Zhang, Y. Yu, F. Dolati, I.T. Ozbolat, Mater. Sci. Eng.: C 39 (2014) 126–133.
[157] J.O. Hardin, T.J. Ober, A.D. Valentine, J.A. Lewis, Adv. Mater. 27 (2015) 3279–3284.
[158] T.J. Ober, D. Foresti, J.A. Lewis, Proc. Natl. Acad. Sci. 112 (2015) 12293–12298.
[159] L.-H. Han, S. Suri, C.E. Schmidt, S. Chen, Biomed. Microdevices 12 (2010) 721–725.
[160] W. Zhu, J. Li, Y.J. Leong, I. Rozen, X. Qu, R. Dong, Z. Wu, W. Gao, P.H. Chung, J. Wang, Adv. Mater. 27 (2015) 4411–4417.
[161] J.-W. Choi, H.-C. Kim, R. Wicker, J. Mater. Process. Technol. 211 (2011) 318–328.
[162] K. Arcaute, B. Mann, R. Wicker, Acta Biomater. 6 (2010) 1047–1054.
[163] C. Zhou, Y. Chen, Z. Yang, B. Khoshnevis, Rapid Prototyp. J. 19 (2013) 153–165.
[164] X. Ma, X. Qu, W. Zhu, Y.-S. Li, S. Yuan, H. Zhang, J. Liu, P. Wang, C.S.E. Lai, F. Zanella, G.-S. Feng, F. Sheikh, S. Chien, S. Chen, Proc. Natl. Acad. Sci. 113 (2016) 2206–2211.
[165] S. Khalil, J. Nam, W. Sun, Rapid Prototyp. J. 11 (2005) 9–17.
[166] H.-W. Kang, S.J. Lee, I.K. Ko, C. Kengla, J.J. Yoo, A. Atala, Nat. Biotechnol. 34 (2016) 312–319.
[167] S. Wust, R. Muller, S. Hofmann, J. Funct. Biomater. 2 (2011) 119–154.
[168] Y. Loo, A. Lakshmanan, M. Ni, L.L. Toh, S. Wang, C.A. Hauser, Nano Lett. 15 (2015) 6919–6925.
[169] A. Panwar, L.P. Tan, Molecules 21 (2016) 685.
[170] D. Chimene, K.K. Lennox, R.R. Kaunas, A.K. Gaharwar, Ann. Biomed. Eng. 44 (2016) 2090–2102.
[171] S. Khalil, W. Sun, J. Biomech. Eng. 131 (2009) 111002.
[172] Z. Wu, X. Su, Y. Xu, B. Kong, W. Sun, S. Mi, Sci. Rep. 6 (2016) 24474.
[173] Q. Xing, K. Yates, C. Vogt, Z. Qian, M.C. Frost, F. Zhao, Sci. Rep. 4 (2014) 4706.
[174] J.W. Nichol, S.T. Koshy, H. Bae, C.M. Hwang, S. Yamanlar, A. Khademhosseini, Biomaterials 31 (2010) 5536–5544.
[175] A. Skardal, J. Zhang, L. McCoard, X. Xu, S. Oottamasathien, G.D. Prestwich, Tissue Eng. Part A 16 (2010) 2675–2685.
[176] C.C. Chang, E.D. Boland, S.K. Williams, J.B. Hoying, J. Biomed. Mater. Res. Part B Appl. Biomater. 98 (2011) 160–170.
[177] L. Koch, A. Deiwick, S. Schlie, S. Michael, M. Gruene, V. Coger, D. Zychlinski, A. Schambach, K. Reimers, P.M. Vogt, B. Chichkov, Biotechnol. Bioeng. 109 (2012) 1855–1863.
[178] M. Yeo, J.S. Lee, W. Chun, G.H. Kim, Biomacromolecules 17 (2016) 1365–1375.
[179] T. Rajangam, S. An, Int. J. Nanomed. 8 (2013) 3641–3662.
[180] M. Gruene, M. Pflaum, C. Hess, S. Diamantouros, S. Schlie, A. Deiwick, L. Koch, M. Wilhelmi, S. Jockenhoevel, A. Haverich, B. Chichkov, Tissue Eng. Part C Methods 17 (2011) 973–982.
[181] A.C. Daly, G.M. Cunniffe, B.N. Sathy, O. Jeon, E. Alsberg, D.J. Kelly, Adv. Healthc. Mater. 5 (2016) 2353–2362.
[182] A.L. Rutz, K.E. Hyland, A.E. Jakus, W.R. Burghardt, R.N. Shah, Adv. Mater. 27 (2015) 1607–1614.
[183] A. Skardal, J. Zhang, L. McCoard, S. Oottamasathien, G.D. Prestwich, Adv. Mater. 22 (2010) 4736–4740.
[184] M.S. Mannoor, Z. Jiang, T. James, Y.L. Kong, K.A. Malatesta, W.O. Soboyejo, N. Verma, D.H. Gracias, M.C. McAlpine, Nano Lett. 13 (2013) 2634–2639.
[185] K. Zhu, S.R. Shin, T. van Kempen, Y.C. Li, V. Ponraj, A. Nasajpour, S. Mandla, N. Hu, X. Liu, J. Leijten, Y.D. Lin, M.A. Hussain, Y.S. Zhang, A. Tamayol, A. Khademhosseini, Adv. Funct. Mater. 27 (2017).
[186] K. Buyukhatipoglu, R. Chang, W. Sun, A.M. Clyne, Tissue Eng. Part C Methods 16 (2010) 631–642.
[187] J.R. Xavier, T. Thakur, P. Desai, M.K. Jaiswal, N. Sears, E. Cosgriff-Hernandez, R. Kaunas, A.K. Gaharwar, ACS Nano 9 (2015) 3109–3118.
[188] G. Gao, A.F. Schilling, T. Yonezawa, J. Wang, G. Dai, X. Cui, Biotechnol. J. 9 (2014) 1304–1311.
[189] F. Pati, J. Jang, D.H. Ha, S. Won Kim, J.W. Rhie, J.H. Shim, D.H. Kim, D.W. Cho, Nat. Commun. 5 (2014) 3935.
[190] M. Kesti, M. Muller, J. Becher, M. Schnabelrauch, M. D'Este, D. Eglin, M. Zenobi-Wong, Acta Biomater. 11 (2015) 162–172.
[191] C. Li, A. Faulkner-Jones, A.R. Dun, J. Jin, P. Chen, Y. Xing, Z. Yang, Z. Li, W. Shu, D. Liu, Angew. Chem. Int. Ed. 54 (2015) 3957–3961.
[192] K. Jakab, C. Norotte, F. Marga, K. Murphy, G. Vunjak-Novakovic, G. Forgacs, Biofabrication 2 (2010) 022001.
[193] J.A. Setterstrom, T.R. Tice, W.E. Myers, in: J.M. Anderson, S.W. Kim (Eds.), Recent Advances in Drug Delivery Systems, Springer US, Boston, MA, 1984, pp. 185–198.
[194] X. Huang, C.S. Brazel, J. Control. Release 73 (2001) 121–136.
[195] C.T. Laurencin, R. Langer, Clin. Lab. Med. 7 (1987) 301–323.
[196] Y.W. Chien, J. Pharm. Sci. 77 (1988) 371.
[197] T.G. Park, S. Cohen, R. Langer, Pharm. Res. 9 (1992) 37–39.
[198] H. Hezaveh, I.I. Muhamad, Chem. Eng. Res. Des. 91 (2013) 508–519.
[199] S.C. Vasudev, T. Chandy, C.P. Sharma, Biomaterials 18 (1997) 375–381.
[200] C.T. Huynh, M.K. Nguyen, G.Y. Tonga, L. Longé, V.M. Rotello, E. Alsberg, Adv. Healthc. Mater. 5 (2016) 305–310.
[201] H. Kim, H. Lee, K.Y. Seong, E. Lee, S.Y. Yang, J. Yoon, Adv. Healthc. Mater. 4 (2015) 2071–2077.
[202] G. Jalani, R. Naccache, D.H. Rosenzweig, L. Haglund, F. Vetrone, M. Cerruti, J. Am. Chem. Soc. 138 (2016) 1078–1083.
[203] H. Epstein-Barash, G. Orbey, B.E. Polat, R.H. Ewoldt, J. Feshitan, R. Langer, M.A. Borden, D.S. Kohane, Biomaterials 31 (2010) 5208–5217.
[204] N. Huebsch, C.J. Kearney, X. Zhao, J. Kim, C.A. Cezar, Z. Suo, D.J. Mooney, Proc. Natl. Acad. Sci. U. S. A. 111 (2014) 9762–9767.
[205] H. Jiang, K. Tovar-Carrillo, T. Kobayashi, Ultrason. Sonochem. 32 (2016) 398–406.
[206] L.M. Geever, C.L. Higginbotham, J. Mater. Sci. 46 (2011) 3233–3240.
[207] M.A. Alam, M. Takafuji, H. Ihara, Polym. J. 46 (2014) 293–300.
[208] C.Y. Gong, S. Shi, P.W. Dong, X.L. Zheng, S.Z. Fu, G. Guo, J.L. Yang, Y.Q. Wei, Z.Y. Qian, BMC Biotechnol. 9 (2009) 8.
[209] R.V. Kulkarni, B. Sa, J. Bioact. Compat. Polym. 24 (2009) 368–384.
[210] A. Servant, V. Leon, D. Jasim, L. Methven, P. Limousin, E.V. Fernandez-Pacheco, M. Prato, K. Kostarelos, Adv. Healthc. Mater. 3 (2014) 1334–1343.
[211] Y. Liu, A. Servant, O.J. Guy, K.T. Al-Jamal, P.R. Williams, K.M. Hawkins, K. Kostarelos, Sens. Actuators B 175 (2012) 100–105.
[212] J.G. Hardy, E. Larrañeta, R.F. Donnelly, N. McGoldrick, K. Migalska, M.T.C. McCrudden, N.J. Irwin, L. Donnelly, C.P. McCoy, Mol. Pharm. 13 (2016) 907–914.
[213] D.M. Nelson, Z. Ma, C.E. Leeson, W.R. Wagner, J. Biomed. Mater. Res. A 100 (2012) 776–785.

[214] X. Hao, E.A. Silva, A. Mansson-Broberg, K.H. Grinnemo, A.J. Siddiqui, G. Dellgren, E. Wardell, L.A. Brodin, D.J. Mooney, C. Sylven, Cardiovasc. Res. 75 (2007) 178–185.
[215] M. Pulat, A.S. Kahraman, N. Tan, M. Gumusderelioglu, J. Biomater. Sci. Polym. Ed. 24 (2013) 807–819.
[216] L.H. Peng, S.Y. Xu, Y.H. Shan, W. Wei, S. Liu, C.Z. Zhang, J.H. Wu, W.Q. Liang, J.Q. Gao, Int. J. Nanomed. 9 (2014) 1897–1908.
[217] J. Parker, N. Mitrousis, M.S. Shoichet, Biomacromolecules 17 (2016) 476–484.
[218] M. Greenwood-Goodwin, E.S. Teasley, S.C. Heilshorn, Biomater. Sci. 2 (2014) 1627–1639.
[219] D.H. Kempen, L. Lu, A. Heijink, T.E. Hefferan, L.B. Creemers, A. Maran, M.J. Yaszemski, W.J. Dhert, Biomaterials 30 (2009) 2816–2825.
[220] S.H. Seo, H.D. Han, K.H. Noh, T.W. Kim, S.W. Son, Clin. Exp. Metastasis 26 (2009) 179–187.
[221] M.S. Hahn, J.S. Miller, J.L. West, Adv. Mater. 18 (2006) 2679–2684.
[222] M.S. Hahn, L.J. Taite, J.J. Moon, M.C. Rowland, K.A. Ruffino, J.L. West, Biomaterials 27 (2006) 2519–2524.
[223] S.-H. Lee, J.J. Moon, J.L. West, Biomaterials 29 (2008) 2962–2968.
[224] J.C. Hoffmann, J.L. West, Soft Matter 6 (2010) 5056–5063.
[225] B.D. Polizzotti, B.D. Fairbanks, K.S. Anseth, Biomacromolecules 9 (2008) 1084–1087.
[226] C.A. DeForest, B.D. Polizzotti, K.S. Anseth, Nat. Mater. 8 (2009) 659–664.
[227] C.A. DeForest, E.A. Sims, K.S. Anseth, Chem. Mater. 22 (2010) 4783–4790.
[228] B.D. Fairbanks, M.P. Schwartz, A.E. Halevi, C.R. Nuttelman, C.N. Bowman, K.S. Anseth, Adv. Mater. 21 (2009) 5005–5010.
[229] D.L. Alge, M.A. Azagarsamy, D.F. Donohue, K.S. Anseth, Biomacromolecules 14 (2013) 949–953.
[230] F. Yu, X. Cao, Y. Li, X. Chen, ACS Macro Lett. 4 (2015) 289–292.
[231] Z. Gu, Y. Tang, Lab Chip 10 (2010) 1946–1951.
[232] Y. Li, B.H. San, J.L. Kessler, J.H. Kim, Q. Xu, J. Hanes, S.M. Yu, Macromol. Biosci. 15 (2015) 52–62.
[233] Y. Luo, M.S. Shoichet, Nat. Mater. 3 (2004) 249–253.
[234] M.J. Mahoney, K.S. Anseth, Biomaterials 27 (2006) 2265–2274.
[235] Y. Luo, M.S. Shoichet, Biomacromolecules 5 (2004) 2315–2323.
[236] J.H. Wosnick, M.S. Shoichet, Chem. Mater. 20 (2008) 55–60.
[237] Y. Aizawa, R. Wylie, M. Shoichet, Adv. Mater. 22 (2010) 4831–4835.
[238] R.G. Wylie, S. Ahsan, Y. Aizawa, K.L. Maxwell, C.M. Morshead, M.S. Shoichet, Nat. Mater. 10 (2011) 799–806.
[239] K.A. Mosiewicz, L. Kolb, A.J. Van Der Vlies, M.M. Martino, P.S. Lienemann, J.A. Hubbell, M. Ehrbar, M.P. Lutolf, Nat. Mater. 12 (2013) 1072–1078.
[240] D.R. Griffin, J. Borrajo, A. Soon, G.F. Acosta-Vélez, V. Oshita, N. Darling, J. Mack, T. Barker, M.L. Iruela-Arispe, T. Segura, Chembiochem 15 (2014) 233–242.
[241] T.T. Lee, J.R. García, J.I. Paez, A. Singh, E.A. Phelps, S. Weis, Z. Shafiq, A. Shekaran, A. del Campo, A.J. García, Nat. Mater. 14 (2015) 352–360.
[242] S. Petersen, J.M. Alonso, A. Specht, P. Duodu, M. Goeldner, A. del Campo, Angew. Chem. Int. Ed. 47 (2008) 3192–3195.
[243] C. Bao, L. Zhu, Q. Lin, H. Tian, Adv. Mater. 27 (2015) 1647–1662.
[244] M.A. Azagarsamy, K.S. Anseth, Angew. Chem. Int. Ed. 52 (2013) 13803–13807.
[245] C.A. DeForest, K.S. Anseth, Angew. Chem. Int. Ed. 51 (2012) 1816–1819.
[246] C.A. DeForest, D.A. Tirrell, Nat. Mater. 14 (2015) 523–531.
[247] N.R. Gandavarapu, M.A. Azagarsamy, K.S. Anseth, Adv. Mater. 26 (2014) 2521–2526.
[248] A.J. Engler, S. Sen, H.L. Sweeney, D.E. Discher, Cell 126 (2006) 677–689.
[249] M. Vicente-Manzanares, X. Ma, R.S. Adelstein, A.R. Horwitz, Nat. Rev. Mol. Cell Biol. 10 (2009) 778–790.
[250] J.L. Young, A.J. Engler, Biomaterials 32 (2011) 1002–1009.
[251] P.J. Nowatzki, C. Franck, S.A. Maskarinec, G. Ravichandran, D.A. Tirrell, Macromolecules 41 (2008) 1839–1845.
[252] S. Khetan, J.S. Katz, J.A. Burdick, Soft Matter 5 (2009) 1601–1606.
[253] S. Khetan, M. Guvendiren, W.R. Legant, D.M. Cohen, C.S. Chen, J.A. Burdick, Nat. Mater. 12 (2013) 458–465.
[254] S. Khetan, J.A. Burdick, Biomaterials 31 (2010) 8228–8234.
[255] M. Guvendiren, M. Perepelyuk, R.G. Wells, J.A. Burdick, J. Mech. Behav. Biomed. Mater. 38 (2014) 198–208.
[256] M. Guvendiren, J.A. Burdick, Nat. Commun. 3 (2012) 792.
[257] S.R. Caliari, M. Perepelyuk, B.D. Cosgrove, S.J. Tsai, G.Y. Lee, R.L. Mauck, R.G. Wells, J.A. Burdick, Sci. Rep. 6 (2016) 21387.
[258] C. Yang, M.W. Tibbitt, L. Basta, K.S. Anseth, Nat. Mater. 13 (2014) 645.
[259] K.M. Mabry, R.L. Lawrence, K.S. Anseth, Biomaterials 49 (2015) 47–56.
[260] R. Tamate, T. Ueki, Y. Kitazawa, M. Kuzunuki, M. Watanabe, A.M. Akimoto, R. Yoshida, Chem. Mater. 28 (2016) 6401–6408.
[261] A.S. Sawhney, C.P. Pathak, J.A. Hubbell, Macromolecules 26 (1993) 581–587.
[262] A.T. Metters, K.S. Anseth, C.N. Bowman, Polymer 41 (2000) 3993–4004.
[263] A.T. Metters, K.S. Anseth, C.N. Bowman, J. Phys. Chem. B 105 (2001) 8069–8076.
[264] K.S. Anseth, A.T. Metters, S.J. Bryant, P.J. Martens, J.H. Elisseeff, C.N. Bowman, J. Controll. Release 78 (2002) 199–209.
[265] S. Sahoo, C. Chung, S. Khetan, J.A. Burdick, Biomacromolecules 9 (2008) 1088–1092.
[266] S.J. Bryant, K.S. Anseth, J. Biomed. Mater. Res. A 64A (2003) 70–79.
[267] B.V. Sridhar, J.L. Brock, J.S. Silver, J.L. Leight, M.A. Randolph, K.S. Anseth, Adv. Healthc. Mater. 4 (2015) 702–713.
[268] D.S. Benoit, A.R. Durney, K.S. Anseth, Tissue Eng. 12 (2006) 1663–1673.
[269] J.L. West, J.A. Hubbell, Macromolecules 32 (1999) 241–244.
[270] B.K. Mann, A.S. Gobin, A.T. Tsai, R.H. Schmedlen, J.L. West, Biomaterials 22 (2001) 3045–3051.
[271] M.P. Lutolf, J.L. Lauer-Fields, H.G. Schmoekel, A.T. Metters, F.E. Weber, G.B. Fields, J.A. Hubbell, Proc. Natl. Acad. Sci. 100 (2003) 5413–5418.
[272] S.B. Anderson, C.-C. Lin, D.V. Kuntzler, K.S. Anseth, Biomaterials 32 (2011) 3564–3574.
[273] Y.S. Jo, S.C. Rizzi, M. Ehrbar, F.E. Weber, J.A. Hubbell, M.P. Lutolf, J. Biomed. Mater. Res. A 93A (2010) 870–877.
[274] J. Patterson, J.A. Hubbell, Biomaterials 32 (2011) 1301–1310.
[275] J.A. Johnson, M.G. Finn, J.T. Koberstein, N.J. Turro, Macromolecules 40 (2007) 3589–3598.
[276] J.A. Johnson, J.M. Baskin, C.R. Bertozzi, J.T. Koberstein, N.J. Turro, Chem. Commun. (2008) 3064–3066.
[277] A.M. Kloxin, A.M. Kasko, C.N. Salinas, K.S. Anseth, Science 324 (2009) 59–63.
[278] A.M. Kloxin, M.W. Tibbitt, K.S. Anseth, Nat. Protocols 5 (2010) 1867–1887.
[279] M.W. Tibbitt, A.M. Kloxin, K.S. Anseth, J. Polym. Sci. A: Polym. Chem. 51 (2013) 1899–1911.
[280] A.M. Kloxin, J.A. Benton, K.S. Anseth, Biomaterials 31 (2010) 1–8.
[281] A.M. Kloxin, M.W. Tibbitt, A.M. Kasko, J.A. Fairbairn, K.S. Anseth, Adv. Mater. 22 (2010) 61–66.
[282] K.J.R. Lewis, M.W. Tibbitt, Y. Zhao, K. Branchfield, X. Sun, V. Balasubramaniam, K.S. Anseth, Biomater. Sci. 3 (2015) 821–832.
[283] M.W. Tibbitt, A.M. Kloxin, K.U. Dyamenahalli, K.S. Anseth, Soft Matter 6 (2010) 5100–5108.
[284] C.M. Kirschner, D.L. Alge, S.T. Gould, K.S. Anseth, Adv. Healthc. Mater. 3 (2014) 649–657.
[285] D.D. McKinnon, T.E. Brown, K.A. Kyburz, E. Kiyotake, K.S. Anseth, Biomacromolecules 15 (2014) 2808–2816.
[286] A.M. Kloxin, K.J.R. Lewis, C.A. DeForest, G. Seedorf, M.W. Tibbitt, V. Balasubramaniam, K.S. Anseth, Integr. Biol. 4 (2012) 1540–1549.
[287] C.A. DeForest, K.S. Anseth, Nat. Chem. 3 (2011) 925–931.
[288] V.X. Truong, K.M. Tsang, G.P. Simon, R.L. Boyd, R.A. Evans, H. Thissen, J.S. Forsythe, Biomacromolecules 16 (2015) 2246–2253.
[289] K.M.C. Tsang, N. Annabi, F. Ercole, K. Zhou, D.J. Karst, F. Li, J.M. Haynes, R.A. Evans, H. Thissen, A. Khademhosseini, J.S. Forsythe, Adv. Funct. Mater. 25 (2015) 977–986.
[290] X. Hu, J. Shi, S.W. Thomas, Polym. Chem. 6 (2015) 4966–4971.
[291] M.A. Azagarsamy, D.D. McKinnon, D.L. Alge, K.S. Anseth, ACS Macro Lett. 3 (2014) 515–519.
[292] B.D. Fairbanks, S.P. Singh, C.N. Bowman, K.S. Anseth, Macromolecules 44 (2011) 2444–2450.
[293] J.F. Mano, Adv. Eng. Mater. 10 (2008) 515–527.
[294] C.d.l.H. Alarcon, S. Pennadam, C. Alexander, Chem. Soc. Rev. 34 (2005) 276–285.
[295] T. Miyata, N. Asami, T. Uragami, Nature 399 (1999) 766–769.
[296] T. Miyata, T. Uragami, K. Nakamae, Adv. Drug Deliv. Rev. 54 (2002) 79–98.
[297] H.Y. Yoshikawa, F.F. Rossetti, S. Kaufmann, T. Kaindl, J. Madsen, U. Engel, A.L. Lewis, S.P. Armes, M. Tanaka, J. Am. Chem. Soc. 133 (2011) 1367–1374.
[298] D. Lin, B. Yurke, N. Langrana, J. Mater. Res. 20 (2005) 1456–1464.
[299] F.X. Jiang, B. Yurke, R.S. Schloss, B.L. Firestein, N.A. Langrana, Biomaterials 31 (2010) 1199–1212.
[300] F.X. Jiang, B. Yurke, R.S. Schloss, B.L. Firestein, N.A. Langrana, Tissue Eng. Part A 16 (2010) 1873–1889.
[301] B.M. Gillette, J.A. Jensen, M. Wang, J. Tchao, S.K. Sia, Adv. Mater. 22 (2010) 686–691.
[302] J.E. Dixon, D.A. Shah, C. Rogers, S. Hall, N. Weston, C.D.J. Parmenter, D. McNally, C. Denning, K.M. Shakesheff, Proc. Natl. Acad. Sci. 111 (2014) 5580–5585.
[303] R.S. Stowers, S.C. Allen, L.J. Suggs, Proc. Natl. Acad. Sci. 112 (2015) 1953–1958.
[304] F.M. Andreopoulos, C.R. Deible, M.T. Stauffer, S.G. Weber, W.R. Wagner, E.J. Beckman, A.J. Russell, J. Am. Chem. Soc. 118 (1996) 6235–6240.
[305] Y. Zheng, M. Micic, S.V. Mello, M. Mabrouki, F.M. Andreopoulos, V. Konka, S.M. Pham, R.M. Leblanc, Macromolecules 35 (2002) 5228–5234.
[306] A.M. Rosales, K.M. Mabry, E.M. Nehls, K.S. Anseth, Biomacromolecules 16 (2015) 798–806.
[307] N. Kong, Q. Peng, H. Li, Adv. Funct. Mater. 24 (2014) 7310–7317.
[308] W.L. Murphy, W.S. Dillmore, J. Modica, M. Mrksich, Angew. Chem. Int. Ed. 46 (2007) 3066–3069.
[309] Z. Sui, W.J. King, W.L. Murphy, Adv. Mater. 19 (2007) 3377–3380.
[310] A.A. Abdeen, J. Lee, N.A. Bharadwaj, R.H. Ewoldt, K.A. Kilian, Adv. Healthc. Mater. 5 (2016) 2536–2544.
[311] Y.S. Kim, M. Liu, Y. Ishida, Y. Ebina, M. Osada, T. Sasaki, T. Hikima, M. Takata, T. Aida, Nat. Mater. 14 (2015) 1002–1007.
[312] K. Yamasaki, H. Hayashi, K. Nishiyama, H. Kobayashi, S. Uto, H. Kondo, S. Hashimoto, T. Fujisato, J. Artif. Organs 12 (2009) 131–137.
[313] J. Duan, X. Liang, K. Zhu, J. Guo, L. Zhang, Soft Matter 13 (2017) 345–354.
[314] H. Fujita, K. Shimizu, Y. Yamamoto, A. Ito, M. Kamihira, E. Nagamori, J. Tissue Eng. Regen. Med. 4 (2010) 437–443.
[315] J.D. Ehrick, S.K. Deo, T.W. Browning, L.G. Bachas, M.J. Madou, S. Daunert, Nat. Mater. 4 (2005) 298–302.
[316] Y. Takashima, S. Hatanaka, M. Otsubo, M. Nakahata, T. Kakuta, A. Hashidzume, H. Yamaguchi, A. Harada, Nat. Commun. 3 (2012) 1270.
[317] J.C. Breger, C. Yoon, R. Xiao, H.R. Kwag, M.O. Wang, J.P. Fisher, T.D. Nguyen, D. H. Gracias, ACS Appl. Mater. Interfaces 7 (2015) 3398–3405.
[318] L. Wang, Y. Liu, Y. Cheng, X. Cui, H. Lian, Y. Liang, F. Chen, H. Wang, W. Guo, H. Li, M. Zhu, H. Ihara, Adv. Sci. (Weinh.) 2 (2015) 1500084.
[319] C. Yang, W. Wang, C. Yao, R. Xie, X.J. Ju, Z. Liu, L.Y. Chu, Sci. Rep. 5 (2015) 13622.

[320] D. Morales, E. Palleau, M.D. Dickey, O.D. Velev, Soft Matter 10 (2014) 1337–1348.
[321] H. Yuk, S. Lin, C. Ma, M. Takaffoli, N.X. Fang, X. Zhao, Nat. Commun. 8 (2017) 14230.
[322] S. Guven, P. Chen, F. Inci, S. Tasoglu, B. Erkmen, U. Demirci, Trends Biotechnol. 33 (2015) 269–279.
[323] S. Ghosh, S.R.P. Kumar, I.K. Puri, S. Elankumaran, Cell Prolif. 49 (2016) 134–144.
[324] E.A. Lee, H. Yim, J. Heo, H. Kim, G. Jung, N.S. Hwang, Arch. Pharm. Res. 37 (2014) 120–128.
[325] N.A. Peppas, J.Z. Hilt, A. Khademhosseini, R. Langer, Adv. Mater. 18 (2006) 1345–1360.
[326] S. Keten, Z. Xu, B. Ihle, M.J. Buehler, Nat. Mater. 9 (2010) 359–367.
[327] N. Stephanopoulos, R. Freeman, H.A. North, S. Sur, S.J. Jeong, F. Tantakitti, J.A. Kessler, S.I. Stupp, Nano Lett. 15 (2015) 603–609.
[328] A. Shaw, V. Lundin, E. Petrova, F. Fordos, E. Benson, A. Al-Amin, A. Herland, A. Blokzijl, B. Hogberg, A.I. Teixeira, Nat. Method 11 (2014) 841–846.
[329] K. Markstedt, A. Mantas, I. Tournier, H. Martínez Ávila, D. Hägg, P. Gatenholm, Biomacromolecules 16 (2015) 1489–1496.
[330] S. Deepthi, K. Jeevitha, M. Nivedhitha Sundaram, K.P. Chennazhi, R. Jayakumar, Chem. Eng. J. 260 (2015) 478–485.
[331] C. Mota, S. Danti, D. D'Alessandro, L. Trombi, C. Ricci, D. Puppi, D. Dinucci, M. Milazzo, C. Stefanini, F. Chiellini, L. Moroni, S. Berrettini, Biofabrication 7 (2015) 025005.
[332] J. Kim, W.-G. Bae, H.-W. Choung, K.T. Lim, H. Seonwoo, H.E. Jeong, K.-Y. Suh, N. L. Jeon, P.-H. Choung, J.H. Chung, Biomaterials 35 (2014) 9058–9067.
[333] K.Y. Morgan, D. Sklaviadis, Z.L. Tochka, K.M. Fischer, K. Hearon, T.D. Morgan, R. Langer, L.E. Freed, Adv. Funct. Mater. 26 (2016) 5873–5883.
[334] T.G. Fernandes, M.M. Diogo, D.S. Clark, J.S. Dordick, J.M.S. Cabral, Trends Biotechnol. 27 (2009) 342–349.
[335] V.I. Chin, P. Taupin, S. Sanga, J. Scheel, F.H. Gage, S.N. Bhatia, Biotechnol. Bioeng. 88 (2004) 399–415.
[336] Y. Li, P. Chen, Y. Wang, S. Yan, X. Feng, W. Du, S.A. Koehler, U. Demirci, B.F. Liu, Adv. Mater. 28 (2016) 3543–3548.
[337] J. Seo, S. Lee, J. Lee, T. Lee, ACS Appl. Mater. Interfaces 3 (2011) 4722–4729.
[338] A.I. Neto, K. Demir, A.A. Popova, M.B. Oliveira, J.F. Mano, P.A. Levkin, Adv. Mater. 28 (2016) 7613–7619.
[339] A. Dolatshahi-Pirouz, M. Nikkhah, A.K. Gaharwar, B. Hashmi, E. Guermani, H. Aliabadi, G. Camci-Unal, T. Ferrante, M. Foss, D.E. Ingber, Sci. Rep. 4 (2014) 3896.
[340] S. Gobaa, S. Hoehnel, M. Roccio, A. Negro, S. Kobel, M.P. Lutolf, Nat. Method 8 (2011) 949–955.
[341] M.-Y. Lee, R.A. Kumar, S.M. Sukumaran, M.G. Hogg, D.S. Clark, J.S. Dordick, Proc. Natl. Acad. Sci. 105 (2008) 59–63.
[342] R. Hull, T. Chraska, Y. Liu, D. Longo, Mater. Sci. Eng.: C 19 (2002) 383–392.
[343] M.B. Oliveira, C.L. Salgado, W. Song, J.F. Mano, Small 9 (2013) 768–778.
[344] C.J. Flaim, D. Teng, S. Chien, S.N. Bhatia, Stem Cells Dev. 17 (2008) 29–40.
[345] C.J. Flaim, S. Chien, S.N. Bhatia, Nat. Method 2 (2005) 119–125.
[346] Y. Mei, K. Saha, S.R. Bogatyrev, J. Yang, A.L. Hook, Z.I. Kalcioglu, S.-W. Cho, M. Mitalipova, N. Pyzocha, F. Rojas, K.J. Van Vliet, M.C. Davies, M.R. Alexander, R. Langer, R. Jaenisch, D.G. Anderson, Nat. Mater. 9 (2010) 768–778.
[347] A. Ranga, S. Gobaa, Y. Okawa, K. Mosiewicz, A. Negro, M. Lutolf, Nat. Commun. 5 (2014) 4324.
[348] T.G. Fernandes, S.J. Kwon, S.S. Bale, M.Y. Lee, M.M. Diogo, D.S. Clark, J. Cabral, J. S. Dordick, Biotechnol. Bioeng. 106 (2010) 106–118.
[349] L. Meli, H.S. Barbosa, A.M. Hickey, L. Gasimli, G. Nierode, M.M. Diogo, R.J. Linhardt, J.M. Cabral, J.S. Dordick, Stem Cell Res. 13 (2014) 36–47.
[350] A.A. Popova, K. Demir, T.G. Hartanto, E. Schmitt, P.A. Levkin, RSC Adv. 6 (2016) 38263–38276.
[351] S. Shin, J. Seo, H. Han, S. Kang, H. Kim, T. Lee, Materials 9 (2016) 116.
[352] D.C. Leslie, A. Waterhouse, J.B. Berthet, T.M. Valentin, A.L. Watters, A. Jain, P. Kim, B.D. Hatton, A. Nedder, K. Donovan, Nat. Biotechnol. 32 (2014) 1134–1140.
[353] W. Feng, L. Li, X. Du, A. Welle, P.A. Levkin, Adv. Mater. 28 (2016) 3202–3208.
[354] M. Hirtz, W. Feng, H. Fuchs, P.A. Levkin, Adv. Mater. Interfaces 3 (2016) 1500469.
[355] M.R. Molla, P.A. Levkin, Adv. Mater. 28 (2016) 1159–1175.
[356] A.A. Popova, S.M. Schillo, K. Demir, E. Ueda, A. Nesterov-Mueller, P.A. Levkin, Adv. Mater. 27 (2015) 5217–5222.
[357] T. Davisson, S. Kunig, A. Chen, R. Sah, A. Ratcliffe, J. Orthop. Res. 20 (2002) 842–848.
[358] S.S. Nunes, J.W. Miklas, J. Liu, R. Aschar-Sobbi, Y. Xiao, B. Zhang, J. Jiang, S. Massé, M. Gagliardi, A. Hsieh, Nat. Methods 10 (2013) 781–787.
[359] J. Lee, A.A. Abdeen, K.L. Wycislo, T.M. Fan, K.A. Kilian, Nat. Mater. 15 (2016) 856–862.
[360] P.J. Ehrlich, L.E. Lanyon, Osteoporos. Int. 13 (2002) 688–700.
[361] N. Tandon, A. Marsano, R. Maidhof, K. Numata, C. Montouri-Sorrentino, C. Cannizzaro, J. Voldman, G. Vunjak-Novakovic, Lab Chip 10 (2010) 692–700.
[362] A. Sathaye, N. Bursac, S. Sheehy, L. Tung, J. Mol. Cell. Cardiol. 41 (2006) 633–641.
[363] C. Moraes, G. Wang, Y. Sun, C.A. Simmons, Biomaterials 31 (2010) 577–584.
[364] H. Liu, J. Usprech, Y. Sun, C.A. Simmons, Acta Biomater. 34 (2015) 113–124.
[365] Y. Li, G. Huang, B. Gao, M. Li, G.M. Genin, T.J. Lu, F. Xu, NPG Asia Mater. 8 (2016) e238.
[366] H.T.H. Au, B. Cui, Z.E. Chu, T. Veres, M. Radisic, Lab Chip 9 (2009) 564–575.
[367] M.Q. Chen, X. Xie, K.D. Wilson, N. Sun, J.C. Wu, L. Giovangrandi, G.T.A. Kovacs, Cell. Mol. Bioeng. 2 (2009) 625–635.
[368] Y. Jin, J. Seo, J.S. Lee, S. Shin, H.J. Park, S. Min, E. Cheong, T. Lee, S.W. Cho, Adv. Mater. 28 (2016) 7365–7374.
[369] X. Dai, W. Zhou, T. Gao, J. Liu, C.M. Lieber, Nat. Nanotechnol. 11 (2016) 776–782.
[370] K.A. Mosiewicz, L. Kolb, A.J. van der Vlies, M.M. Martino, P.S. Lienemann, J.A. Hubbell, M. Ehrbar, M.P. Lutolf, Nat. Mater. 12 (2013) 1072–1078.